Masters Theses   Graduate School

5-2017

Influence of Environmental Conditions and Inundation History on Bacterial Diversity of Salt Marsh Soils in Southern Louisiana

Brandon M. Bagley
University of Tennessee, Knoxville, bbagley2@vols.utk.edu

To the Graduate Council:

I am submitting herewith a thesis written by Brandon M. Bagley entitled "Influence of Environmental Conditions and Inundation History on Bacterial Diversity of Salt Marsh Soils in Southern Louisiana." I have examined the final electronic copy of this thesis for form and content and recommend that it be accepted in partial fulfillment of the requirements for the degree of Master of Science, with a major in Geology.

<div align="right">Annette S. Engel, Major Professor</div>

We have read this thesis and recommend its acceptance:

Edumnd Perfect, Mike L. McKinney, Sean M. Schaeffer

<div align="right">Accepted for the Council:
<u>Dixie L. Thompson</u></div>

<div align="right">Vice Provost and Dean of the Graduate School</div>

(Original signatures are on file with official student records.)

Influence of Environmental Conditions and Inundation History on Bacterial Diversity of Salt Marsh Soils in Southern Louisiana

A Thesis Presented for the
Master of Science
Degree
The University of Tennessee, Knoxville

Brandon M. Bagley
May 2017

ACKNOWLEDGEMENTS

ABSTRACT

Diversity patterns and controls on bacterial community composition were investigated from coastal salt marsh soils in southern Louisiana (USA) from 2012 – 2014. These salt marshes are part of an extensive coastal landscape that is experiencing land loss due to subsidence, sea-level rise, and anthropogenic activities, including from the impacts of the Deepwater Horizon oil spill in 2010. Prior to the oil spill, microbiology research focused predominately on biogeochemical roles and not on taxonomic representation in the soils or on understanding the significance of taxonomic diversity at the microbial level to marsh food webs or ecosystem dynamics. The purpose of this research was to characterize the taxonomic diversity of marsh soils and examine which sets of environmental parameters, including water inundation frequency and depth, vegetation, and salinity, contributed to the most variance in microbiome taxonomic diversity through time. Historical datasets and on-site measurements from the marshes were used to model marsh elevation and local flooding history, and multivariate statistical analyses were applied to determine bacterial community structure and variance. Regardless of sampling time or geographic location, bacterial communities were 80% similar at the phylum level, meaning that marshes were comprised of similar bacterial groups that likely reflected comparable ecosystem function. Subtle differences in marsh bacterial communities were coupled to geographic region, the depth of water that flooded the marsh surfaces, and salinity of that water, with most of the compositional variations being among the Alphaproteobacteria, Gammaproteobacteria, different classes of Chloroflexi, and subgroups within Cyanobacteria. Collectively, these results indicate that some bacterial groups are ubiquitous in natural salt marsh soils, and that efforts to remediate or restore coastal marshes after a disturbance need to consider the importance of key

environmental drivers, like salinity, to how marsh soil bacterial communities are structured and

how ecological function can be maintained.

TABLE OF CONTENTS

LIST OF TABLES

LIST OF FIGURES

xii

CHAPTER ONE - BACKGROUND

The coastal marshes of the Mississippi River delta are important, both environmentally and economically, because they provide habitats for fisheries that generate greater than $10 billion annually in fish stocks and tourism (CWPPRA Task Force, 2015). Louisiana marshes provide ecosystem services for approximately 30% of the United States commercial fishery production (Mac et al., 1998). Saltwater marshes also protect the mainland from storm surges, buffer salinity for the mainland, sequester 44.6 Tg yr^{-1} of carbon, and have the capacity to enhance water quality and remove anthropogenic contamination, such as crude oil (Chmura et al., 2003). Despite their importance, marshes are threatened by chronic natural stressors that are compounded by anthropogenic activities. Natural stressors include sea-level rise, subsidence, and hurricanes, whereas anthropogenic activities include draining marshland for agriculture, crude oil spills, and river diversions (Couvillion et al., 2011; Tweel and Turner, 2012; Turner et al., 2016). During the Deepwater Horizon oil spill of 2010, 4.9 million barrels of MC252 crude oil were released from the Macondo well into the Gulf of Mexico (Mendelssohn et al., 2012). Prior to the oil making landfall, little information was known about how the Gulf ecosystems, including salt marshes, would respond to oiling and how the oil would affect microbial communities in marsh sediments (King et al., 2015).

Microbial communities are responsible for many biogeochemical processes that occur in salt marshes (e.g., nitrogen fixation, sulfate reduction, methanogenesis). Microbes provide these essential ecosystem services, being at the base of the ecosystem, and contribute to nutrient storage or conversion for food webs (Valiela et al., 2002). However, most microbial communities in marsh soils have been studied at a broad, ecosystem-scale. A better

understanding of the nearshore processes that govern salt marsh ecosystems has been needed (Blum et al., 2004; Joye et al., 2014). Moreover, few studies have identified the diversity of bacterial communities from Louisiana marshes, including community structure and taxonomic representation, or characterized changes in diversity spatially and temporally, as was done for other salt marsh systems (Bowen et al., 2009; Kostka et al., 2008; Bowen et al., 2011).

Therefore, the purpose of this thesis project was to examine the 16S rRNA gene sequences retrieved from 2012 until 2014 in southern Louisiana marshes. The research goal was to uncover bacterial diversity in salt marsh soils and determine which sets of environmental parameters, including water inundation frequency and depth, vegetation, and salinity, contributed to the most variance in the taxonomic diversity of marsh soil microbiomes through time. This research project was part of a large, consortium effort to understand salt marsh ecosystem dynamics following the Deepwater Horizon oil spill. The consortium, Coastal Waters Consortium (CWC), sampled marshes in three areas of southern Louisiana, at core sites studied by all the investigators, beginning in August 2011 and continuing through at least 2017.

There are three main research hypotheses: 1) Marsh bacterial communities will share a core microbiome. 2) Marsh bacterial communities in the different study regions are influenced by different environmental conditions, such as salinity, temperature, and depth of water over the marshes. 3) Marsh flooding history explains bacterial community variation through time. The findings from this research will significantly improve our understanding of salt marsh bacterial communities and environmental controls. This thesis is organized into chapters for Materials and Methods (Chapter 2), Results (Chapter 3), and Discussion (Chapter 4). The remainder of Chapter 1 focuses on the background for southern Louisiana marsh geology, geomorphology,

and previous microbiological research from coast salt marshes. Tables and figures are included at the end of each chapter, and references for the entire thesis are at the end of the Discussion, prior to the Appendices.

Geologic History of Southern Louisiana Marshes

As of 2010, coastal marshes covered 14,666 km^2 of land in southern Louisiana (Couvillion et al., 2011). This area includes nine saline to fresh water basins formed as the ancestral Mississippi River began to develop deltas due to rising sea level caused by melting glaciers in the Pleistocene, roughly 15,000-17,000 years ago (Kolb and Van Lopik, 1958). As sea level rose, the deeply incised Mississippi River channel began to fill and deposit increasingly finer sediment along the coastal margins (Kolb and Van Lopik, 1958). The coastal marshes we see today began to develop 5,000 to 6,000 years ago during the relatively stable period (Mac et al., 1998). From 1,000 to 1,500 years ago, natural growth and decay of the delta lobes occurred as the Mississippi River changed course upstream (Mac et al., 1998). Natural levees or embankments channelized river flow and allowed for further seaward land formation (Mac et al., 1998). Repeated breeches of the natural levees abandoned older delta lobes and formed new lobes seaward of the breech (Kolb and Van Lopik, 1958; Mac et al., 1998). In southeast Louisiana, in order from oldest to youngest, the deltaic lobes are Sale-Cypremort, Cocodrie, Teche, St. Bernard, Lafourche, Plaquemines, and Balize, which is known as the bird foot delta and is the active lobe (Figures 1.1 and 1.2).
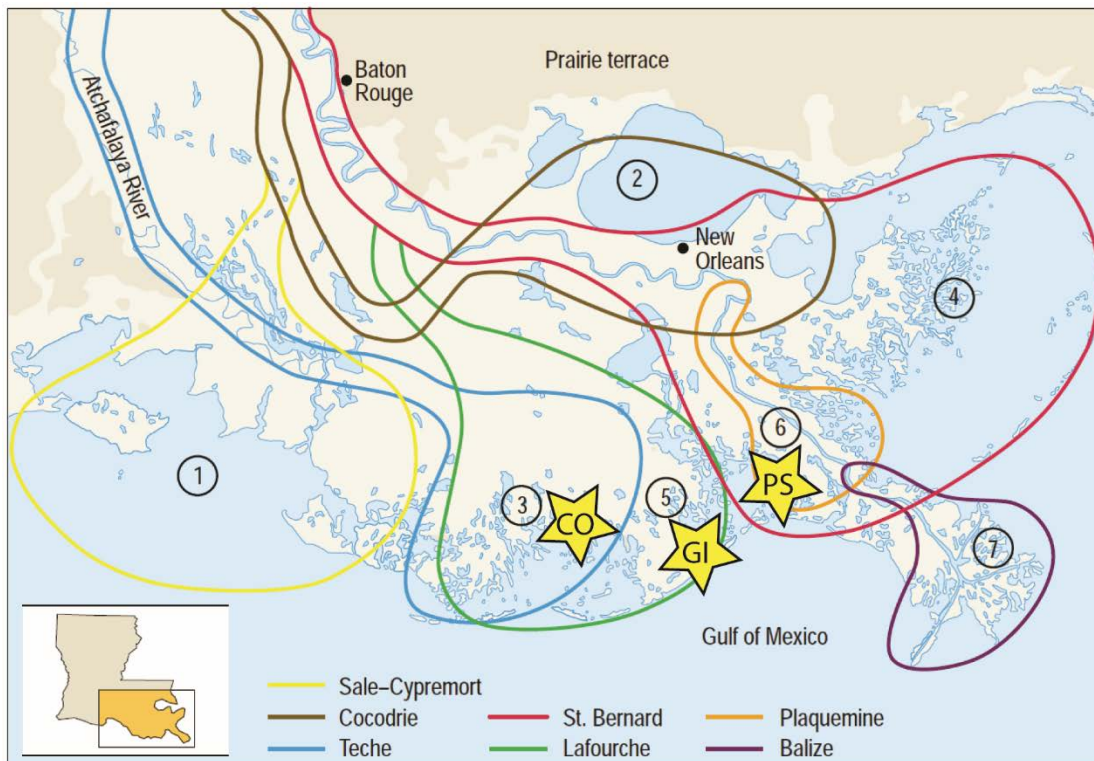
Figure 1.1:   Mississippi River delta lobes, numbered in chronological order of
formation (modified from Kolb and Van Lopik, 1958). Light yellow shading indicates
the extent of current coastal marsh and bottomland forest. Yellow stars are the
sampling regions with the two letters indicating the sampling region name. Each
sampling region is within a lobe of different deltaic age, labeled CO–Cocodrie, GI–
Grand Isle, PS–Port Sulphur. Base map from Mac et al. (1998).
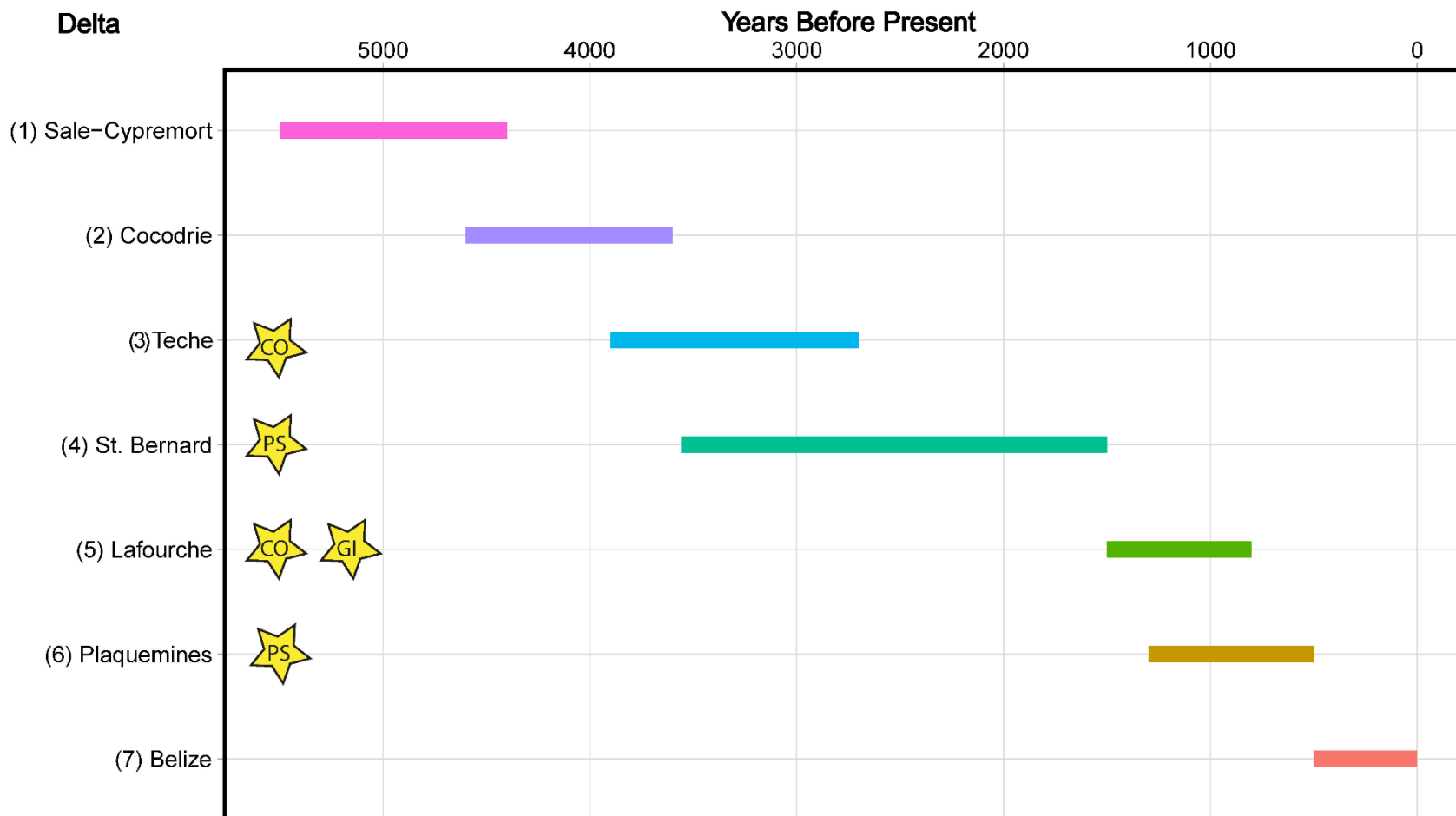
Figure 1.2: Approximate age of Mississippi River Deltas derived from C14 isotopic samples, from Kolb and Van Lopik (1958) with updated chronology from Tornqvist et al. (1996). Relative age of the sample areas noted by stars with the regional acronym, and the corresponding delta lobe number from Figure 1.1 are labeled.

Coastal Marsh Geomorphology

The Mississippi River delta has the largest marsh system in the conterminous United States. The Mississippi River drains a watershed of roughly 4.76 million km^2 of land across the United States and Canada (Louisiana Department of Natural Resources, 2011). Currently, the Mississippi River and a major tributary, the Atchafalaya River, discharge 15,400 m^3 sec^{-1} and carry approximately 240 billion kg of sediment annually (Mac et al., 1998). Sediment input drives the marsh development and decay cycles. But, land use changes and anthropogenic river alterations have decreased the sediment load and increased base flow since the 1800s (Tweel and Turner, 2012). Reduction in sediment from the Mississippi River has been implicated as causing major wetland land loss in southern Louisiana (Boesch et al., 1994; Mac et al., 1998; Tweel and Turner, 2012).

Depending on the stage of delta lobe development, the marshes along coastal Louisiana have varying geomorphic properties and dominant processes (Sasser, 1994). All the studied marshes for this thesis are in decay (Figure 1.1), which begin as the river diverted water and sediment into a most recent, Balize lobe that began to form 500 years ago. The marshes on the abandoned, decaying lobes now experience transport and reworking of existing material (Sasser, 1994). The study region includes Terrebonne Bay (Cocodrie sampling area) to the west on the Teche and Lafourche lobes, the barrier island Grand Isle on the Lafourche lobe, and Barataria Bay (Port Sulphur sampling region) to the east on St. Bernard and Plaquemines delta (Figure 1.1). The relative ages of each of these lobes are shown in Figure 1.2, with the oldest being Teche and the youngest being Plaquemines (Kolb and Van Lopik, 1958; Tornqvist et al., 1996). The Teche delta lobe formed as the Mississippi River re-routed to form the Atchafalaya River,

approximately 4,000 years ago (Mac et al., 1998). The lobe was abandoned and reworked during the development of the Lafourche lobe ~1,500 years ago that resulted in the formation of the barrier islands of Grand Isle (Tornqvist et al., 1996). Soon after the initiation of the Lafourche delta, the Plaquemines lobe began to form ~1,300 years ago (Tornqvist et al., 1996).

Marsh ground surface elevation is affected by opposing forces. Subsidence in the region is occurring at a rate of -10 to -15 mm yr^{-1}, which may be caused by tectonic activity or compaction of sediments over the past ~11,000 years (Shinkle and Dokka, 2004). In addition, sea level rise (SLR) globally averages +2.9 mm yr^{-1} (National Oceanic and Atmospheric Association, 2013). Within southern Louisiana, SLR averages +9.05 mm yr^{-1}, which is +0.025 mm day^{-1}, due to ground surface variation, prevailing winds, and differences in regional precipitation (Shinkle and Dokka, 2004; Center for Operational Oceanographic Products and Services, 2015). But, the rate of subsidence varies from -2.3 mm yr^{-1} to -12.29 mm yr^{-1}, which has caused lateral shifts in datum (Shinkle and Dokka, 2004). To maintain equilibrium with sedimentation rates and sea level rise, marshes in southern Louisiana need to accumulate sediment (and organic matter) at the same rate of SLR or greater (Glick et al., 2013).

Organic matter in marshes is mainly sourced from the dominant standing vegetation. Plant diversity is affected by flood inundation, flooding frequency, as well as the water body salinity (Penfound and Hathaway, 1938; Valiela et al., 2002). Marshes in low-lying areas are marine, while freshwater marshes receive water with salinities (practical salinity units) <0.5 and lie at generally higher elevations and are buffered from tidal influences being further from the ocean. Changes in elevation and salinity create plant zonation from lowland to upland marsh regions (Mac et al., 1998; Valiela et al., 2002). Tidal salt marshes, with salinity influences

ranging from marine (salinity 30-35) to brackish (salinity 0.5 to 17), have lower plant species

diversity and are dominated by only one to two species of cordgrass or rush grass, specifically

Spartina alterniflora or *Juncus roemerianus* (Rietl et al., 2016). Below the surface, each of these

plants will alter the soil in the area surrounding the roots, known as the below ground

rhizosphere, due to colonization by microorganisms and the addition of oxygen (Koretsky et al.,

2008). Previous research on marsh ecosystem dynamics and biological diversity in Louisiana

mostly focused on marsh geochemistry and control on vegetation, but there has been relatively

limited research done on marsh soil microbial communities, especially compared to other marsh

systems (Blum et al., 2004; Koretsky et al., 2005; Weston et al., 2006; Beazley et al., 2012; King

et al., 2015).

Overview of Water Sources and Environmental Influences

Precipitation

Precipitation in southern Louisiana is highest in June and lowest in October based on

monthly rainfall averages from the National Atmospheric Deposition Program (NADP) (Figure

1.3) (National Atmospheric Deposition Program, 2015). Regional precipitation ranges from pH

4.7 to 5.1 and contains varying concentrations of sulfate, nitrate, ammonium, sodium, chloride,

and calcium (Figure A.1) (National Atmospheric Deposition Program, 2015). August

precipitation has the highest concentrations of sulfate and nitrate, and the lowest concentrations

in chloride and sodium (Figure A.1). Changes in concentrations have been attributed to the

complex interplay among climate, ocean gas and particle exchange, and atmospheric chemical

transformations (Koster and Suarcz, 1995; Iavorivska et al., 2016). Precipitation on marshes
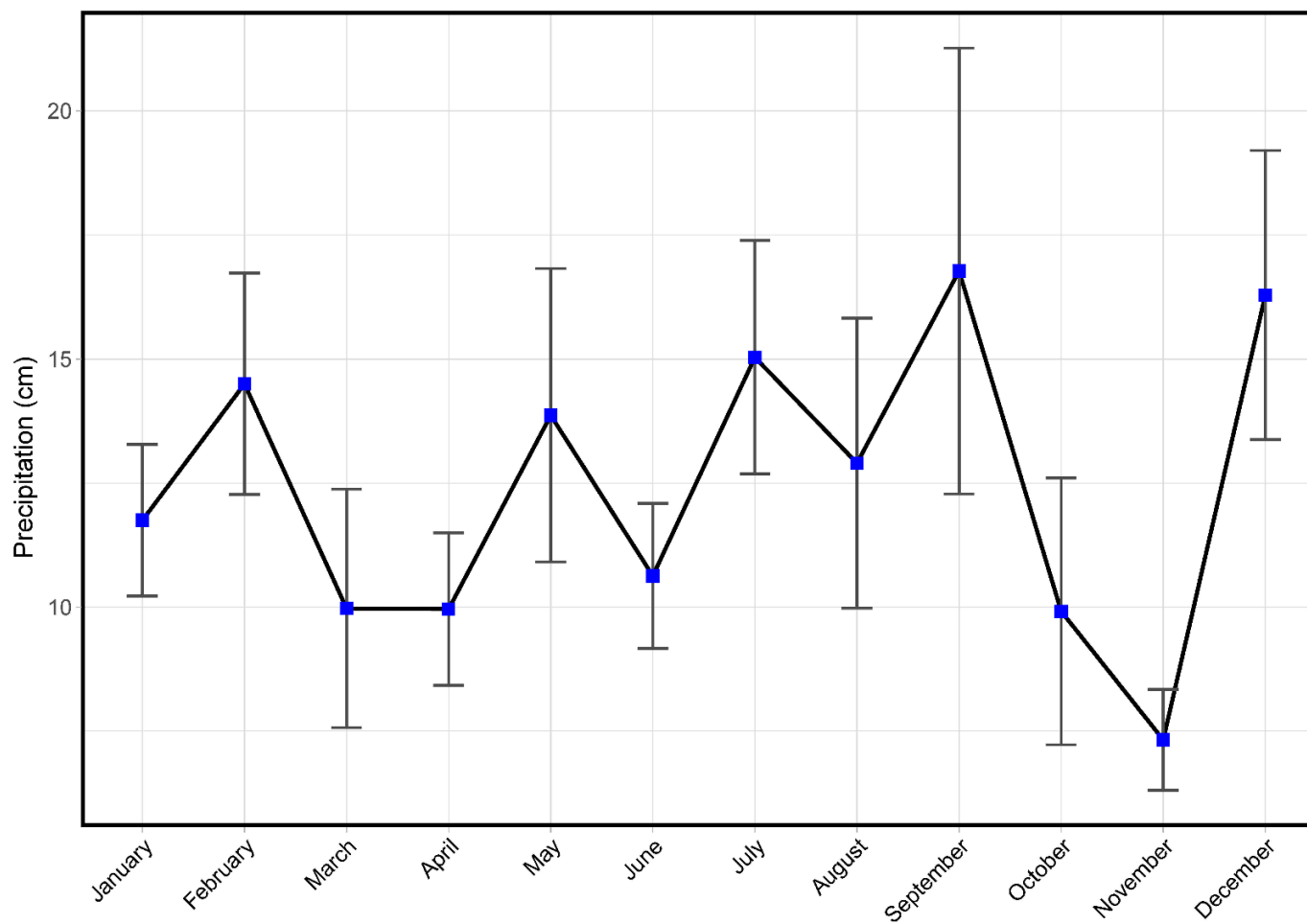
Figure 1.3: Average monthly precipitation (±1SE) from 2006-2015 from monthly precipitation data recorded by the National Atmospheric Deposition Program (NADP) at site LA30 located near Franklinton, LA. The data were accessed from the NADP data repository (National Atmospheric Deposition Program, 2015). The mean monthly precipitation (points), and standard error (error bars) were calculated.

have the potential to impact microbial communities, such as from solute introduction, but are likely minimal due to mixing and dilution with marine water (Valiela et al., 1978).

Mississippi River influences

Mississippi River inputs are primarily enriched in nutrients derived from overland flow and precipitation. This water will pick up dissolved and particulate matter from weathering bedrock and from anthropogenic inputs depending on land use. Land use changes in the Mississippi River basin have caused nitrate and phosphorus concentrations to increase and silicate concentrations to decrease (Turner and Rabalais, 1991; Tweel and Turner, 2012).

Flow data throughout the year for the Mississippi River are collected by the United States Geological Survey (USGS) at several locations in Louisiana. The Belle Chasse station is the closest to the study area (U.S. Geological Survey, 2016) (Figure 1.4). River diversions along the Mississippi River have been constructed by the Army Corps of Engineers, the USGS, and restoration agencies for flood control and to increase the potential for sediment introduction into the marshes (CPRA, 2017b). River diversions predominantly affect the sampling area near Port Sulphur, where riverine input has decreased salinity throughout the year, but mostly during the spring (Figure 1.4 & 3.7). In addition, river diversions have been projected to decrease salinity at Grand Isle from 16.07 in 2008 during median diversion flow average to 9.92 (standard deviation (SD) = 4.75) at a maximum proposed flow from the diversions (Roblin, 2008). The efficacy of river diversions as a method of restoring marshes in southern Louisiana is uncertain, and the effects on alterations to the microbial communities have only recently been studied (Boustany, 2010; Couvillion et al., 2013; Glick et al., 2013; Mason et al., 2016; Marks et al., 2016).
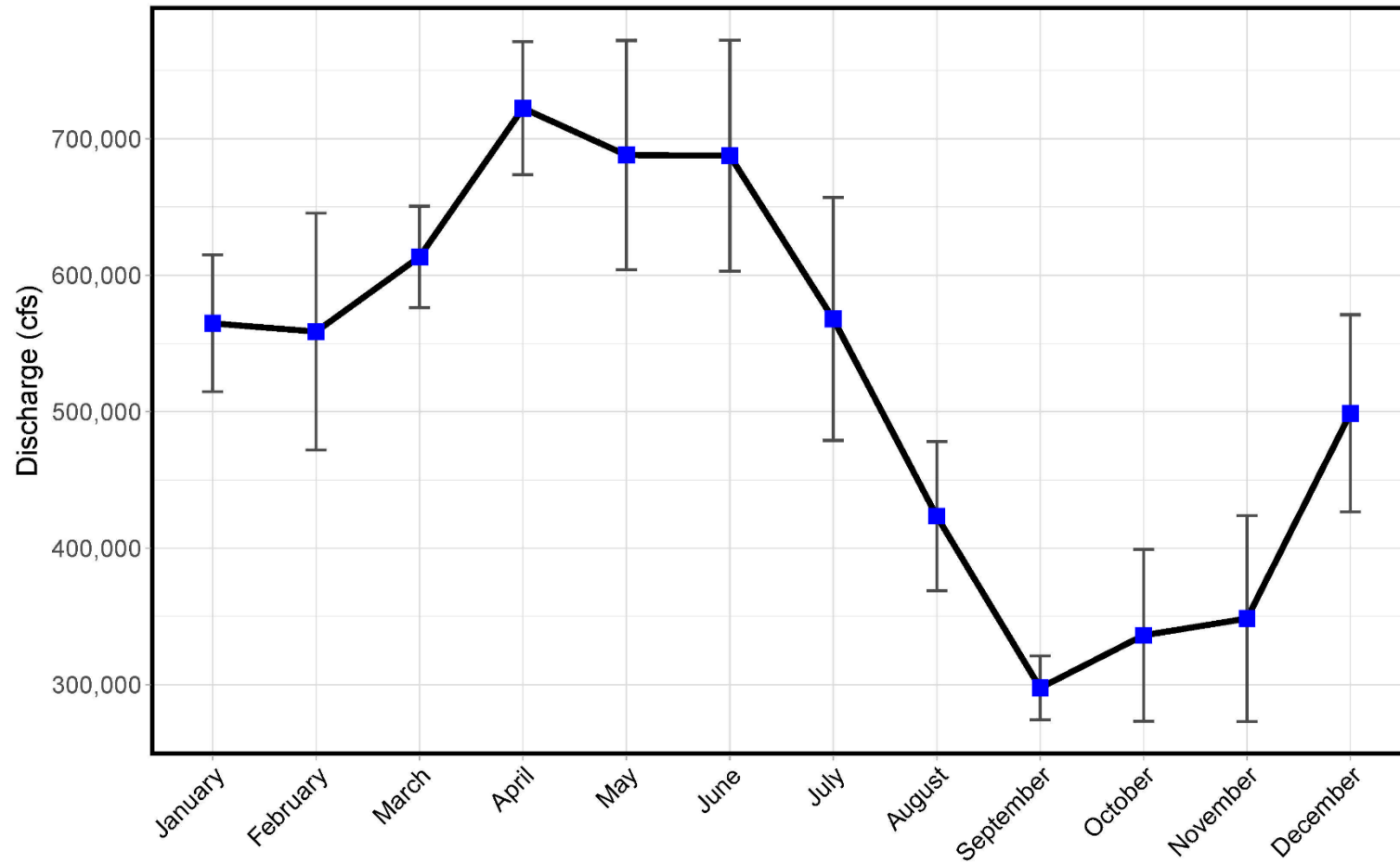
Figure 1.4: Average monthly discharge rate (±1SE) of the Mississippi River from 2008-2015 at Belle Chasse station (site #07374525). Monthly discharge data was obtained from the USGS data repository (U.S. Geological Survey, 2016) at the Belle Chasse station for the extent of data available. Monthly mean discharge values (points), and standard error (error bars) were calculated for each month.

Marine water influences

Ocean water is limited in nitrogen compounds and phosphorus but abundant in chloride, sulfide, sulfate, magnesium, and potassium (Lyman and Fleming, 1940). Eutrophication, oil spills, and bacterial or diatom bloom events can alter the seawater composition locally (Cerco and Cole, 1993; Falkowski et al., 1998; Yang et al., 2014; Joye et al., 2014). However, due to global circulation patterns, concentrations of these ions do not vary widely in the ocean, and remain at the N:P:K "Redfield" ratio (Redfield, 1942).

Depending on the time of year, the tidal variations control the flow of water into the marshes (Pethick, 1981). Water flux occur on daily to annual time scales based on data from tide predictions calculated by the National Oceanic and Atmospheric Administration (NOAA), NOAA Station #8762928 (Figure 1.5). NOAA tide predictions are calculated from tidal datums of extreme high and low tides occurring as the sun and moon move water masses due their gravitational pull, which are corrected by current and historical observations (CO-OPS and NOAA, 2016). Daily variation in the tidal range can be significantly different from year to year; however, the annual trends remain consistent (Figure 1.5). Tides in southern Louisiana are highest in October through November and lowest during January and February.

The Coastwide Reference Monitoring System (CRMS) was established under the Coastal Wetlands Planning, Protection and Restoration Act (CWPPRA) as a network of up to 391 stations that record marsh conditions and effectiveness of marsh restoration in the area (CWPPRA Task Force, 2015). The network of tidal stations record water level and water quality, as well as monitor local and reginal marsh vegetation changes and land surface elevations along the coast (CWPPRA Task Force, 2015). Average annual water level in the sampling areas of
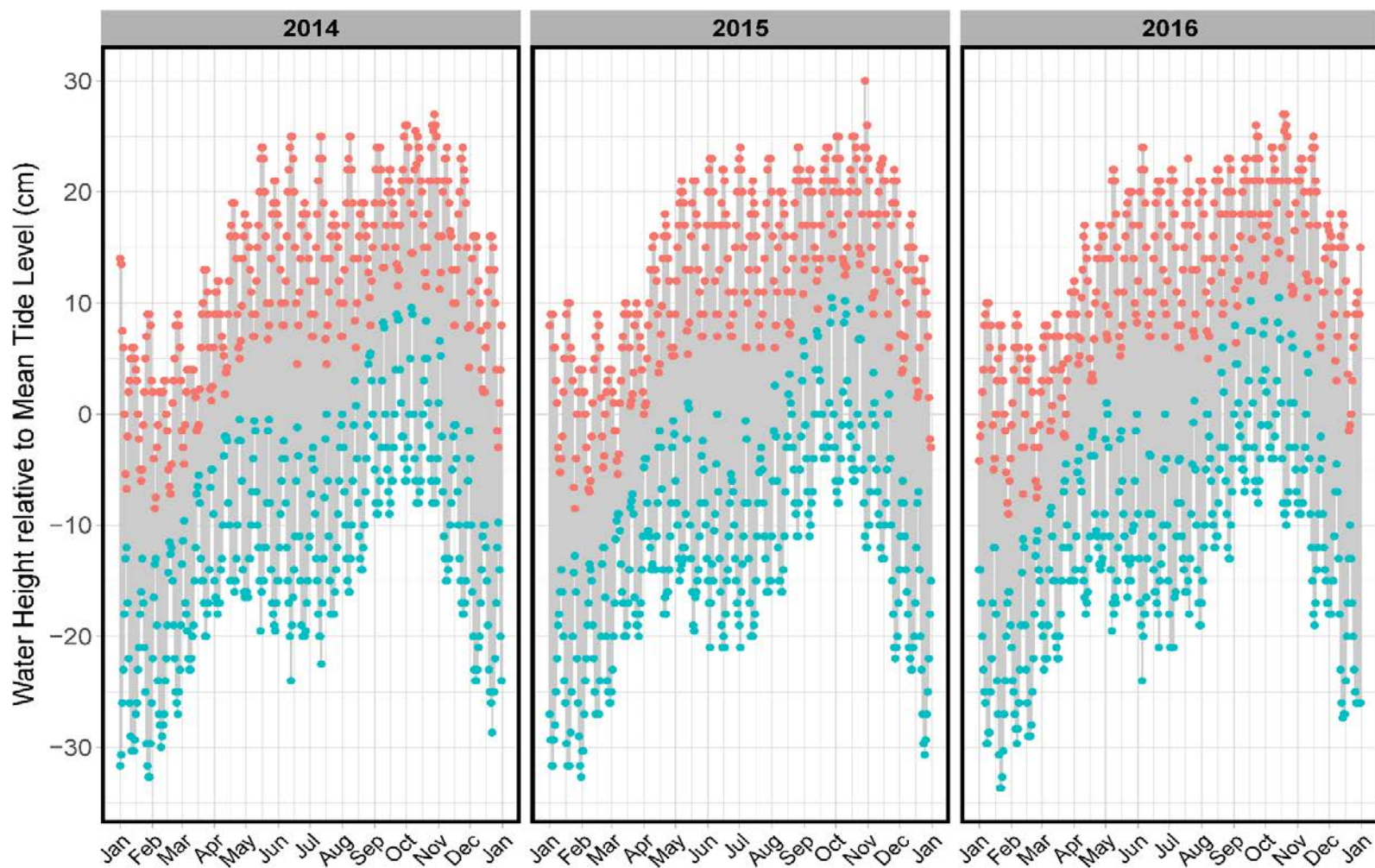
Figure 1.5: Tide predictions from the Cocodrie, LA, NOAA station (#8762928) from 2014-2016 with red points indicating daily high tide and blue points indicating daily low tide with shading in between these values. All water height values are referenced to the station mean tide level of 1.14 m above the standard datum (CO-OPS and NOAA, 2016).

Port Sulphur, Grand Isle, and Terrebonne Bay closely follow tidal predictions (Figure 1.6), with average daily water heights measured at CRMS stations from 2006 to 2016 peaking during October and being lowest in January through March (Figure 1.6).

Salinity influences on vegetation

Within the marshes of southern Louisiana, the water quality of one region is expected to vary from another region based on marsh elevation (DeLaune and Pezeshki, 1994), marsh accretion and erosion rates (Chmura et al., 2003), tide stage (Chambers et al., 2013), dominant vegetation (Visser et al., 2013; Koretsky et al., 2008), salinity (Jackson and Vallaire, 2009; Morrissey et al., 2014), among other factors. However, when water from precipitation, riverine, and marine sources interact within the marshes, salinity is considered to be one of the main controls associated with plant zonation patterns (Pennings et al., 2005). This is because salinity can change due to tides, meteorological activities and events (i.e., from changes in wind patterns due to storm fronts or from hurricanes), and river diversions, which affect flooding frequency and inundation depth (DeLaune and Pezeshki, 1994; Chambers et al., 2013; Glick et al., 2013).

The effect of salinity on plant zonation is seasonal due to river or tidal flooding (Morris, 2000), with more halotolerant plant species occupying upland marshes and more flood tolerant species colonizing marshes inundated by marine waters. As such, zonation results in variable biomass production, degradation rates, carbon fixation pathways (C_3 vs C_4), and symbiotic microbial relationships within the rhizosphere (Blum et al., 2004). Specifically for freshwater marshes, salinity increases reduce soil organic content, increases sulfate reduction rates and total nitrogen storage, and potentially alters microbial communities (Jackson and Vallaire, 2009; Ikenaga et al., 2010; Chambers et al., 2013).

14
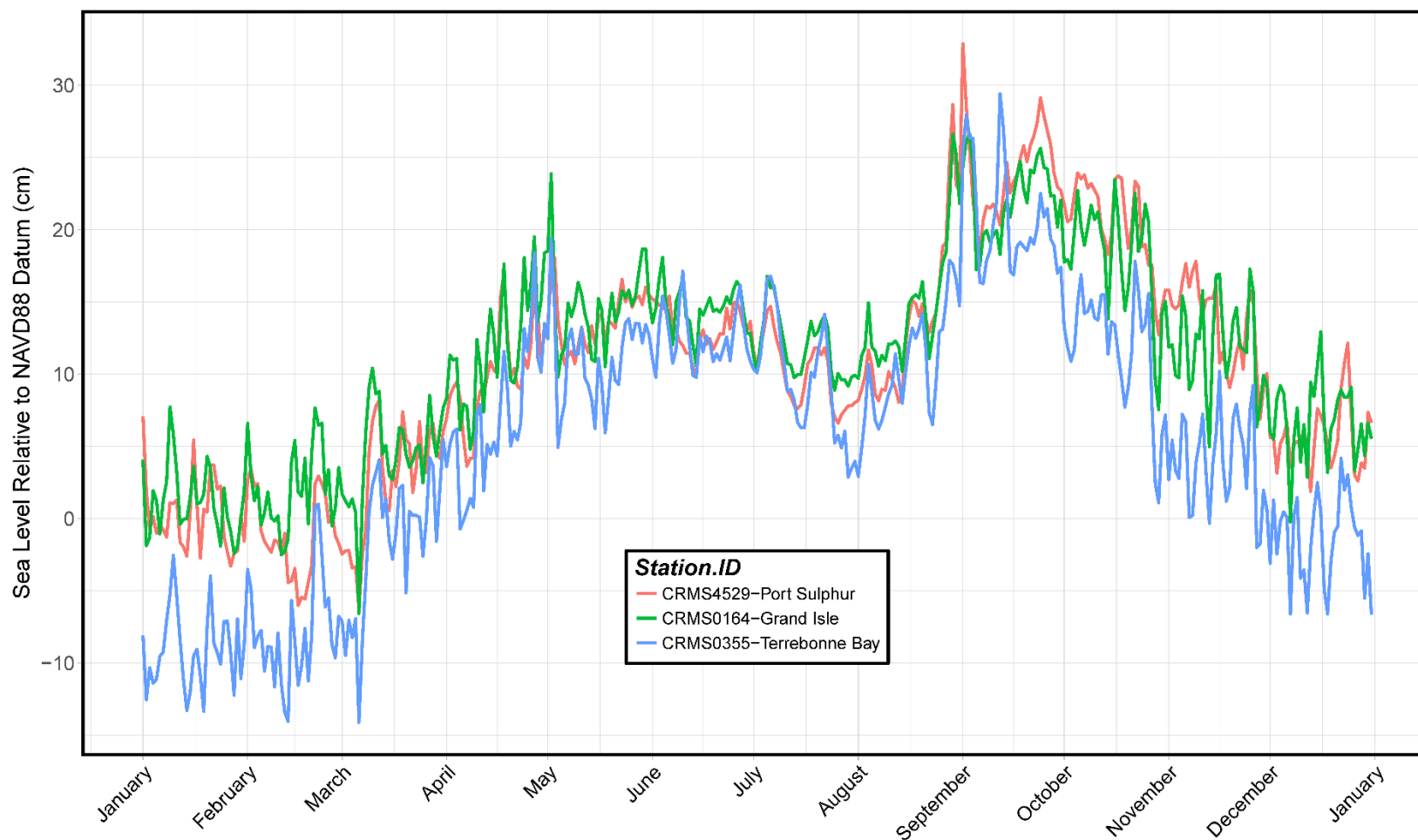
Figure 1.6: Time series of average daily sea-level (in cm) in the three sampling regions from 2006 to 2016, colored by regional gauging station. Hourly water level data, relative to the NAD88 datum, were accessed from the CIMS data repository (CPRA, 2017a) for each of the three regional CRMS stations. The hourly water level values prior to October 2013 were corrected to the current Geoid 99 and mean water level for each day at each station was calculated for each day and plotted for a single calendar year.

15

In contrast, during the summer months when flooding is less frequent, the maximum available incoming solar radiation is converted to biomass, and upland marshes, which are also predominately freshwater systems, accumulate reduced nutrients (Cronk and Fennessy, 2016).

Primary production in salt marshes varies widely, estimated at an average of 1873 g m^{-2} yr^{-1} (Kaswadji et al., 1990), and is a combination of production from standing vegetation and microphytobenthos. For some marshes, up to 75% of organic matter in salt marsh sediments can originate from phytoplankton (Gebrehiwet et al., 2008). Estimates of production for *S. alterniflora* are upwards of 7000 g m^{-2} yr^{-1} for dry above- and below-ground biomass. Although predominately composed of lignocellulose, a highly refractory polymeric complex that is not easily broken down by animals (Benner et al., 1984), plant biomass can be completely decomposed in as little as seven months (White et al., 1978; Schubauer and Hopkinson, 1984) due to bacterial and fungal mineralization (Benner et al., 1986; Buchan et al., 2003). The bacterial dominance of lignocellulose breakdown in salt marshes is unique, as the same process on land is controlled primarily by fungal processes (Benner et al., 1986).

Current Understanding of Bacterial Communities in Salt Marshes

Soils in salt marshes are typically characterized by strong reduction potential and are generally anoxic at ~1-2 cm below the surface (King, 1988; Kostka et al., 2008), being dominated by the reduction of sulfate and nitrate linked to decomposing organic matter by microbial activity (White et al., 1978; Valiela and Teal, 1979; King, 1988; Kostka et al., 2008). The transition from aerobic to anaerobic conditions is important to controlling rates of organic matter and other transformations, although bioturbation has the potential to mix biogeochemical gradients (Kostka et al., 2008). Nevertheless, microbial communities are critical in regulating

marsh biogeochemistry (Hartman et al., 2008) and are responsible for much of the nitrogen fixation, pH buffering, and oxidation of reduced compounds, in addition to organic matter decomposition (Lamers et al., 2012; Rietl et al., 2016).

Although there have been many long-term studies focused on salt marsh geochemistry and studies of singular bacterial function (e.g., ammonium oxidation, sulfate reduction), the microbial composition within Louisiana marsh sediments and soils is not well defined and few studies have obtained a complete understanding of microbial diversity changes through time (Blum et al., 2004; Koretsky et al., 2005; Hartman et al., 2008; Gebrehiwet et al., 2008; Kostka et al., 2008; Bowen et al., 2009; Jackson and Vallaire, 2009; Ikenaga et al., 2010; Bowen et al., 2011, 2012; Campbell and Kirchman, 2012; Graves et al., 2016). Since the Deepwater Horizon in 2010, research focused on salt marsh microbial diversity in southern Louisiana has shifted from basic biogeochemical studies to investigations that attempt to quantify microbial diversity changes and the impacts of the oil spill on microbes (Beazley et al., 2012; Mendelssohn et al., 2012; Mahmoudi et al., 2013; Joye et al., 2014; King et al., 2015). Specifically, studies highlight the potential for persistence, resilience, and functional redundancy of the microbial communities, particularly those impacted by natural stressors like hurricanes or from the spill. Diverse microbes, based on 16S rRNA gene sequencing, were found that could potentially utilize different electron acceptors to enhance the degradation of crude oil (Amaral-Zettler et al., 2008; King et al., 2015) . Because phylogenetic information does not yield functional information and can provide inconsistent results about functional changes (Graves et al., 2016), metagenomics approaches seek to identify microbial functional responses (Bowen et al., 2013; Rodriguez-R. et al., 2015). However, correlation of bacterial diversity over large spatial scales using 16S rRNA

17

gene sequencing can provide more statistically significant results than functional gene markers (Angermeyer et al., 2016).

Considering these recent results and emphasis on understanding broad scale patterns of bacterial diversity, this thesis research goal was to uncover bacterial diversity in salt marsh soils and determine which sets of environmental parameters, including water inundation frequency and depth, vegetation, and salinity, contributed to the most variance in the taxonomic diversity of marsh soil microbiomes through time. Theoretically, each sampling event collected soils from the dynamic system that was changing through time and space. The marsh soil was considered to represent a snapshot in time that was also part of a sequence of depositional and erosion events. With every centimeter into the soil, the microbial communities and sediment properties would become separated temporally, and so the research had to consider that successional patterns would be apparent. This research did not attempt to assign function to bacterial data collected from 16S rRNA genes, and geochemical and environmental controls were statistically analyzed. The bulk of the effort focused on collecting a wide array of data, including information about SLR and subsidence rates for the marshes. The connection between SLR and subsidence to marsh microbial communities in southern Louisiana has not been studied previously, but similar research has been done elsewhere (Larsen et al., 2010; Simon, 2013; Dini-Andreote et al., 2014).

CHAPTER TWO - MATERIALS AND METHODS

Field Sampling

Prior to the current project, thirty marshes across the region were monitored to assess the impacts of the 2010 Deepwater Horizon oil spill with National Science Foundation funding (Turner et al., 2014). In 2012, the Coastal Waters Consortium (CWC) was funded by the Gulf of Mexico Research Initiative (GOMRI) and the CWC established 12 core sampling locations, and the CWC installed boardwalks (Hooper-Bui et al., 2014). After 2014, the CWC was refunded by GOMRI as CWC-II until 2017. For this project, salt marshes were sampled twice a year from 2012 until 2014. Four marshes were selected near Cocodrie in western Terrebonne Bay (TB), which was the westernmost sampling area. Five marshes were used near Grand Isle (GI) on the western edge of Barataria Bay. A total of eight different sites were used near Port Sulphur (PS) on the easternmost sampling area in Barataria Bay and closest to the Mississippi River (Figure 2.1). The higher number sites for PS was because the original CWC sites in 2012 had landowner permission revoked and new sites had to be chosen (and landowner permission granted) in 2013. At each of the marshes, soil samples were collected using push-cores at 5 m inland from the marsh vegetation edge directly off of boardwalk. Push-cores were 10 cm in diameter and sectioned into sterile Whirlpak bags in the field at four 1 cm depths; 0-1cm (A), 1-2cm (B), 4-5cm (C), and 9-10 cm (D). Soil cores were collected in duplicate to have sufficient material for molecular and geochemical analyses. A homogenized soil sample from up to two cm deep in the marsh soil surface was also collected (MS) in 50-ml tubes. Soil samples were placed on ice and transferred to -20 °C within 48 hours. For some select locations, MS samples were collected in
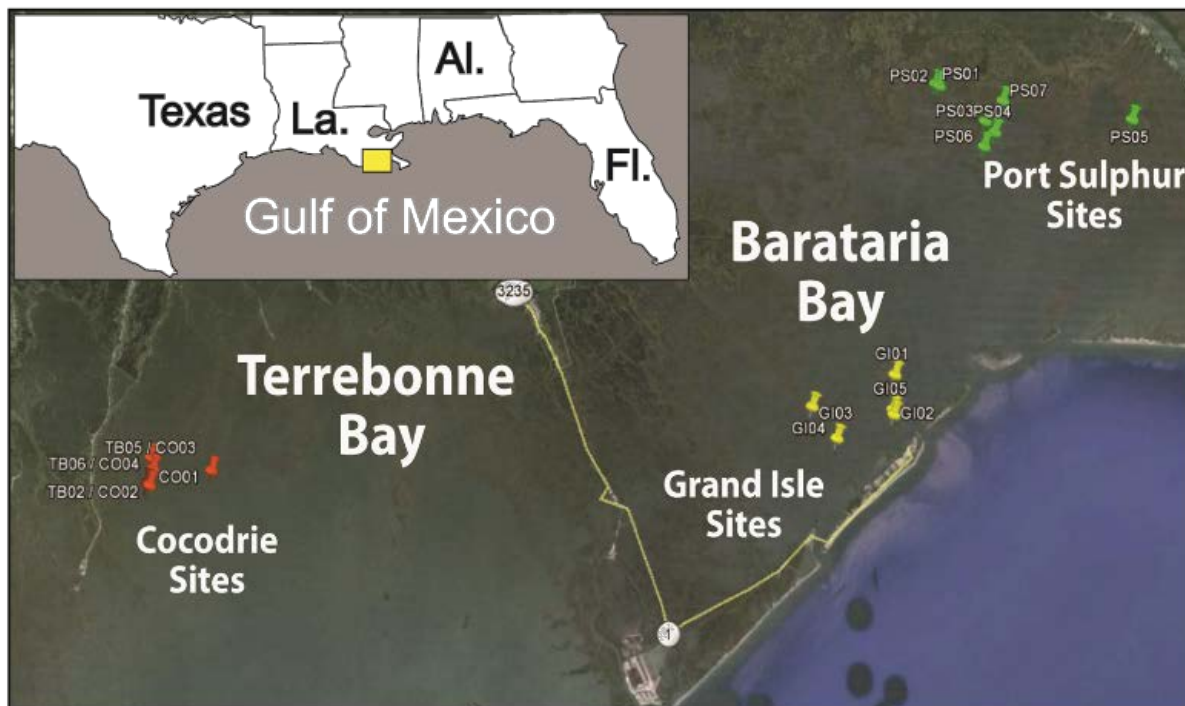
Figure 2.1: Map of the sampling sites where sediment cores were collected twice a year from 2012 to 2014. See Table 2.1 for details for each sample site.

2011, and extreme weather and landowner issues caused some samples to go uncollected periodically (Table 2.1).

Physical measurements at each of the marshes included the height of water over the marshes (if water was present), and inland soil pH, temperature, and salinity (see pages 21-22). Generalized sketches of the submerged and un-vegetated marsh bottom were constructed. From the open water at ~3m offshore, pH and temperature were measured with a 3-point calibrated Accumet Thermo (Fisher) meter, and salinity, dissolved oxygen, and temperature were measured at the surface and bottom of the water column using with a YSI meter. A raw water sample was collected from ~0.25 m below the open water surface for major anion and cation geochemical analysis and for DNA extractions. Water samples were frozen at -20°C within 24–48 hours of collection.

Table 2.1:   Samples were collected twice a year from 2012-2014. Each cell contains the letter(s) corresponding to the sample depth. MS-Marsh surface (0-2cm grab sample), A (0-1 cm) core section, B (1-2 cm) core section, C (4-5cm) core section, D (9-10cm) core section. Colors indicate the type of samples collected; Red-Marsh Surface only, Yellow-Core samples only, Blue-Marsh Surface and core.

Site	Jun-12	Oct-12	May-13	Oct-13	May-14	Oct-14
GI-01	MS	MS		A-D, MS		A-D, MS
GI-02	MS	MS		A-D, MS		A-D, MS
GI-03		MS	A-D, MS	A-D	A-D, MS	A-D, MS
GI-04		MS	A-D, MS	A, C, D	A-D, MS	A-D, MS
GI-05	MS	MS		A-D	A-D, MS	A-D, MS
PS-01	MS					
PS-02	MS					
PS-03	A-D, MS					
PS-03A				A-D, MS		A-D, MS
PS-04	A-D, MS					
PS-05			A-D, MS	A-D	MS	A-D, MS
PS-06			A-D, MS	A-D	A-D, MS	A-D, MS
PS-07				A-D, MS	A-D, MS	A-D, MS
TB-04/CO-01	MS					
TB-02/CO-02	MS		A-D, MS		A-D, MS	A-D, MS
TB-05/CO-03			A-D, MS	A-D	A-D, MS	A-D, MS
TB-06/CO-04			A-D, MS	A-D	A-D, MS	A-D, MS
TB-01/CO-05			A-D, MS	A-D	A-D, MS	A-D, MS

Data for individual field measurements are archived in the Gulf of Mexico Research

Initiative Information and Data Cooperative (GRIIDC) database:

http://dx.doi.org/10.7266/N7XW4GQG, http://dx.doi.org/10.7266/N7RB72JB,

http://dx.doi.org/10.7266/N70V89RN, http://dx.doi.org/10.7266/N7W37T8P,

http://dx.doi.org/10.7266/N7S46PVP, http://dx.doi.org/10.7266/N74M92GC,

http://dx.doi.org/10.7266/N7Q23X55.

Additional sample collection

Other research groups within the CWC concurrently collected samples and took

additional measurements from the marshes as soil collection. Additional parameters from 1 m

inland and 10 m inland from the marsh edge included porewater dissolved hydrogen sulfide

measured using Chemetrics colorimetric chemistries (Calverton, VA), vegetation coverage from

stem counts, average plant height, and the number of unique observed plant species in the

sampling area (Turner and Swenson, 2016). Samples of marsh soil were also collected at 1 m

and 10 m inland for hydrocarbon analysis, including normal (*n*)-alkanes and polycyclic aromatic

hydrocarbon compounds and alkylated homologs. Hydrocarbon characterization was done using

previously described methods (Turner et al., 2014).

Laboratory Analysis

Aliquots of homogenized soil from each depth were separated from thawed samples in

the lab for measurements of gravimetric water content (% H_2O), total organic carbon (TOC), pH,

and total nucleic acids extractions.

Soil analyses

The % H_2O and TOC concentrations of the 2012-2014 soils were measured using the thermogravimetric loss-on-ignition method modified from Veres (2002). Triplicate 3 g aliquots were weighed and placed in pre-weighed tins. Samples were dried for 12 h at 105°C to determine the % H_2O by weighing cooled dry samples and calculating the percentage of water (Equation 1):

$$Water\ content = 100 * \frac{(mass\ of\ soil+tin)-(mass\ of\ dry\ soil+tin)}{mass\ of\ dry\ soil}$$ *Equation 1*

The dried soils were heated to 550°C for 6 h, then placed into a desiccator to cool before weighing at room temperature to calculate TOC, following the methods outlined by Schulte and Hopkins (1996) (Equation 2):

$$TOC = 100 * \frac{(mass\ of\ dry\ soil+tin)-(mass\ of\ soil\ after\ combustion+tin)}{mass\ of\ dry\ soil}$$ *Equation 2*

The contribution of carbonate to TOC was determined to be insignificant after several analyses (<0.1% TOC). Therefore, the LOI values were as TOC.

Soil pH was determined from each sample according to the method outlined by Thomas (1996). Duplicate 2 g aliquots from each core section (A-D depths) and marsh surface (MS) sample were added to 10 mL of 0.01M $CaCl_2$ solution and mixed at 100 rpm for one hour. Aliquots were centrifuged at 4°C for 10 min and the supernatant was pushed through an 11μm filter to remove particulate organic matter. The measurements of the filtered supernatant were done using a calibrated Accumet Thermo (Fisher) glass electrode and pH meter. The readings from two measurements were averaged for each sample.

Water analyses

Frozen water was thawed, sonicated in the collection bottles for 10 minutes, and filtered into HDPE bottles through a 0.22 μm Sterivex PES filter to obtain filtered water that would be analyzed for major anion and cation concentrations on a Dionex (Thermo Fisher) dual column ion chromatograph (IC) reagent free system. Cation samples were preserved with nitric acid, and no preservation was used for anions prior to IC measurements done with six cation and seven anion standards. Ion data are archived in the GRIIDC database: https://data.gulfresearchinitiative.org/data/R1.x139.143:0056.

Microbial diversity analyses

For the 2012–2014 soil samples, total nucleic acids were extracted using the sucrose lysis method, which was modified from Guerry et al. (1973), Somerville et al. (1989), Zhou et al. (1996), and Mitchell and Takacs-Vesbach (2008). Methods were consistent with previous research done from marsh sediments before and after the Deepwater Horizon oil spill (Liu, 2011). Briefly, each of the soil core depths were thawed at room temperature. Triplicate extractions were done for each soil sample, whereby 0.5–2.0 g of thawed soil were mixed with sucrose lysis buffer and centrifuged at maximum speed in 15 mL conical centrifuge tubes for 3 to 5 min prior to incubation at 37°C for 60-90 min. After the first incubation, a mixture of proteinase K/CTAB/SDS was added to each extraction prior to incubation at 55°C for 12-16 hours at 100 rpm on a rocking platform. Following the last incubation, slurries were centrifuged at 10,000 x g to separate solids from the supernatant. In triplicate volumes, 1 mL of supernatant was mixed with 10M ammonium acetate prior to centrifugation at 10,000 x g for 10 min. The three separate volumes were mixed with 100% isopropanol to precipitate the nucleic acids at -

20°C, prior to centrifugation at 10,000 x g for 10 minutes. Pellets were washed twice using molecular grade ethanol. After drying, nucleic acid pellets were re-suspended in TE buffer.

For each core section, the triplicate extractions that were each used for three precipitation volumes that were pooled and homogenized. The 260/280 nm and 230/280 nm adsorption values were quantified by using a Nanodrop spectrophotometer (ThermoFisher Nanodrop ND1000), and DNA extractions were also visualized by using electrophoresis with ethidium bromide stained TBE gels. The homogenized extractions were sent for 454 tag pyrosequencing of the V1-V3 region of 16S rRNA genes using Titanium series Roche 454 at the Molecular Research (MRDNA) laboratory in Shallowater, Texas (Dowd et al., 2008). The Texas facility cleaned, tagged, and amplified the 16S rRNA gene amplicons prior to sequencing. The raw amplicons were compiled by sample and reported back to the lab with quality scores.

Use of Coastal Wetland Monitoring Datasets

To assess the frequency and duration of flooding over the marshes in southern Louisiana, data from the NOAA (https://tidesandcurrents.noaa.gov/tide_predictions) and CRMS (https://www.lacoast.gov/crms2) websites and were acquired. Data are stored in the Coastal Protection and Restoration Authority's Coastal Information Management System (CIMS), as per the data plan outlined in the Master Plan (CPRA, 2017b). CRMS data are available publicly from the Coastwide Information Management System (CIMS) data repository (http://cims.coastal.la.gov/).

NOAA tidal predictions

NOAA creates predictions of the currents based on harmonic constants and tidal datums from the position of the earth and moon. Calculations at each station include the high and low tidal heights and times for each NOAA station (CO-OPS and NOAA, 2016). Tidal stations were separately selected for the regions of Port Sulphur (8761819), Grand Isle (8761724), and Terrebonne Bay (8762928). Hourly tide predictions were downloaded for each station from 2014-2016, aggregated, and Similarity Percentage (SIMPER) analysis was run on different groupings of the predicted water height using the packages vegan, dplyr, and reshape2 in R (Oksanen et al., 2007; Wickham, 2012; Wickham and Francois, 2015). SIMPER analysis based on Bray-Curtis dissimilarity matrices were used to determine the similarity of daily high and low tides between regions during the months of sampling.

CRMS marsh accretion rates and station data

The CRMS data having the longest coverage, proximity to the sampling sites, and rate of marsh accretion from three stations closest to each marsh sampling location for each region were acquired. Marsh accretion data were used to indicate if marshes are accreting or subsiding and to evaluate the regional variability of marsh elevation, water height, subsidence, and productivity.

Briefly, marsh accretion is determined by CRMS network staff by collecting soil cores and measuring the thickness of marsh sediment and organic matter from an insoluble powder of feldspar applied surrounding a survey pin at each location during installation (Folse et al., 2014). CRMS cores are collected at 6-12 month intervals. Accretion rates for each candidate CRMS station used in this study were plotted in Figure 2.2. Accretion results were not spatially referenced to a datum, and could not be used in correlation with another dataset. Therefore,

selecting a CRMS marsh with the median value of marsh accretion for an area was assumed to

provide more accurate measurements than the highest or lowest accretion rates from any single

site. CRMS stations with median rates of marsh accretion were selected from Port Sulphur and

Terrebonne Bay, but because the marshes at Grand Isle were accreting at roughly the same rate,

the station with the longest sampling duration (until October 2016) and largest coverage was

selected. The CRMS stations that were selected to represent each region were Port Sulphur –

CRMS-4529, Grand Isle – CRMS-0164, and Cocodrie – CRMS-0355.
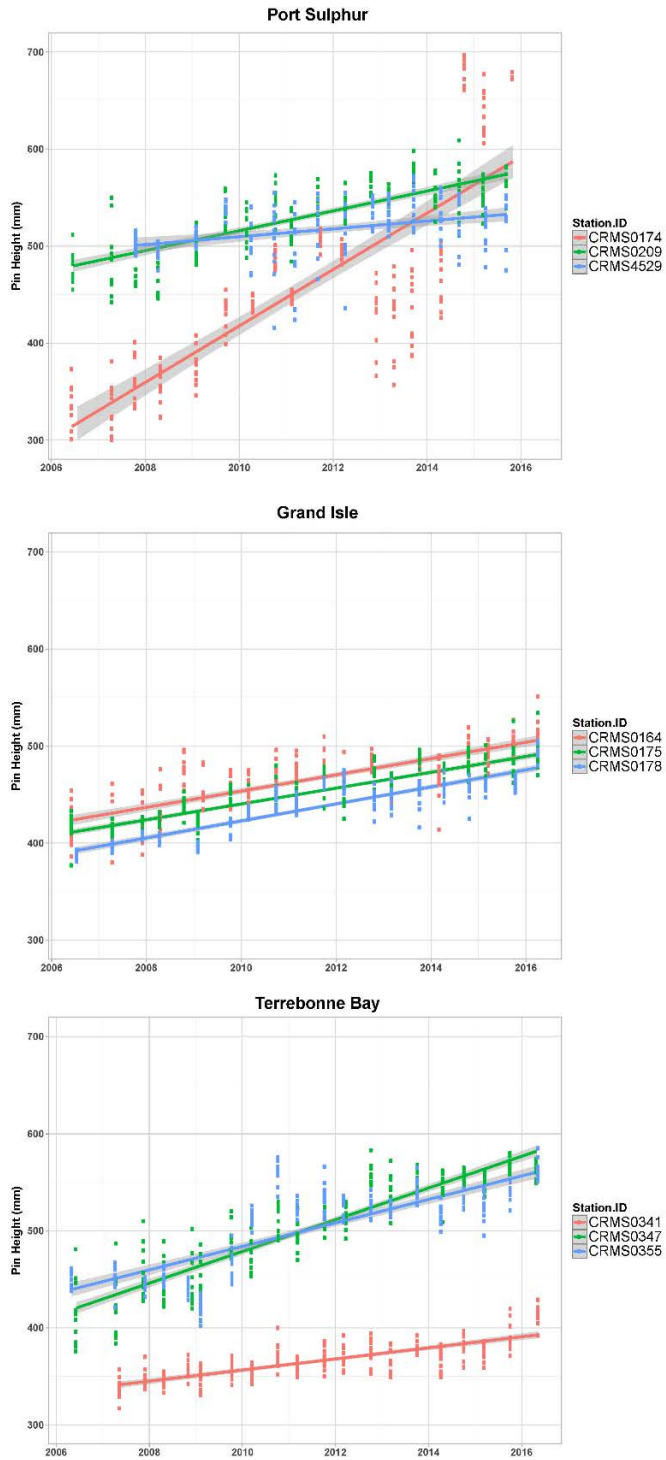
Figure 2.2: Marsh accretion for three stations from each region. A linear regression line was plotted with a 95% confidence interval in gray. Pin height was reported in mm from each of the nine directions around the pin above the NAVD88 datum.

Data coverage assessed as a percentage of the data collected from the start of each station's recorded measurements were 94.5% for Port Sulphur, 97.5% at Grand Isle, and 98.3% at Cocodrie. The length of time sampled among the CRMS sites in Port Sulphur, with data only extending back to July 2007 (one year prior to the other two regional datasets). During the sampling period of 2007 to 2015, the coverage was 94.5%, but data coverage was 99.9% from 2012 to 2014, the duration of this study.

The CRMS network records hourly water levels at each gauging station, as well as surface water salinity and temperature (CPRA, 2017a). The gauge height accuracy at each station is assessed twice a year based on surveys conducted in the field by CRMS staff. Each station records the "*Raw Water Level,*" which is corrected for biofouling, instrument drift, and/or instrument malfunction and reported as "*Adjusted Water Level*" (Folse et al., 2014). As such, these measurements are not comparable through time or across different gauging stations, and the water level measurements had to be referenced to a datum. At each station, the reported water level is converted to the North American Vertical Datum 1988 (NAVD88). During this study, datum conversions had two different geoid models through time, Geoid12A was used prior to October 1, 2013, and GEOID99 was used from October 2013 to the present. A correction factor is available for each station to correct from GEOID99 to GEOID12A on the CRMS website, referred to as "*Shifted Water Elevation.*" For each station selected, the correction factor from GEOID99 to GEOID12A was -0.73 ft (Grand Isle Station #164), -0.9 ft (Terrebonne Bay station # 0355), and -0.86 ft (Port Sulphur station # 4529). For this thesis, after the correction for each station was applied, the average daily water heights were plotted through time; refer to Figure 1.6.

Marsh elevation determination

At each representative CRMS station, CRMS research staff measure the elevation of the marsh surface roughly twice a year from nine cardinal directions around a collared survey pin near each station (Folse et al., 2014). The distance from each measurement point around the collar of the pin to the marsh surface is subtracted from the survey results of the collar to ensure that the average measurement of elevation from the location captured the variability in topography at each location, as well as between survey events (Figure 2.3) (Folse et al., 2014). Marsh elevation differs from accretion because elevation is referenced to a datum and can provide comparable results between datasets and through time.

For this thesis, marsh elevation was assumed to change at a rate of change equal to marsh accretion adjusted to the mean elevation of on-site water height over the marsh in each region. The marsh elevation of each region was evaluated based on two calculations: 1) From a nearby marsh elevation calculated by CWPPRA (Folse et al., 2014); 2) a linear regression model of elevation change through time using the CRMS surveyed marsh elevation from a nearby marsh adjusted to sampled marsh elevation based on regional CWC field observations. CRMS reported water marsh height over the marsh and CWC staff observed data were assessed using a paired t-test to determine if the groups were significantly different. If the test yields that the two groups are significantly different, a calculated marsh elevation will be used for the marsh elevation at CWC sites.

The first method of evaluating marsh elevation is calculated by CWPPRA at each of their monitoring stations obtained using on site measurements (Equation 3).
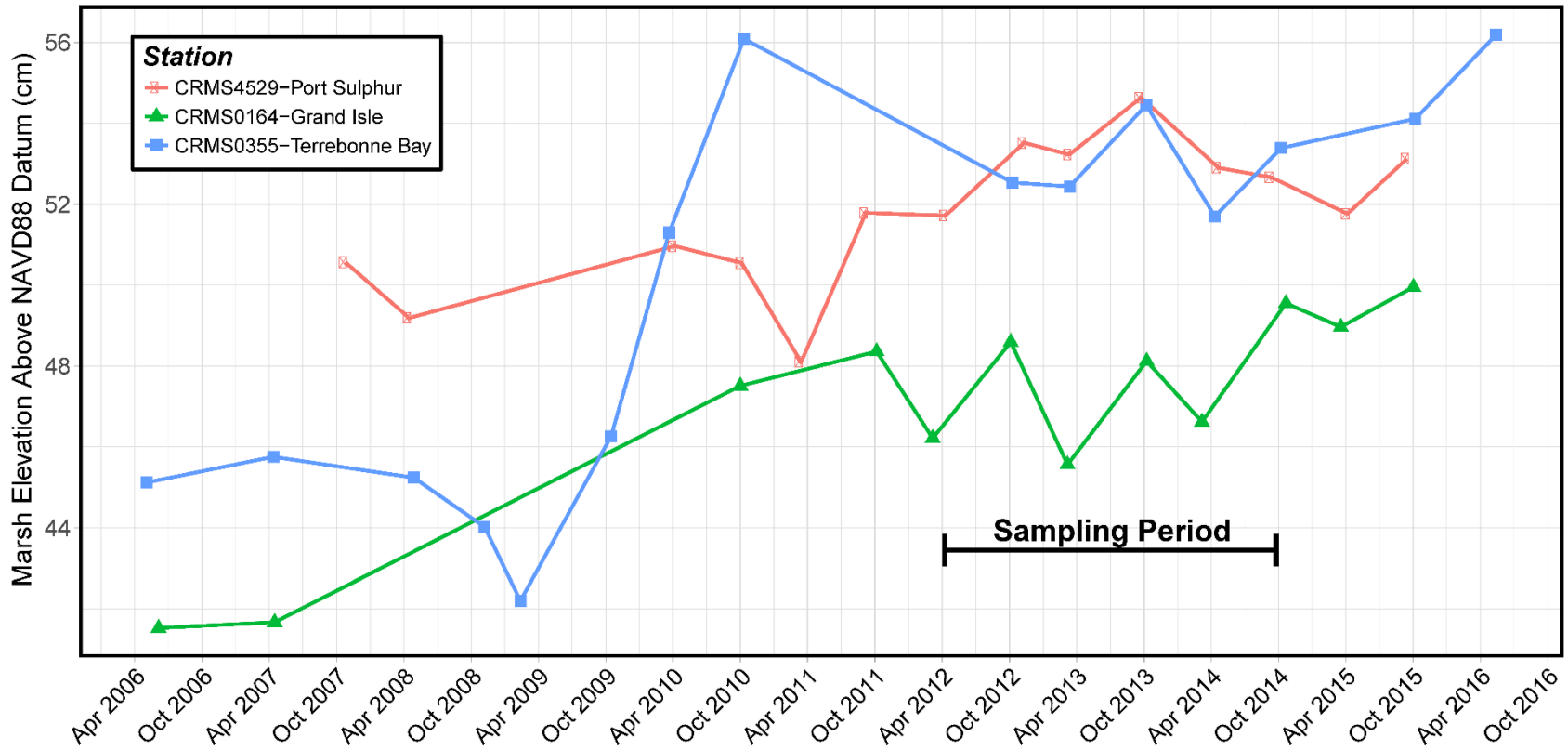
Figure 2.3: Time series data from marsh surface elevation, 2006–2016. Average marsh surface elevations from each survey period from CRMS stations are representative of each sampled region in the thesis. Each point is the average value of measurements around a pin above the datum. The values are not the actual marsh elevation but distance above the datum collected at 6 month to 12 month intervals by CRMS staff.

The mark elevation is collected during survey events by CRMS staff approximately two times a year and elevation is adjusted roughly annually to once every two years (Folse et al., 2014):

$$Marsh\ Elevation\ (NAVD88, ft) = Mark\ Elevation\ (NAVD88, ft) - Mark\ to\ Marsh\ Surface\ (ft)$$

Equation 3

Water elevation from the associated CRMS station is subtracted from the marsh elevation to obtain the reported in the CRMS data as "*Adjusted Water Elevation to Marsh (ft),*" in which positive values represent water over the marsh surface and negative values represent water levels below the marsh surface. These values for water elevation over the marsh were compared to the observed height of water over the marsh during field sampling for this study using a paired t-test.

The second method of determining marsh elevation was done by analyzing the change in marsh surface elevation through time from the representative regional CRMS station elevation data. Unlike the CRMS calculated marsh elevations that provide a static elevation, the marsh surface elevation was calculated as the linear regression, changing with time. The regional rate of marsh elevation change was calculated as the slope of the best fit linear regression from 2006/2007 – 2016 of the corrected pin height measurements. The slope of the line was assumed to represent the average regional elevation change. However, the first coefficient or y-intercept was not based on marshes sampled by the CWC. The elevation of CWC sampled marshes has not been determined. So, for this thesis, marsh elevation was calculated as the difference in means between CRMS water elevation at the hour of sampling and the CRMS recorded water height over the marsh at each sampling location within a region. A total of 45 water height observations were made from 5–10 m inland at all sampling sites during 2011–2016 sampling. Differences were noted if ponded water was on the marsh, and ponded water depths were not used.

The CWC-measured water heights over the marsh were compared to the residuals of the linear regression of CRMS sea-level elevation at the hour of sampling at each region. The two means were compared at each region using a paired t-test. The difference in means from the observed water heights and residuals was calculated, and the values were subtracted to obtain a correction factor in centimeters. The correction factor was applied to the first coefficient (y-intercept) of the marsh elevation linear regression. The resulting equation yielded hourly marsh elevation at each region.

Marsh flooding and Marsh Inundation Index

Once the marsh elevation was calculated for each region, the hourly water elevation relative to the marsh surface was calculated. Hourly water level measurements adjusted to NAVD88 datum were subtracted from the calculated marsh elevation to yield water height over the marsh. Positive values of water over the marsh indicate flooding, and negative values indicated periods where water level is below the average marsh surface.

The tidal cycle of the Gulf of Mexico is generally diurnal, and a single cycle occurs every 24 hours and 50 minutes (DiMarco and Reid, 1998). A 24-hour cycle was chosen to represent a tidal cycle, and the hourly water level data were divided into 24-hour segments. For each time period, data for adjusted water depth over the marsh were analyzed, which totaled 10,454 intervals from July 2006 until October 2016 at Grand Isle and Terrebonne Bay, and from July 2007 until October 2016 at Port Sulphur. From the 24-hour water height over the marsh measurements, the maximum water height and flooding duration were determined. Maximum water heights relative to the NAVD 1988 datum in a 24-hour period varied from -10.01 cm to + 195.7 cm for all regions. The range of maximum water heights over the marsh in 24 hours

ranged from <10 cm to over 45 cm above the marsh. The percentage of time a marsh was

flooded was calculated as the number of hours with positive values of marsh water heights

divided by the number of hours in each interval (24), multiplied by 100.

The Marsh Inundation Index (MII) is a new calculation developed for this thesis research

to categorize water depths and flooding duration, ranging from zero to four and based on the

mean and standard deviation of the maximum water heights. The least flooded time periods were

assigned a MII value of 0, which represented less than 30% of the time (5 hours) being flooded

by 10 cm or less water over the marsh surface. A value of MII 1 indicated a marsh was flooded

less than 50% of the time (12 hours) by a maximum water height of between 10.1 cm and 20 cm.

A value MII 2 indicated inundation greater than 54% (13 hours) and a maximum water height of

less than 30 cm. MII 3 corresponded to inundation duration greater than 62% (15 hours) and a

maximum water height of between 30 cm and 45 cm. MII 4, the highest value, represented

marsh surface inundation greater than 62% of the time and a maximum water height of greater

than 45 cm. Of the 10,454 observations, the average maximum water height in 24-hour cycle

from 2006 to 2016 was 15.74 cm (MII 1), the first quartile was 5.22 cm (MII 0), the third

quartile was 25.6 cm (MII 2), and a SD = 16.8 cm.

16S rRNA Gene Sequence Processing

Raw amplicon files for the 2012-2014 samples were provided by MRDNA, which totaled

4,522,073 reads. All failed reads, low-quality reads (Q-score <30), and non-bacterial rRNA

sequences were removed using the computer program MOTHUR V1.36.1

(http://www.mothur.org/wiki/Main_Page), following the pipeline modified from Schloss et al.

(2011). Amplicons were aligned to the Silva reference alignment database release 119 (Pruesse

et al., 2007) modified for MOTHUR by Schloss (http://blog.mothur.org/2014/08/08/SILVA-v119-reference-files). Amplicons were chimera-checked using the aligned Silva gold reference database with the program Uchime (Edgar et al., 2011). Taxonomic identities were assigned to each read also using Silva release 119 reference file in MOTHUR (Pruesse et al., 2007; Schloss et al., 2009). Data for each sample is archived in the GRIIDC database: http://dx.doi.org/10.7266/N7GT5K39, http://dx.doi.org/10.7266/N7C24TCW, http://dx.doi.org/10.7266/N73N21BJ, http://dx.doi.org/10.7266/N77D2S2W, https://data.gulfresearchinitiative.org/data/R1.x139.143:0044, https://data.gulfresearchinitiative.org/data/R1.x139.143:0045.

Operational taxonomic units (OTUs) were generated to describe and compare the marsh bacterial communities across sample depth, marsh location, and region. Sequences from each file were merged and clustered using an average neighbor algorithm (Schloss and Westcott, 2011). Sequences were "denoised" by clustering at a distance threshold of 85% with an OTU cutoff of 0.03 (97%) and 0.05 (95%) (Schloss and Westcott, 2011). OTUs were classified based on the consensus taxonomic identification at the 85% cutoff using the Silva reference file release 119 (Pruesse et al., 2007). Clusters at the different OTU cutoffs were used to assess the α- and β-diversity (Schloss et al., 2009). Bacterial community richness was estimated using the Chao1 and nonparametric bootstrap calculations (Smith and van Belle, 1984; Colwell, 2006). Community diversity was assessed using the Shannon and Simpson indexes, and the overall coverage of sampling was assessed using Good's coverage for an OTU definition (Good, 1953; Magurran, 2013). After processing, the presence of shared OTUs in a sample at a relative abundance of greater than 1% was determined using the commands *make.shared* and

get.microbiome in MOTHUR to evaluate core microbiomes (Schloss and Westcott, 2011). The *make.shared* command produced a count of each identified OTU from the merged samples, and *get.coremicrobiome* returned a shared file to calculate the relative abundance of each OTU within all merged samples present from 1–100%. The datasets created were curated using the most recent updates to the R computer program packages dplyr, and reshape2 (v 3.3.2 "Sincere Pumpkin Patch") (R Core Team, 2015; Wickham, 2012; Wickham and Francois, 2015).

A core microbiome is defined as one or more OTUs that are one percent relatively abundant within all of the samples. OTUs were assessed at a 95% similarity threshold, and OTUs shared in at less than 1% of any sample are not detectable by the method, and may be considered part of the rare core microbiome (Shade and Handelsman, 2012; Bowen et al., 2012). A 95% similarity threshold was chosen which do not group samples at the species level of identification, but is associated with genus-level taxonomic identification. Genus level taxonomic identification yields a reduced number of singletons and doubletons, and more identification due to the many unidentified species within marsh environmental samples. Samples were grouped initially by site at each sampling time, for each region. When selecting the samples to merge, only groups with at least 3 samples were used. Comparing a core microbiome from 2 samples would not be statistically relevant.

All bacterial data were converted into relative abundance values, ranging from 0 to 1 (or 0% to 100%). The total sum of each bacterial community within a phylogenetic level was divided by the count of individual reads from each species. This was performed for each phylogenetic level, for each sample. This technique allows samples to be compared but assumes that the number of bacterial reads and the taxonomic identifications within the sample are

36

representative of the entire population in situ. One downfall of using relative abundance

transformations for bacterial data is that each value is not an independent variable because they

are fractions of the whole (Paliy and Shankar, 2016). The change in one value affects the

relative abundance values of all communities within a sample at a specific taxonomic level.

Other methods of assessing bacterial community abundance could have been used, but because

the data encompasses many zero values, the number of approaches diminishes due to potential

error (Paliy and Shankar, 2016). Total normalization is a well-established method when

assessing bacterial community composition (Paliy and Shankar, 2016).

Statistical Analyses

Data Transformation

Multiple types of data transformation were used for measurements that encompass long

gradients, short gradients, zeros, and discrete response variables (Paliy and Shankar, 2016).

Transforming the data was completed to create equal variances between measurements of

different units and magnitudes. Categorical data such as region and depth were not transformed

into continuous variables. Transformations applied to all n=245 observations in this research

included: Hellinger transformation: $\sqrt{(x_{ij}/\sum_{i=1}^{n} x_{i+})}$; where *i*-species, *j*-object and *i+*-denotes all

i's (Rao, 1995); log transformation: $\log_{10}(x+1)$ (Paliy and Shankar, 2016); normalization:

$(x_i/\sum_{i=1}^{i} x_i)*100$; where i-species completed for each samples (Paliy and Shankar, 2016).

Environmental variables were collected using a variety of techniques, and the data were

both discrete and continuous. Counts, categorical, time, and quantitative values were all used

and transformed to reduce dimensionality and scaling when comparing datasets. To reduce

statistical error, diversity index values were transformed using the Hellinger transformation that is well suited for large values within a dataset, and those containing many zeros (Paliy and Shankar, 2016). All field measured environmental variables measured both in the field and from the lab were log10(n+1) transformed. The log transformed variables included the measurements of normal alkane concentrations, salinity, water depth, sulfide concentrations, vegetation coverage, canopy height, pH, and temperature. Missing values were assigned an NA and were handled through various methods, including deletion of entire samples or pairwise deletion.

The hypothesis that the sample has a sufficient coverage can be assessed by Good's coverage and rarefaction curves (Good, 1953; Morales et al., 2009). Good's coverage gives a value from 0-1 (or 0-100%) that indicates if the number of OTUs identified at a similarity cutoff is representative of the overall population. Adequate Good's coverage values indicate that the number of sequences and identified OTUs for a sample are representative of the entire population, assessed for this thesis as >80% coverage.

Data Validation

Data assessment and validation were completed for each measurement and dataset used in this thesis. Each laboratory analysis or collaborator provided measurements that met three criteria: 1) have adequate coverage (>90%) from 2012 – 2014; 2) use previously established collection methods in the field or by following standards (ASTM, USGS); 3) be comprised of minimal outliers or easily explained outliers.

Bray-Curtis Dissimilarity matrix based analyses

To determine the similarity or difference among bacterial diversity grouped by time, depth, and spatial distribution, the similarity percentage analysis (SIMPER) was used from the vegan package in R (Oksanen et al., 2007). SIMPER is based on Bray-Curtis dissimilarity matrices and provides the percentage of dissimilarity between groupings, as well as the contribution of taxonomic assessment to that total dissimilarity from a comparison (Clarke, 1993). To determine the significance of these relationships 99 permutations of the analysis were run to evaluate the P-values associated with each analysis. The Bray-Curtis Dissimilarity Index (BCDI) assesses dissimilarity between two groups as a value from 0–1, with 1 being the most dissimilar.

Principal Component Analysis

Principal Component Analysis (PCA) is a multivariate analysis used to identify bacterial community relationships using relative abundance data. PCA plots visualize two or more axes that are linear components that explain variance among communities (Legendre and Gallagher, 2001). The axes are listed from most to least variance, and thus the first two axes should identify the taxa or loadings that explain the most variance, which is farthest away from the central point in either the positive or negative direction. Communities that explain low variance plot very close to one another, near the central point. The total number of axes (ranks) explains how many dimensions the data have based on orthogonal projections from the previous axis, starting with the first (Legendre and Gallagher, 2001). PCA has its drawbacks in that rare and low abundance communities can skew the interpretations (Paliy and Shankar, 2016), although low abundance

communities can be removed so that only the upper 95% of all bacterial communities were assessed.

Canonical Correspondence Analysis

Canonical Correspondence Analysis is based on Chi-squared distance matrices and performs weighted linear mapping of the variables. The CCA is most widely accepted with the abundance and environmental data due to the presence of gradients that exist within the relative abundance and environmental parameters (Paliy and Shankar, 2016). Variables to be used in the CCA were selected to identify and explain the variation related to the MII. Hypothesis two focused on the interaction of bacterial communities and the MII values, which was the only continuous variable paired with a categorical value of either region or depth. When using categorical variables, dummy variables were decomposed into n-1 CCA axes, where n is the total number of factors of the variable. For a regional classification variable, two dummy variables were created of binary indication of the variable were assessed, since regional differences are not continuous. The results were plotted as centroids, and not vectors.

A stepwise CCA model was completed using forward and backward modeling based on variable significance at a threshold P-value of 0.01 using the R program and "vegan package" (Oksanen et al., 2007). To reduce model instability, only parameters with low multicollinearity were used in the model, tested using a variance inflation factor of less than or equal to nine (Craney and Surles, 2002).

General Linear Models

To determine what environmental variables were meaningful in explaining variation in the bacterial communities, a lasso regularized general linear model was done using the package "glmnet" in the program R (Friedman et al., 2009). The environmental variables used in the model were screened first for collinearity using a variance inflation factor (VIF) cutoff of 9 from linear regression (Craney and Surles, 2002). The Lasso regression method was used to select a sparse number variables that were associated with bacterial changes by analyzing the parameter lambda (λ[lambda]) in the form of Equation 4 (Tibshirani, 1996).

$$\sum_{i=1}^{n} \left(y_i - \beta_0 - \sum_{j=1}^{p} \beta_j x_{ij} \right)^2 + \lambda \sum_{j=1}^{p} |\beta_j| = RSS + \lambda \sum_{j=1}^{p} |\beta_j| \text{ } Equation\text{ }4$$

Lasso regularization was used to minimize the predicted coefficient of lambda, the tuning parameter, using an L1 penalty. In Equation 4, y is the dependent response variable with p predictors of the ith sample, β[beta] is the coefficients vector, with β[beta]0 being the intercept and RSS is the residual sum of squares of the jth predictor.

To select a lambda value that minimize MSE, cross-validation sampling approach was used with 10 folds to approximate the MSE of all 245 samples (Friedman et al., 2009). When running the sample for each region, the sampling folds were decreased to 5 or 6 due to a reduction in sample size. Lambda selection for the selection of parameters can be extended beyond the minimum MSE to +1MSE, which could reduce the total number of parameters that are useful in the model. For the entire dataset, the model was used at a +0.5MSE cutoff, and all regional models were extended +0.5SE to reduce variables with lower total number of samples.

CHAPTER THREE - RESULTS

Environmental Physiochemistry Based on Field Sampling

Seventeen environmental parameters were measured in conjunction with a collection of 245 marsh soil samples (Table 2.1). For all parameters used in this study, the averages and maximum and minimum values were calculated (Table 3.1). Measurement coverage was determined and utilization of a measurement for statistical purposes was evaluated. From the field data, although inland water depth was only measured for 109 (44%) of the soil samples, average water depth when measured was 11.69 cm at Port Sulphur, 9.47 in Grand Isle, and 23.5 cm in Terrebonne Bay. These values were compared to CRMS data during sampling. Because of incomplete records, inland sulfide data and incoming solar radiation were not used for statistical analyses. Specifically, the average concentration for inland sulfide was 27.36 ppm for 48% of the samples, mostly because there was no water available for which to measure dissolved sulfide. The average incoming solar radiation was 929 W m^{-2} for 50% of samples when measured.

Hydrocarbon data had 96% sampling coverage, with all but 10 samples having analyses. The average total n-alkane concentration for all samples during the study was 20.7 mg kg^{-1}. Total n-alkane concentrations from inland soils were used to calculate proportions of n-alkane chain length, with 5.8% low (C_{10} –C_{18}), 34.9% medium (C_{19} –C_{26}), and 57.1% high (C_{27} –C_{35}) chain length values (Figure 3.1). These values differed significantly between regionals base on ANOVA calculations (P-value = <0.0001) (Table 3.1). Total n-alkane data were also used to calculate carbon preference index (CPI), average chain length (ACL), and the C_{29}/C_{19} ratio.
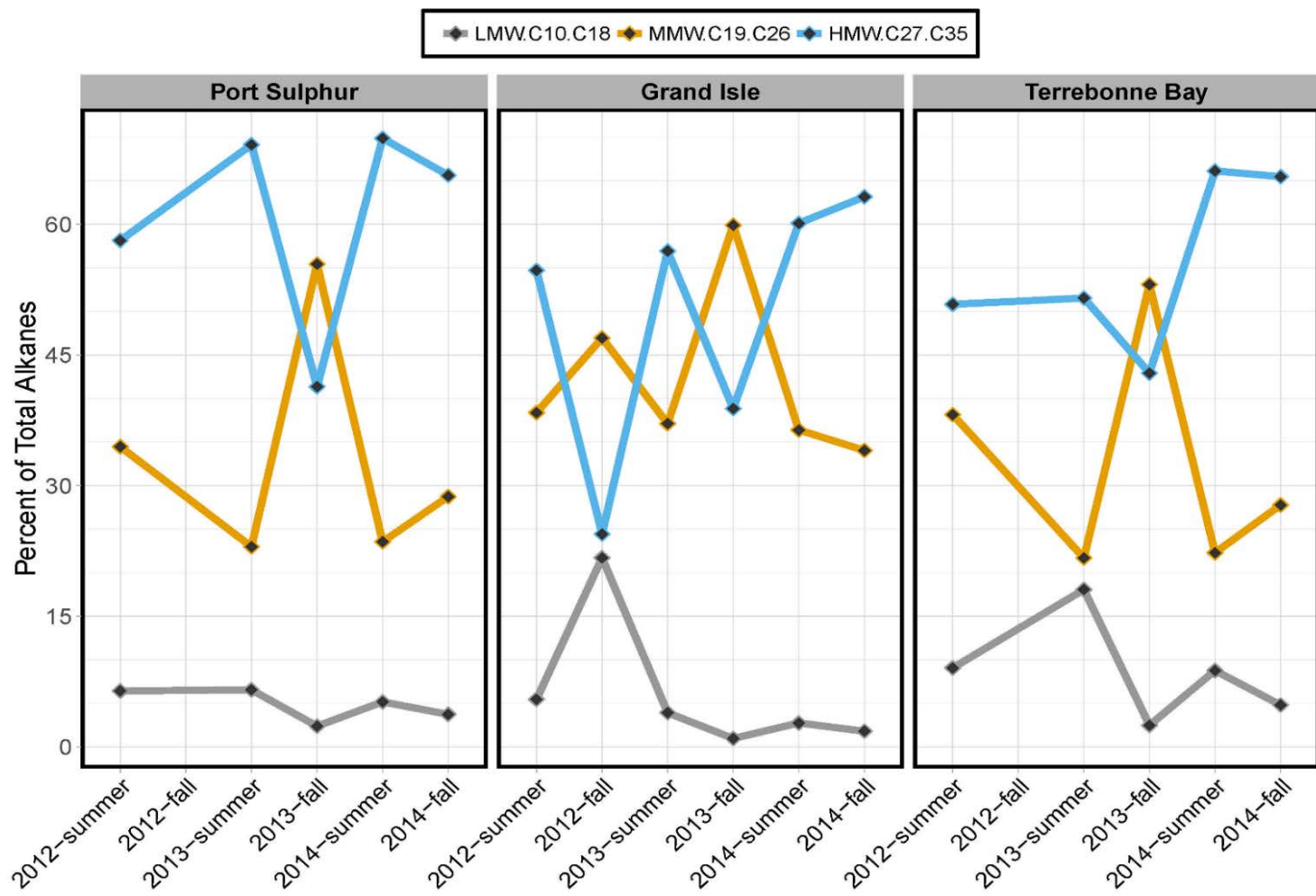
Figure 3.1:   *n*-alkane chain length as a percentage of the total *n*-alkane concentrations from 2012 through 2014 measured at each site. Average total concentrations are listed in Table 3.1.

Table 3.1:   Summary average values from the environmental parameters collected in the field and diversity values obtained from 95% similarity threshold OTU calculation.

Parameter	Port Sulphur			Grand Isle			Terrebonne Bay		
	Max	Mean	Min	Max	Mean	Min	Max	Mean	Min
Plant Species Observed (Count)	4	2.08	1	2.00	1.57	1	2	1.39	1
Vegetation Coverage (%)	88	34.89	4	75.00	36.01	8	95	29.98	2
Cano opy Height (cm)	98.50	65.86	38.50	120	63.57	30.00	145	66.00	45.00
Inland Water Depth (cm)	30.50	7.57	0	18.50	4.51	0	55.00	12.53	0
MII	4	2.73	1	2	1.17	0	3	1.71	1
Edge Water pH	8.08	7.62	7.17	8.39	8.04	7.10	7.89	7.65	7.10
Edge Water Temp (°C)	29.60	27.41	25.30	32.50	26.86	24.50	31.20	28.29	24.60
Salinity field (ppt)	16.18	11.57	7.10	35.20	19.10	7.50	22.40	14.64	9.40
Salinity CRMS (ppt)	17.82	10.88	8.25	25.30	20.19	15.96	19.89	16.88	12.64
Conductivity CRMS (ms/cm)	28.91	18.93	13.72	39.63	27.81	18.93	40.56	27.48	21.36
Total alkanes (mg/Kg)	33.60	14.84	2.29	64.01	29.43	6.00	88.26	19.27	1.68
LMW Alkanes ($C_{10} - C_{18}$) (%)	13.51	4.79	0.722	41.50	3.68	0.346	21.64	9.11	0.753
MMW Alkanes ($C_{19} - C_{26}$) (%)	68.34	32.25	8.19	62.47	44.05	18.28	65.71	29.35	16.96
HMW Alkanes ($C27 - C_{35}$) (%)	84.89	61.63	30.69	73.77	50.96	17.26	72.37	57.63	29.03
CPI	4.82	3.26	1.17	6.74	3.71	1.30	4.11	3.03	1.35
ACL Tanner	29.97	28.19	25.84	29.05	27.11	25.69	28.90	28.26	26.35
OTUs (Count)	4,484	2,415	1,258	5,246	2,595	1,188	6,331	3,162	1,525
Chao1 Diversity	7,307	4,323	2,032	8,546	4,816	2,155	13,666	5,937	2,661
Shannon Diversity	7.63	6.84	5.86	7.68	6.90	5.40	7.71	6.84	5.24
Simpson Diversity	0.001	0.003	0.015	0.001	0.003	0.026	0.001	0.003	0.031
Bootstrap Diversity	5,416	3,001	1,529	6,310	3,177	1,488	7,887	3,850	1,854

The salt marsh plant observations differed by region, the highest average number of plant species observed was at Grand Isle with an average of 2.1 species per site, and lowest at Terrebonne Bay where there were only 1.4 species on average observed per site (Table 3.1). The canopy height was highest at Terrebonne Bay, with plants averaging 66 cm tall. The greatest vegetation coverage occurred at Port Sulphur, with an average coverage of 36% (Table 3.1).

Salinity measured from edge water in the field was the highest at Port Sulphur, with an average value measured of 19.1. Salinity was also measured at CRMS gauging stations, and this dataset was used to evaluate long-term changes in salinity regionally. The highest average salinity recorded was at Grand Isle, and the lowest average salinity values was at Port Sulphur (Figure 3.2). Differences between the salinity measured at the CWC sites during field research

and the CRMS network during the same time period, particularly for the spring of 2013 data, were because CRMS stations used were not proximal to CWC sites. Local hydrological variations likely affected the values.

Marsh Surface Elevations and Inundation History

By definition, coastal salt marshes are flooded periodically, and tidal cycles are the underlying cause of daily fluctuations in water elevation. Changes in marsh surface elevation affect how much of a marsh is flooded over time. If marshes are flooded for longer periods of time, and to greater water depths, then this may be because surface elevation is not keeping up with sea-level rise. Marshes need to accrete faster than the local to regional sea-level rise, or subsidence rates, to keep from being flooded for longer periods of time. Changes in marsh surface elevation may affect marsh vegetation and microbial ecosystems, which is why marsh surface elevation, accretion rates, and flooding histories were derived in this study from the regional CRMS station data using linear regressions of marsh accretion rates (Figure 3.3) and gauged water heights (Figure 3.4). These changes were used to determine marsh elevation and flooding histories.

For the three regions, average accretion rates were slower than changes in water level at the marshes, which resulted in modest changes in marsh elevations over time. For instance, at Port Sulphur, the average accretion rate was +0.37 cm yr^{-1} from 2007 to 2016, and +0.86 cm yr^{-1} during the sampling period (Figure 3.3), but water level changes were faster at an average of +1.00 cm yr^{-1} from 2007 to 2016 and +1.62 cm yr^{-1} during the sampling period (Figure 3.4).
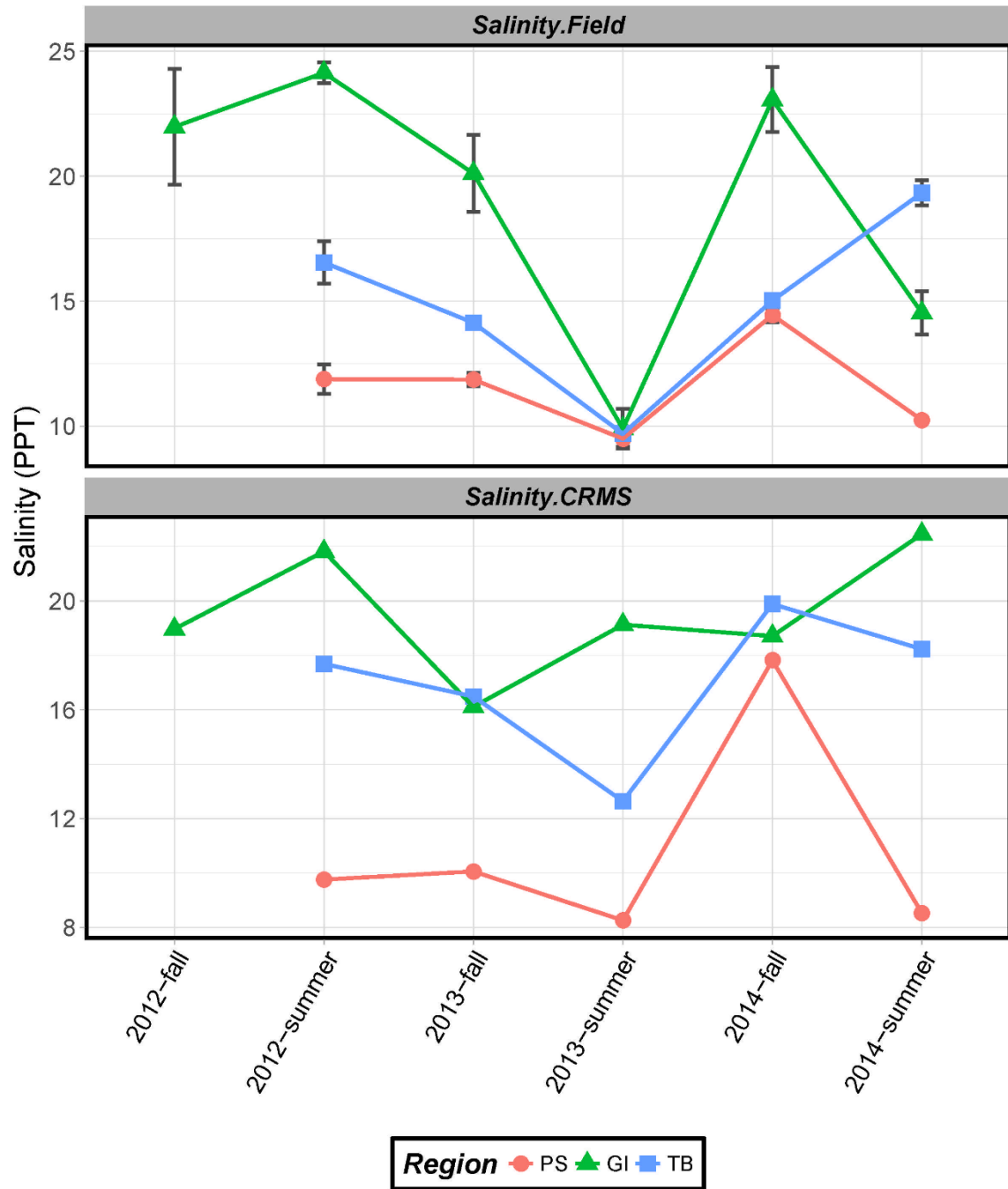
Figure 3.2: Salinity at each region as an average (± 1 SE) of the ~3m offshore measurements at each sampling site, and from regional CRMS Stations during the time of sampling. Both measurements were adjusted for temperature. Error bars that are not shown are smaller than the symbols used for the average value of the field salinity, no error bars are displayed for the CRMS data since there were no calculations used in the creation of the value.
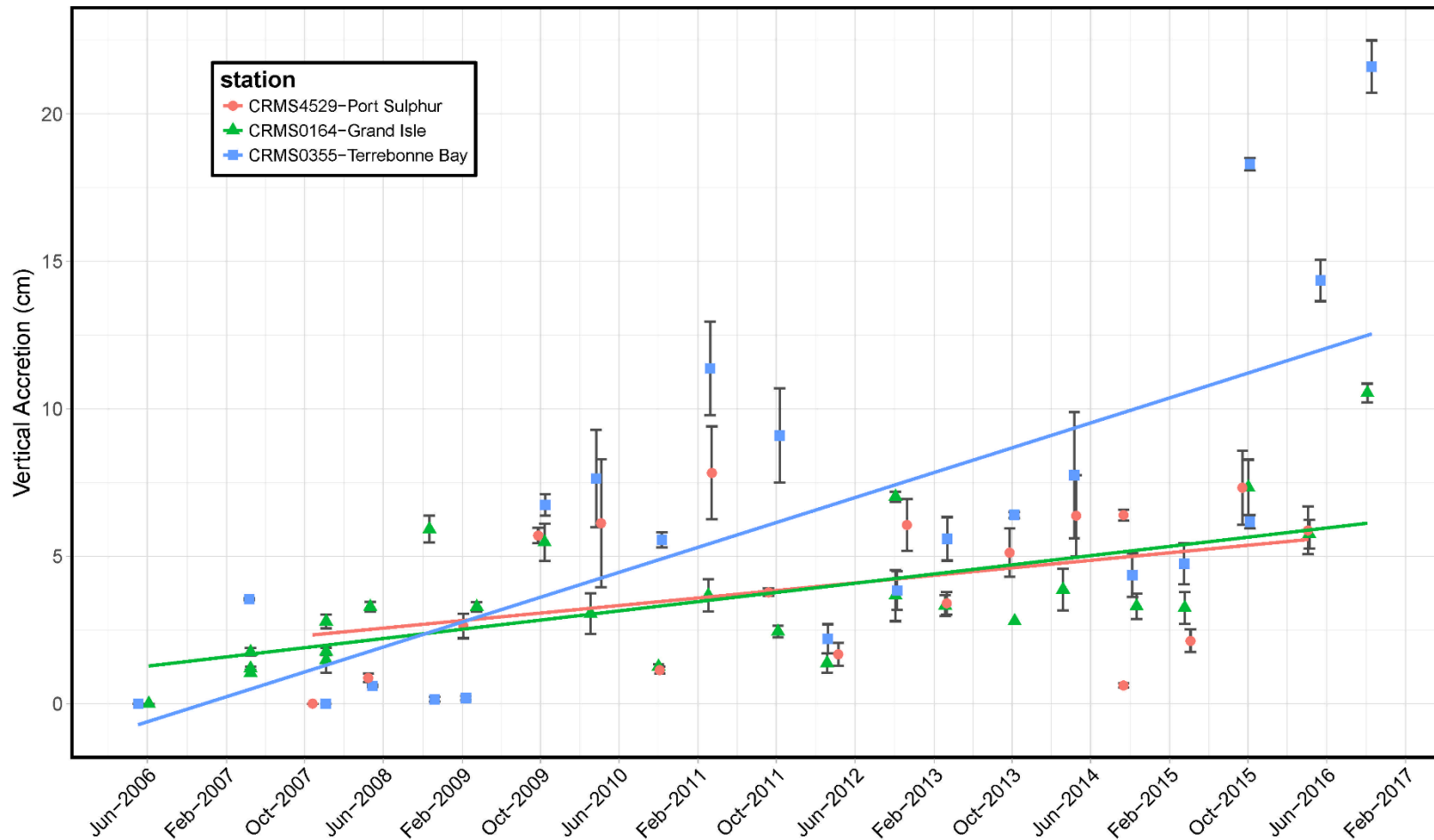
Figure 3.3: Time series data from marsh accretion (±1SE) and linear regression colored by CRMS station, 2006-2016. Marsh accretion was measured from the surface to a marker horizon in cores collected on site roughly twice a year. The feldspar marker horizon was placed on site during the CRMS station instillation.
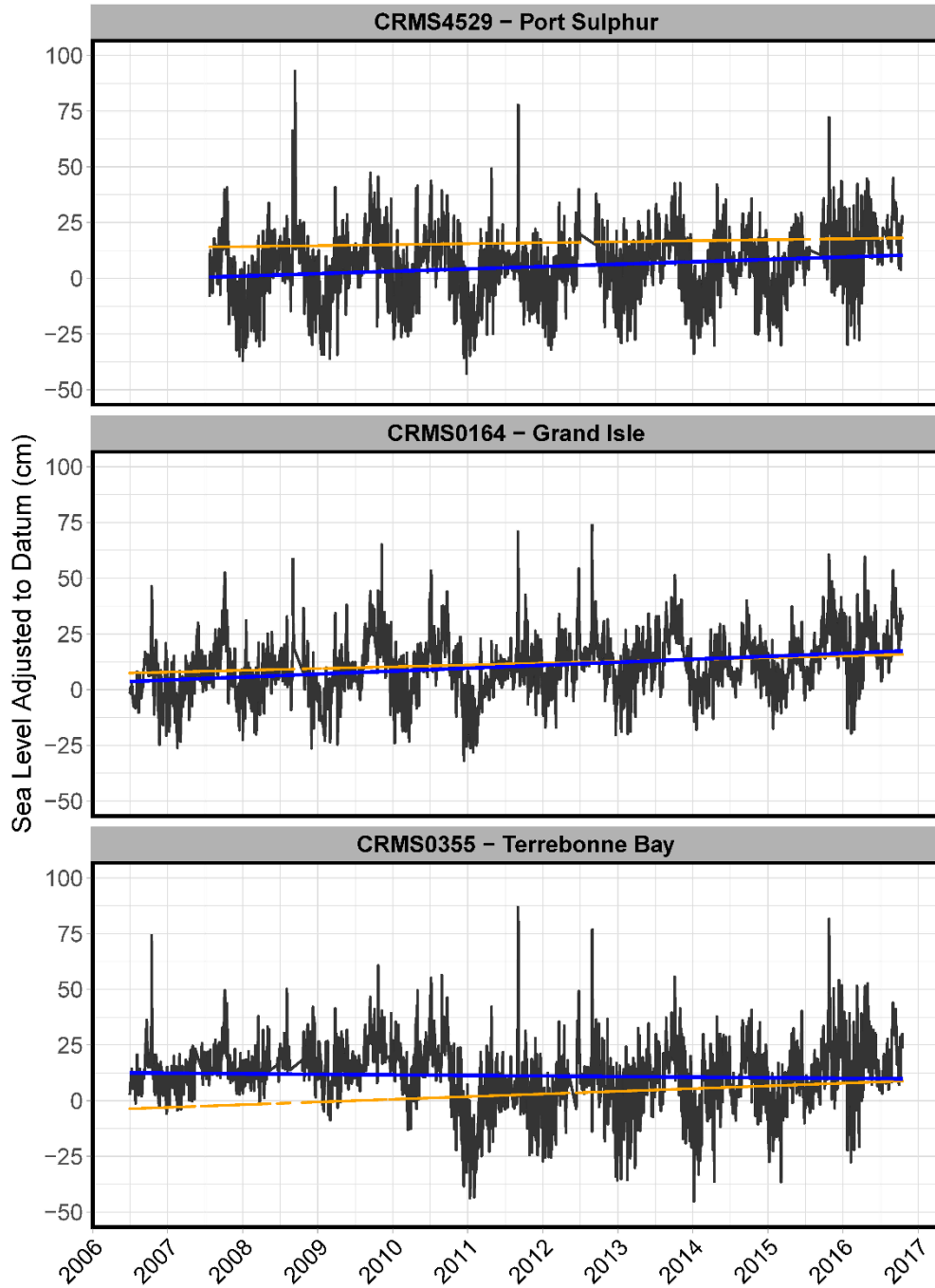
Figure 3.4: Hourly water level adjusted to the NAVD88 datum for each representative station from the regions of Grand Isle, Terrebonne Bay, and Port Sulphur. Yellow lines indicate the calculated marsh elevation through time. Blue lines are the liner regression by least squares method for the water elevation through time.

Consequently, extrapolated marsh elevation changes were +0.43 cm yr^{-1} (R^2 = 0.13, P-value=<0.001) from 2007 to 2016, and +0.26 cm yr^{-1} (R^2 = 0.009, P-value = 0.16) during the sampling period. This meant that from 2012 to 2014, the marsh surface did not change by more than 0.5 cm, and samples taken from cores were not significantly affected by the addition of new material to the marsh. Similarly, accretion rates at Grand Isle were slower, being +0.37 cm yr^{-1} from 2006 to 2016 and +0.33 cm yr^{-1} during the sampling period, compared to water level changes at +1.32 cm yr^{-1} from 2006 to 2016 and +0.73 cm yr^{-1} for the sampling period. But, extrapolated marsh surface elevation changes at Grand Isle were faster at +0.81 cm yr^{-1} (R^2 = 0.58, P-value = <0.001) from 2006 to 2016, and the same rate during the sampling period +0.81 cm yr^{-1} (R^2 = 0.14, P-value = <0.001). At Terrebonne Bay, the average accretion rate was +1.08 cm yr^{-1} from 2006 to 2016, and +1.52 cm yr^{-1} during the study period. Accretion rates for each of the regions represented the median value of the three closest stations, and were similar to other reported values in the region. Water level measured at the Terrebonne Bay CRMS station changed in 2010, noted in Attachment C3-23.2 of the CPRA (2017b) master plan. For the 2010 to 2016 data, the long-term increase in water depth was +2.90 cm yr^{-1}, and +2.32 cm yr^{-1} during the specific sampling interval. The marsh elevation changes were +1.20 cm yr^{-1} (R^2 = 0.63, P-value = <0.001) from 2006 to 2016, and +0.44 cm yr^{-1}(R^2 = 0.08, P-value = <0.001) at Terrebonne Bay.

Based on the calculated hourly marsh elevation and water depth at each region, the average height of water at Port Sulphur was -11.4 cm, meaning that water levels, on average, were below the marsh surface. Similarly, at Grand Isle, water levels were also, on average, below the marsh surface, at -0.719 cm. At Terrebonne Bay, however, likely due to faster increases in

water height and lower accretion rates, water depth over the marsh was, on average, +2.73 cm. The marshes at Port Sulphur were flooded 31.4% of the year (or 114.7 days per year) from 2007 to 2016, whereas the marshes at Grand Isle were flooded 47.1% annually (or 171.7 days), and Terrebonne Bay marshes were flooded the most at 73.8% of the time (or 269.3 days per year).

To assess whether these changes reflected differences in tidal cycle patterns regionally and over time, SIMPER was used to compare daily high and low tidal predications during the sampling period and trends in the long-term data. Results indicated significantly similar values (P-value <0.001) for daily tidal predictions during sampling period and from the long-term data. Tidal cycles in May or October, when field sampling occurred, were 91% similar between all regions. Tidal variations at Terrebonne Bay were >90% similar over the three years of prediction data, and >87% similar at both Grand Isle and Port Sulphur. Therefore, fluctuations in tidal cycles could not be linked to changes in water flooding the marshes.

Marsh Inundation Index (MII) through time

Using the calculated marsh elevations, the Marsh Inundation Index (MII) was used to categorize flooding height and duration of time water was over the marsh surfaces. From a total of 10,4564 intervals (i.e., days) calculated for the three regions, inundation duration ranged from 0 to 24 hours, and the maximum water height over the marsh in any 24-hour interval ranged from -40.45 cm to +195.7 cm. For each region, the MII values were normally distributed (Figure 3.5), averaging 0.88 (n = 3,204 intervals) at Port Sulphur, 1.32 (n = 3,688) at Grand Isle, and 2.06 (n = 3,582) at Terrebonne Bay. As expected, considering the extrapolated changes in water height over time, average MII values increased through time at each region (Figure 3.6).
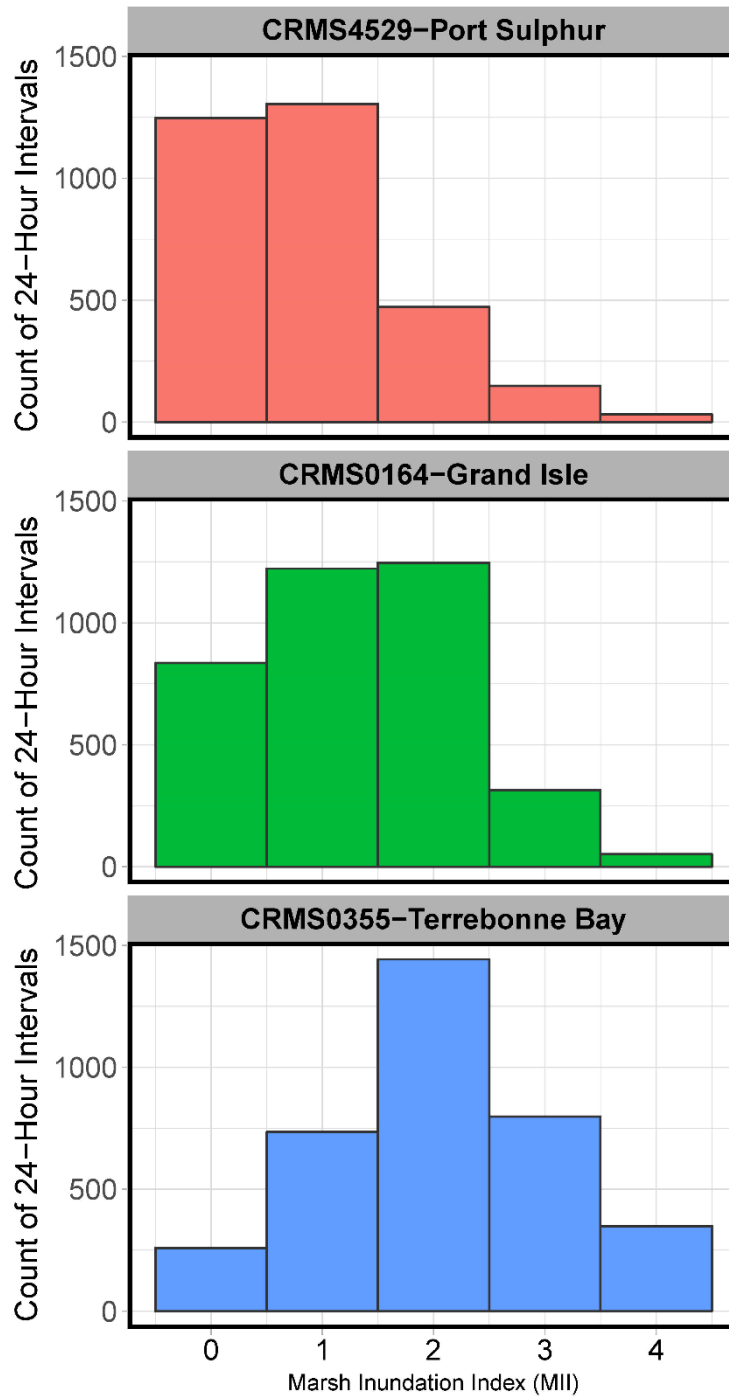
Figure 3.5: Marsh Inundation Index (MII) from the calculated marsh height and hourly water level from the CRMS stations within each region. The y axis is a count of the total number of intervals matching the parameters for each MII value, 1 - 4 shown on the x axis.
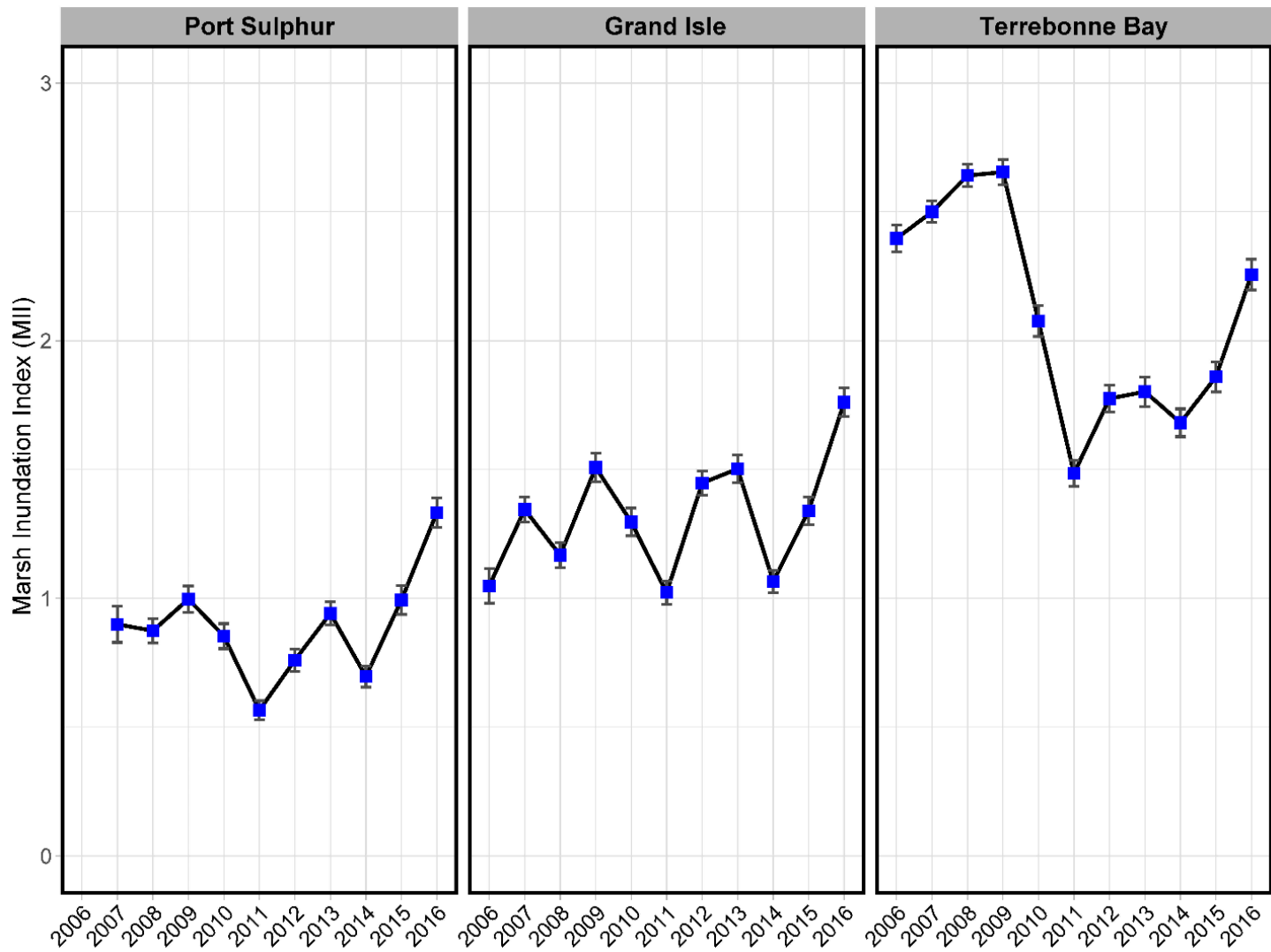
Figure 3.6:   Annual average MII values from each region (±1SE) from 2006-2016.

These results confirmed that water depth over the marshes, and the duration of flooding of the marsh surfaces, increased through time in all regions because marsh accretion rates were less than the rates of water level rise. Overall, Grand Isle marshes experienced less flooding than at Port Sulphur or Terrebonne Bay during the sampling period.

Changes in flooding history were compared to salinity changes from each region to evaluate the type of water that had flooded the marshes based on MII (Figure 3.7) and water height over the marsh (Figure 3.8). For Port Sulphur and Terrebonne Bay, higher MII values were significantly related to lower salinities (R^2 = 0.042 and 0.006, P-values = 0.002 and 0.0003, respectively), but higher salinities were related to higher MII values for Grand Isle, although this relationship was not significant (R^2 = 0.03, P-value = 0.12). These results mean that when marshes at Port Sulphur and Terrebonne Bay were inundated for longer periods of time and to greater water depths, the water was, on average, less saline and likely associated with regional riverine input rather than input from the marine waters in the Gulf.

Bacterial Community Diversity and Structural Differences

The most abundant taxonomic groups retrieved from the soils are listed in Table 3.2. The phylum Proteobacteria represented an average of 53% of all amplicons (SE = 0.45, SD = 7.0, n = 245). The top three most abundant classes were Deltaproteobacteria, Gammaproteobacteria, and Alphaproteobacteria. The most abundant class of bacteria at each depth differed for the samples collected below the surface (B, C, and D) compared to those sampled collected from the surface (MS and A). However, the most abundant bacterial class at depth from each region belonged to the Deltaproteobacteria, on average 18.9% at Port Sulphur, 19.9% at Grand Isle, and 20.0% at Terrebonne Bay.
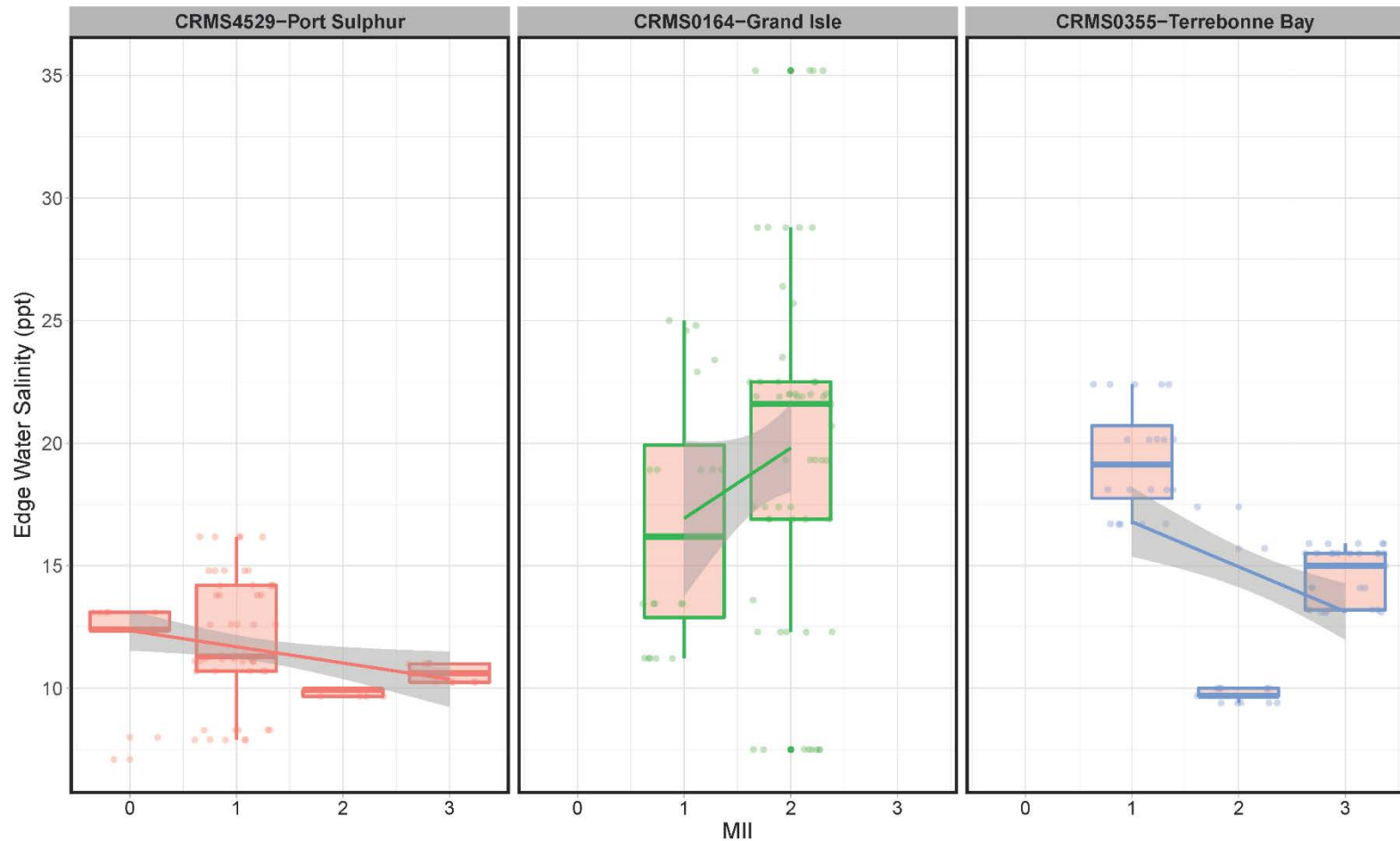
Figure 3.7: Salinity vs MII boxplot for all samples grouped by MII per region. Salinity was measured at each sampled marsh and the MII values were calculated from flooding duration and water depth based on changes in marsh surface elevation. The linear regression comparisons were significant for Terrebonne Bay ($R^2 = 0.1$, P-value=0.006) and Port Sulphur ($R^2 = 0.05$, P-value=0.042,), but not for Grand Isle. The linear regression and 95% standard error are shown in grey, and each data point is also plotted in the background.
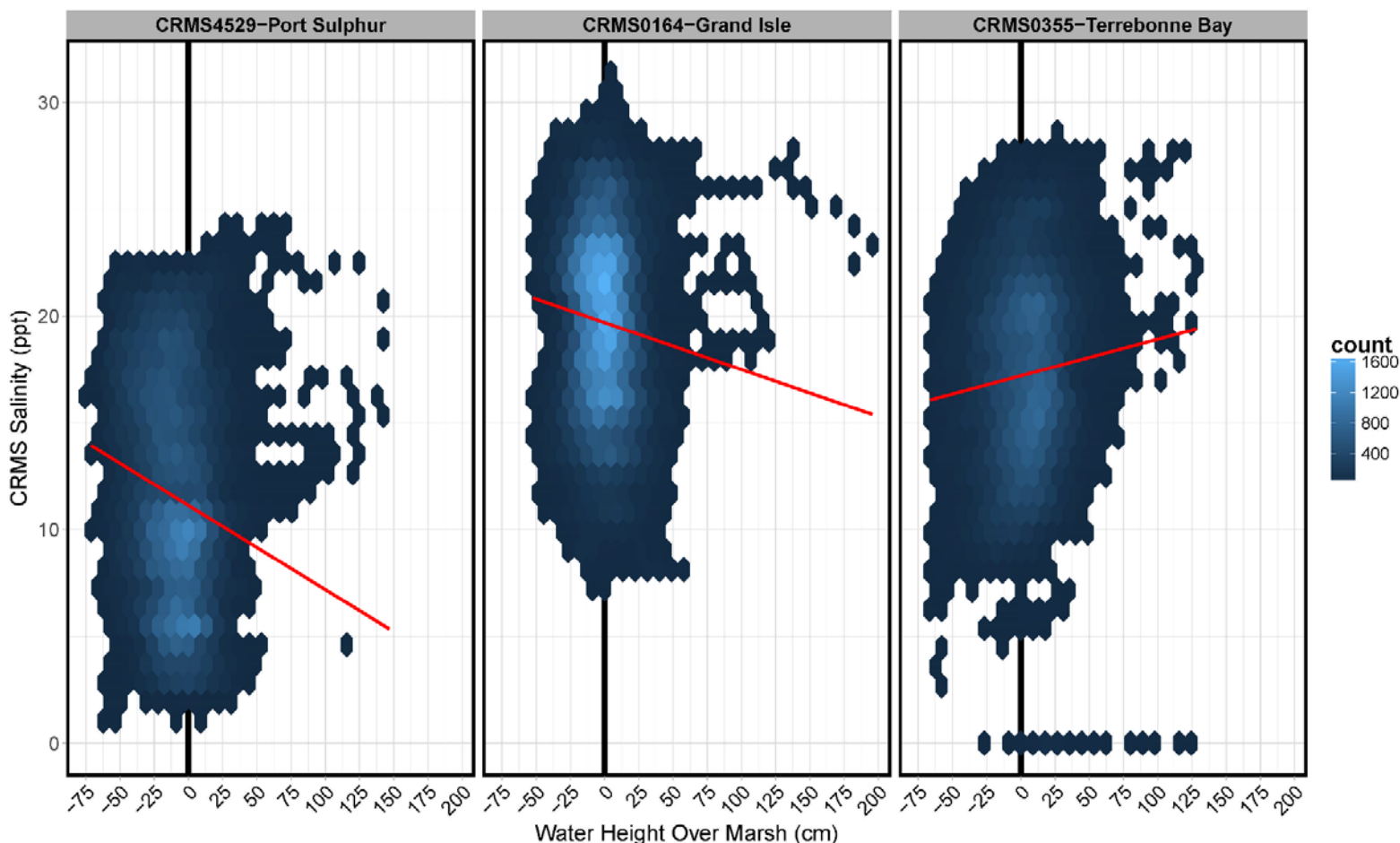
Figure 3.8: Salinity vs water height over the marsh from CRMS collected salinity and calculated marsh elevations of all hourly samples and from 2006-2016. The plot is a modified point cloud where the number of points within each geometric hex are noted on the right with lighter colors having higher number of points. Red lines indicate linear relationship with the slope at Port Sulphur = -0.61 (R^2=0.02, P-value <0.001), Grand Isle = -0.39 (R^2=0.01, P-value <0.001), and Terrebonne Bay =0.44 (R^2=0.01, P-value <0.001). The dark vertical line lies along the marsh elevation of zero, negative values indicated water below the marsh and positive values are the water height over the marsh.

Table 3.2: Average relative abundance percentage of the most abundant bacterial classes from 2012 to 2014, grouped by sampling year, season, year and season, depth, and region. The highest average relative abundance for each bacterial taxon is shaded in blue. All values are the average relative abundance percent of the bacterial class per group.

Grouping	Delta-proteobacteria (%)	Gamma-proteobacteria (%)	Alpha-proteobacteria (%)	Planctomycetacia (%)	Sphingobacteria (%)
Year					
2012	16.23	16.59	14.39	5.17	6.43
2013	17.76	17.94	12.43	4.71	4.68
2014	19.00	13.20	13.59	4.62	3.20
Season					
Fall	19.26	15.04	12.58	4.71	3.81
Spring	17.17	15.96	13.79	4.72	4.46
Year and Season					
2012-Spring	16.90	16.91	11.96	5.28	7.04
2012-Fall	13.69	15.39	23.62	4.75	4.15
2013-Spring	16.00	18.41	13.86	4.82	5.29
2013-Fall	19.44	17.49	11.06	4.60	4.08
2014-Spring	18.35	13.37	14.38	4.43	2.78
2014-Fall	19.54	13.05	12.94	4.78	3.56
Depth					
Marsh Surface (0-2 cm)	15.67	16.14	16.79	6.08	5.71
A (0-1 cm)	16.89	17.09	15.39	5.97	5.18
B (1-2 cm)	18.94	16.78	13.19	5.05	4.18
C (4-5 cm)	19.87	14.74	11.51	3.65	3.09
D (9-10 cm)	20.03	12.67	8.58	2.62	2.29
Region					
Grand Isle	17.93	18.89	14.56	5.24	4.69
Port Sulphur	18.80	14.71	12.06	4.63	3.93
Terrebonne Bay	17.83	12.73	13.01	4.23	3.76

At the A depth, the class Gammaproteobacteria (17.1%) was the most abundant, but the Alphaproteobacteria (16.8%) were the most abundant from the marsh surface samples (MS). There were seasonal differences among the bacterial classes (Table 3.2)

The relative abundances of bacteria identified to the class level were analyzed via SIMPER and calculated BCDI values to determine similarities in community compositions by depth, season, and region. Overall, the bacterial communities averaged 67.6% similarity at the class level and 81.6% similarity at the phylum level. When compared by depth, the bacterial communities were 67.6% similar to one another. Depths A and B were 71.9% similar, and depths MS and D being the least similar at 60.6% (Figures 3.9 – 3.12). Differences in the relative abundances in Alphaproteobacteria, Gammaproteobacteria, Deltaproteobacteria, Betaproteobacteria, and Flavobacteria explained the BCDI values. Compared to the sampling season (Figures 3.10 & 3.11), bacterial communities were 67.8% similar, with the most dissimilar times being between spring 2012 and spring 2014 (65.4% similarity) and the most similar times being between spring 2013 and fall 2013 (69.6% similarity). Deltaproteobacteria, Alphaproteobacteria, Gammaproteobacteria, Sphingobacteria, and Flavobacteria explained the differences among the communities seasonally. Compared by region, the bacterial communities were 67.2% similar. The most dissimilar regions were Terrebonne Bay and Grand Isle (65.9% similarity), and the most similar regions were Grand Isle and Port Sulphur (69.3%) (Figures 3.9 & 3.11). Based on the average contribution to the overall similarity between Grand Isle and Port Sulphur, Alphaproteobacteria, Gammaproteobacteria, Betaproteobacteria, Deltaproteobacteria, and Chlorobia explained the differences. But, between Terrebonne Bay and Grand Isle samples, Flavobacteria and Planctomycetacia contributed to the compositional differences.
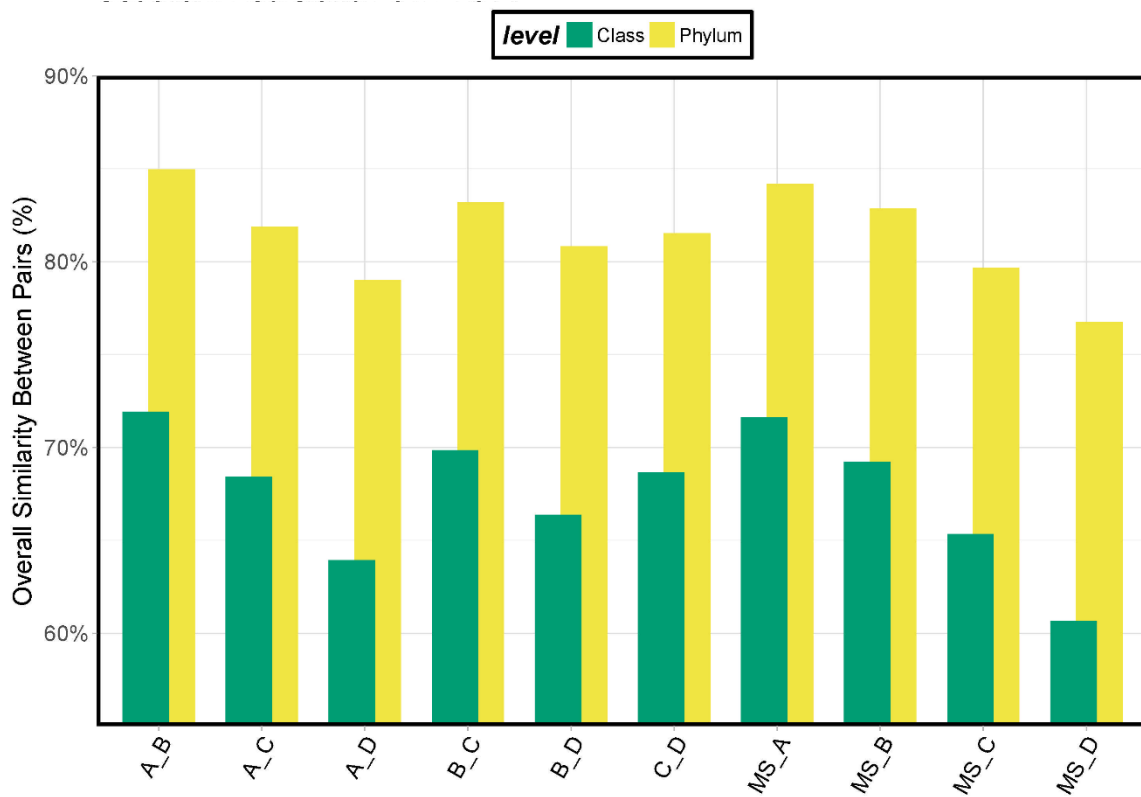
Figure 3.9: SIMPER overall similarity results from comparison at the phylum and class level between sampling depths from the soil cores.
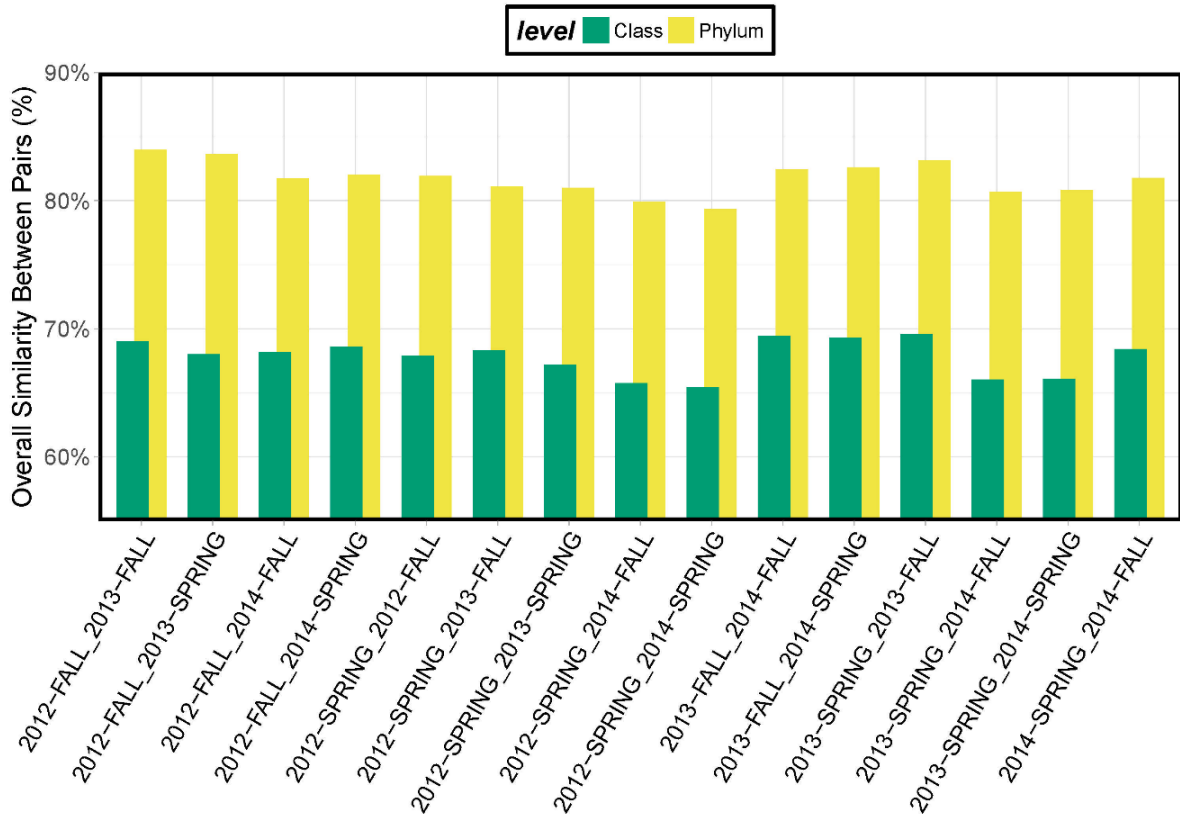
Figure 3.10:   SIMPER overall similarity between of phylum and class level bacteria grouped by sampling period.
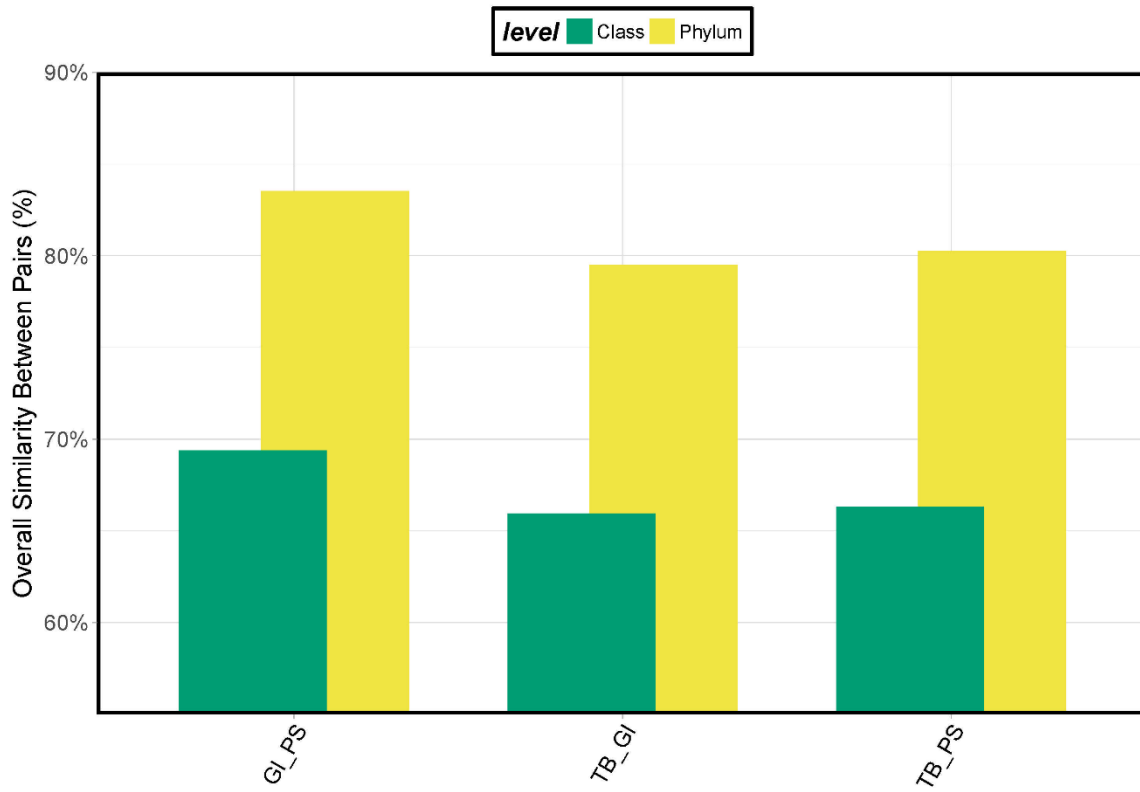
Figure 3.11:   SIMPER analysis and overall similarity between phylum and class level bacterial grouped by sampling region.
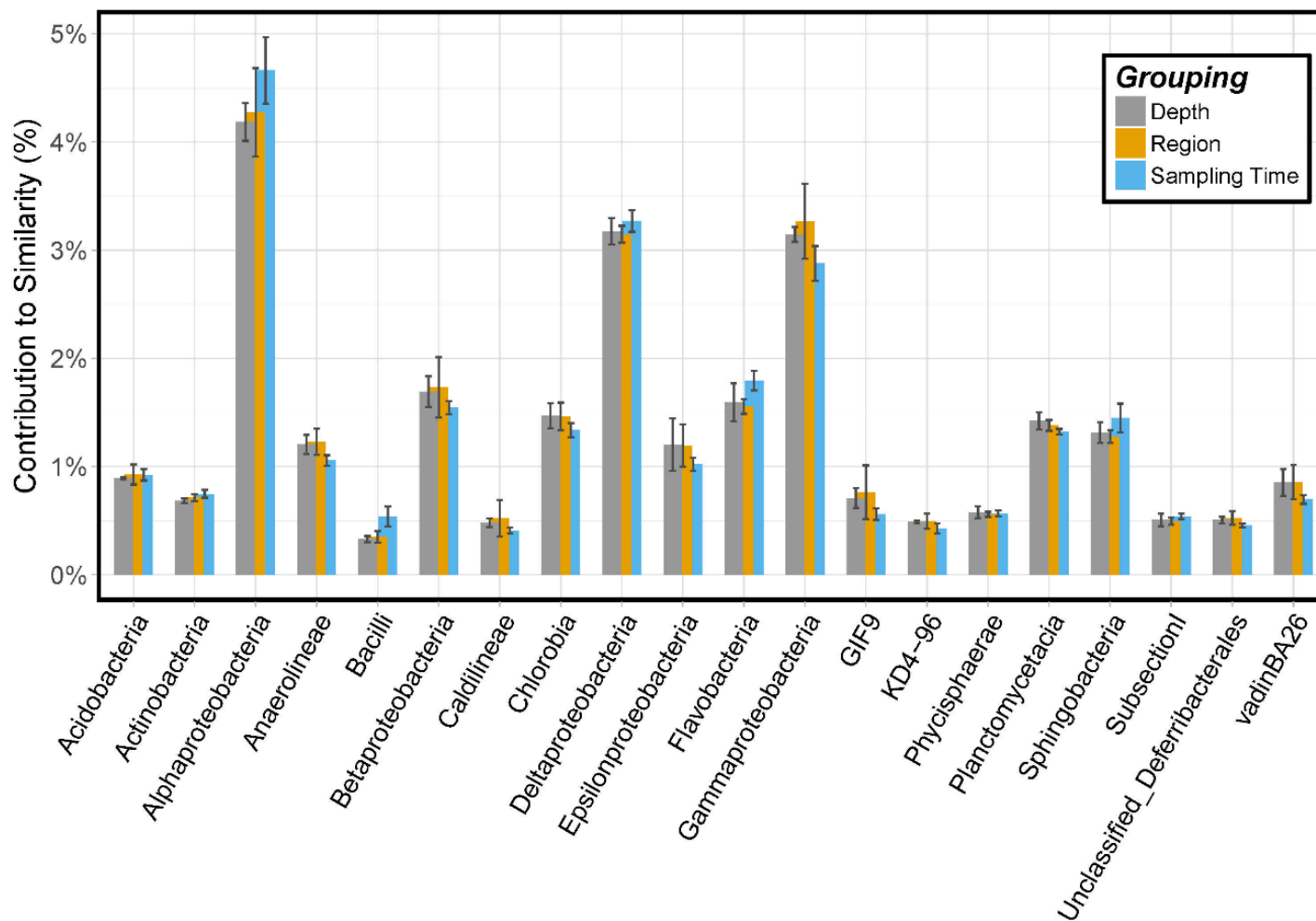
Figure 3.12:   Results from the SIMPER analysis of the bacterial relative abundances at the class level. Each bar represents the average contribution to the overall similarity from each grouping, with the error bars displaying ±1SE. The top 20 most influential bacterial classes are displayed, which all had an average contribution to the overall similarity > 1%.

PCA was used to identify the underlying compositional variation within the data where there is inherent multicollinearity between variables (Graham, 2003). The relative abundances of all bacterial classes were used and diversity data were grouped by sampling time, region, and depth to determine patterns and multivariate trends among samples. The PCA according to the compositions explained 82% of the variation in the first two principal components (axes) among communities at the phylum level and 65% at the class level (Figures 3.13 and 3.14). At the phylum level (Figure 3.13), PC1 explained 57.2% of the variation and the most influential loadings were Chloroflexi, Proteobacteria, and Bacteroidetes (Table 3.3). PC2 explained 24.8% of the phylum level variation, due to loadings of Proteobacteria, Chlorobi, Chloroflexi, and Bacteroidetes. The PCA at the phylum level indicated that the Terrebonne Bay communities were distinct from the communities in the other two regions. Similarly, the PCA completed at the class level along PC1 explained 45.6% from the loadings of Alphaproteobacteria and Deltaproteobacteria (Figure 3.13 and Table 3.3). PC2 controlled 18.9% of the variance and was explained by Gammaproteobacteria. In addition, for these results, PC3 was included in Table 3.3 and was identified to be explained by Betaproteobacteria, Chlorobia, Deltaproteobacteria, and Epsilonproteobacteria. When the PCA was grouped by region (Figure 3.13), Terrebonne Bay communities from 2013 and spring 2014 were skewed in the negative loading direction explained by Chloroflexi and Alphaproteobacteria. Along PC2, also in the negative direction, the Grand Isle communities from spring and fall 2013 were explained by Gammaproteobacteria. Additional PCA were constructed based on the same variance and loadings, grouped by sampling year and depth (Figures A.2 – A.4) to identify that the phylum Chloroflexi explained the greatest loadings for deeper sampling depths (C and D), specifically in 2014 and from Terrebonne Bay.

Table 3.3: PCA loadings for bacterial classes. The Eigenvalue and variance, as a percentage, are displayed, and the individual class levels are listed with their loadings for the first three PC axes; only PC1 and PC2 were plotted.

PC 1		PC 2		PC 3	
Eigenvalue	96.89	40.22		22.92	
% variance	45.60	18.93		10.79	
Bacterial Class Loadings					
Deltaproteobacteria	0.4743	Alphaproteobacteria	0.2938	Betaproteobacteria	0.4488
Anaerolineae	0.1480	Epsilonproteobacteria	0.1487	Chlorobia	0.4049
Chlorobia	0.1155	Chlorobia	0.1474	Deltaproteobacteria	0.3793
Epsilonproteobacteria	0.0991	Anaerolineae	0.1432	Alphaproteobacteria	0.2470
vadinBA26	0.0938	vadinBA26	0.1137	Acidobacteria	0.1932
Sphingobacteria	-0.0978	Planctomycetacia	-0.0653	Sphingobacteria	-0.1502
Gammaproteobacteria	-0.0979	Chloroplast	-0.0718	vadinBA26	-0.1815
Planctomycetacia	-0.1494	Flavobacteria	-0.1888	Flavobacteria	-0.2016
Flavobacteria	-0.1497	Sphingobacteria	-0.1895	GIF9	-0.2651
Alphaproteobacteria	-0.7956	Gammaproteobacteria	-0.8434	Epsilonproteobacteria	-0.3317

Figure 3.13: PCA of phylum level bacterial relative abundances with the vectors indicating the loadings of specific phyla. The ordinal hulls group samples by region.
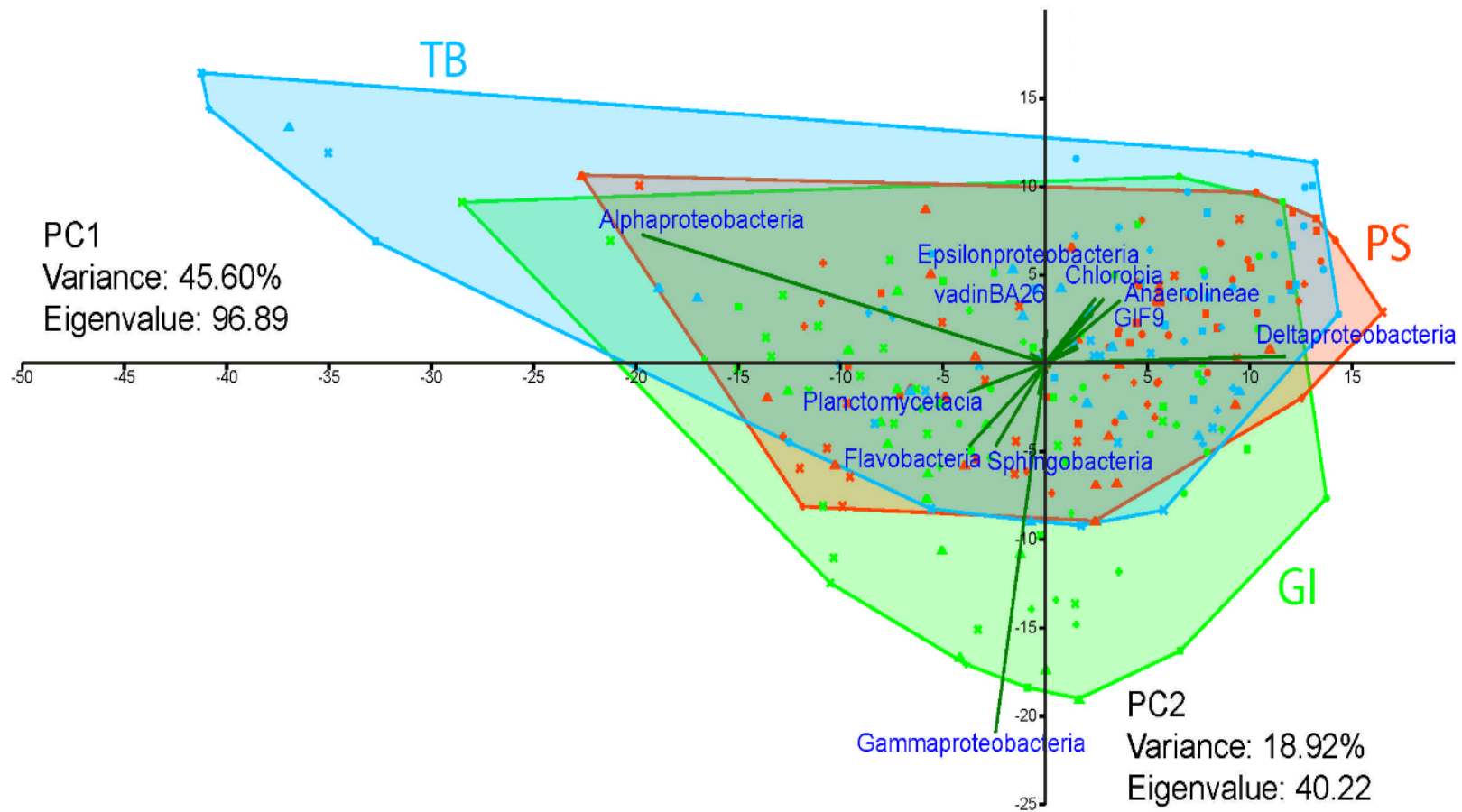
Figure 3.14: PCA of class level bacterial relative abundance with the vectors indicating the loadings of specific phyla. The ordinal hulls group samples by region.

Core Microbiome Membership

To evaluate the presence and membership of a core microbiome, samples from each sampling event were merged, which included the MS sample if collected (Table 2.1). Good's coverage values for the merged samples range from 88.3% to 90.1%, indicating adequate coverage of the total bacterial community for OTU-based analyses. OTUs calculated at 95% similarity for each sample totaled 662,450 and each sample contained an average of 2,704 OTUs. Of the 47 merged samples, only 20 samples (42%) shared OTUs that comprised 1% or more of the community, and only 3 (15%) of the samples had shared OTUs at greater than 2% of the community relative abundances. For the shared OTUs, 73% were affiliated with Proteobacteria, of which 52% were Deltaproteobacteria and 31% were Gammaproteobacteria (Figure 3.15). The most common core OTU belonged to the Deltaproteobacteria, either being closely related to previously uncultured groups or the Desulfobacteraceae, and specifically to the genus *Desulfococcus*. These groups are sulfate-reducing bacteria that can utilize low chain length *n*-alkanes (C_4 to C_{18}) (Rueter et al., 1994; Aeckersberg et al., 1998). Gammaproteobacteria, comprised some shared OTUs, mostly at Grand Isle, and Deltaproteobacteria were only shared at Port Sulphur and Terrebonne Bay.

When grouped by depth from each region, only 21 (32.8%) shared OTUs at the 1% relative abundance level from 64 merged samples were obtained, and 4 (6.3%) samples shared OTUs at greater than 2% relative abundance (Figure 3.16). Alpha-, Beta-, Delta-, and Epsilonproteobacteria, as well as Chlorobia, Flavobacteria, Planctomycetacia, Sphingobacteria, and one subsection of Cyanobacteria, were represented.
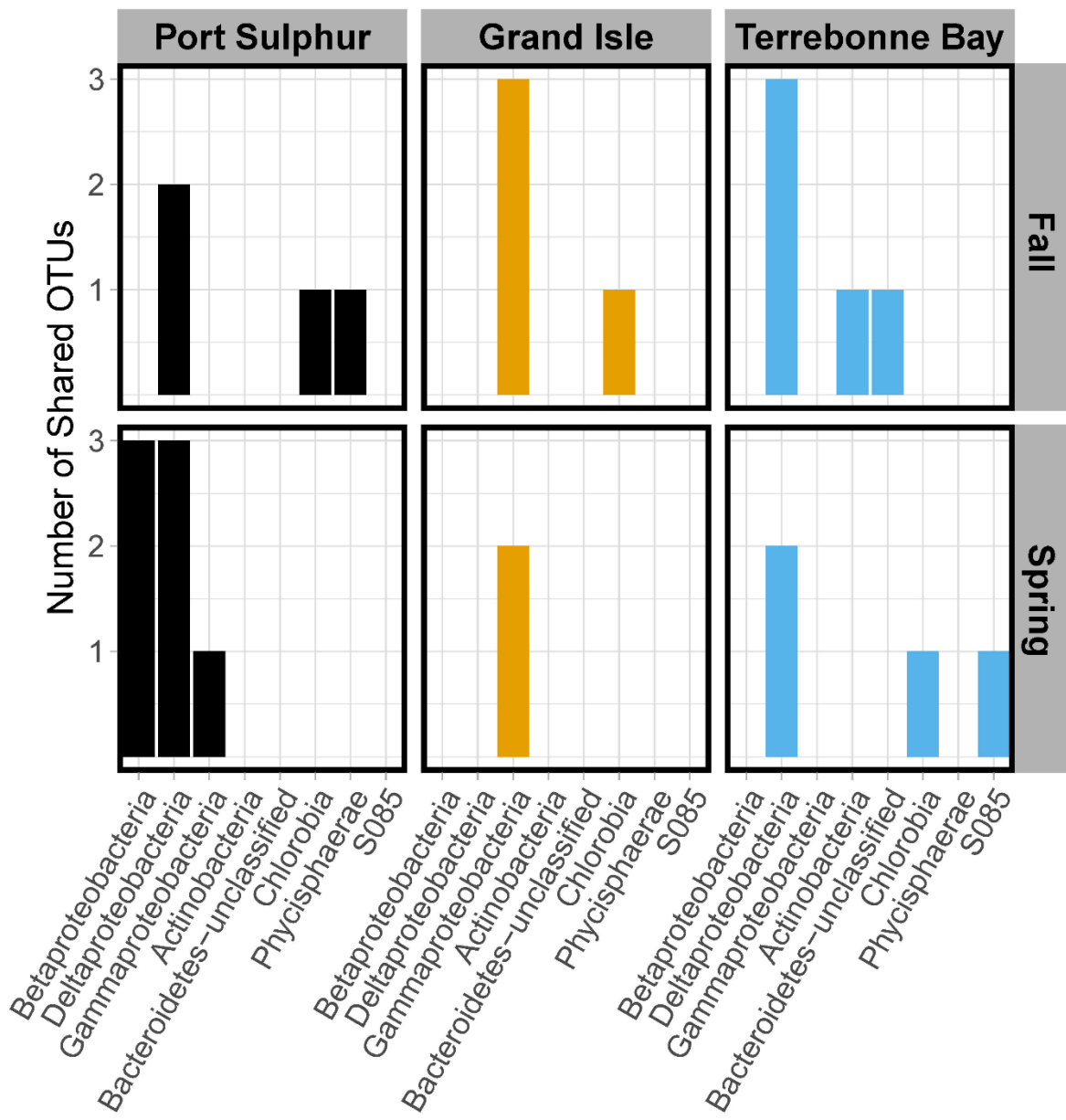
Figure 3.15: Histogram of the OTU counts of bacterial class from samples merged by site at each region for each sampling event at 95% sequence similarity that contain a core microbiome at 1% or greater by relative abundance. The season is noted on the right side of the plot.
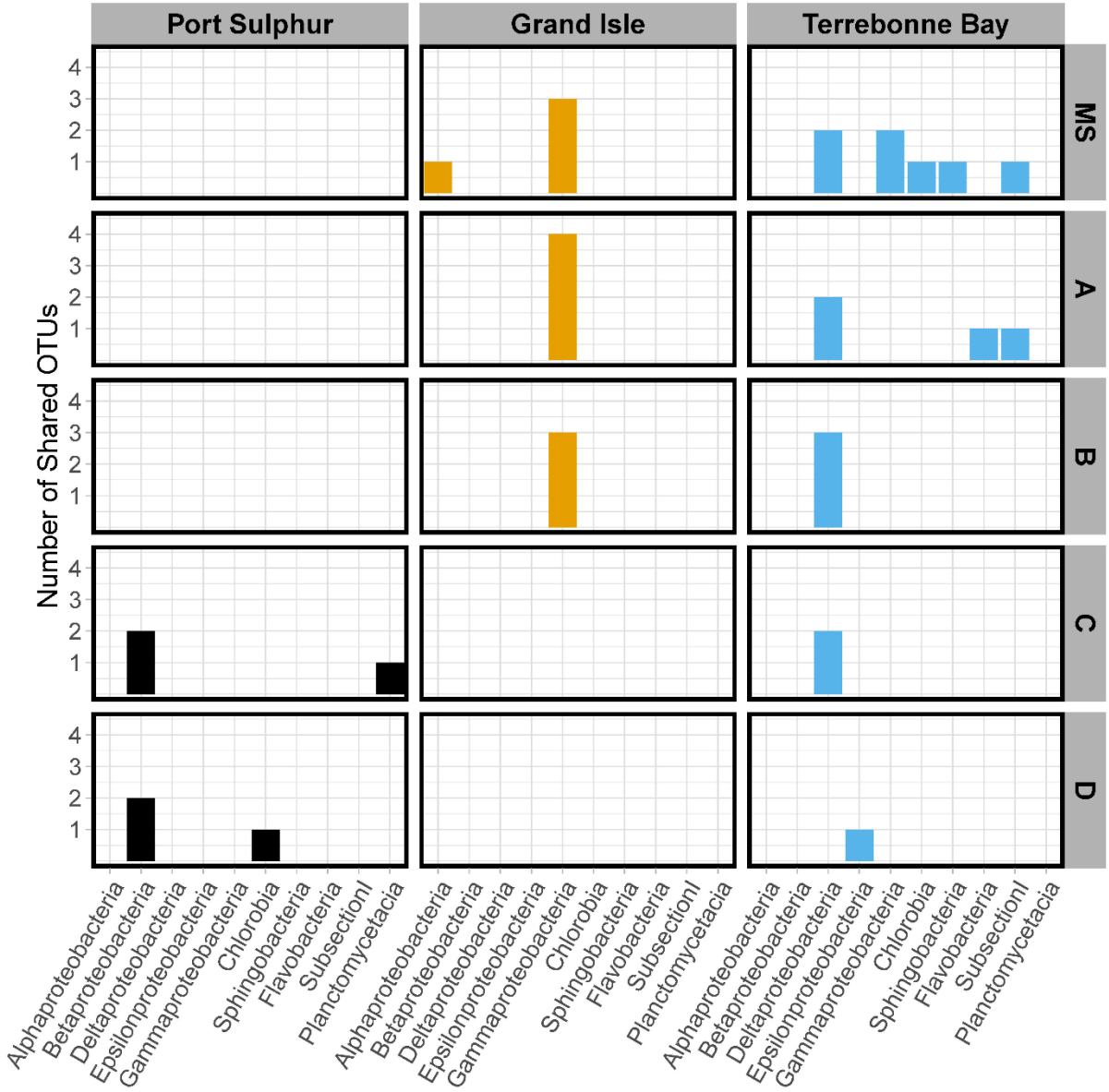
Figure 3.16: Histogram of the OTU counts of bacterial class from samples merged by depth at each region for each sampling event. The depth is noted on the right side of the plot. Plots with no bars did not contain a taxonomic group in the microbiome at 1% or greater by relative abundance.

The shared OTUs were predominantly related to the Gammaproteobacteria (35%) at

Grand Isle within upper depths (MS, A, B), or to the Deltaproteobacteria (26%) at Terrebonne

Bay from the upper depths (MS, A-C). All Deltaproteobacteria at Terrebonne Bay belonged to

the family Desulfobacteraceae. The shared OTUs at Port Sulphur were only from the lower soil

depths (C, D), and were predominantly related to Betaproteobacteria, and specifically, the

Nitrosomonadales that are known to be ammonium-oxidizers (Rosenberg, 2013).

Environmental Controls on Bacterial Communities

To determine what environmental controls were potentially significant in explaining

compositional variability in the dataset, and at each region, a general linear model was run with a

Lasso regularization. The model parameters were reduced from a total of 34 measured

parameters to 11 based on the VIF: number of plant species observed, MII value, CPI, low

molecular weight n-alkanes (C10-C18), inland water depth, canopy height, vegetation coverage

(%), edge water pH, edge water salinity (field collected), edge water temperature, and salinity

(CRMS collected). Based on the general linear model for all samples, a lambda was selected

with +0.05 minimum MSE ($\lambda = 1.54$, % deviance = 23). The selected lambda reduced the

number of influential variables from 11 to 10 (Table 3.4 & Figure 3.17). The same generalized

linear modeling using Lasso parameter selection and 5-fold cross validation was completed for

each region using a lambda selection +0.5 SE of the calculated model minimum MSE (Figure

3.18). In Port Sulphur, the lambda selection ($\lambda = 1.27$, % deviance = 37.5) reduced the number

of influential variables from 11 to 10. In Grand Isle, the lambda selection ($\lambda = 1.71$, % deviance

= 38) reduced the number of influential variables to 9, and in Terrebonne Bay, the lambda

selection ($\lambda = 2.5$, % deviance = 42.7%) reduced the variable number to 6.

Table 3.4: Parameter selection based on a general linear model using Gaussian lasso regularization and a lambda selection of +0.5SE from cross validation calculated MSE. Environmental parameters that were selected to be predictive in the model are denoted with a check and highlighted in green. Parameters not selected are denoted with a dash. All parameters were either log(n+1)-transformed or Hellinger-transformed prior to modeling.

Environmental Parameter	All Samples	Port Sulphur	Grand Isle	Terrebonne Bay
LMW Alkanes (C10-C18)	✓	✓	✓	✓
Carbon Preference Index	✓	-	✓	-
Canopy Height	✓	✓	✓	-
Vegetation Coverage	✓	✓	✓	✓
Inland Water Depth	✓	✓	✓	✓
Salinity-CRMS Station Logger	✓	✓	-	✓
Salinity-Field Measured	✓	✓	✓	-
Edge Water pH	✓	✓	✓	✓
Edge Water Temp	✓	✓	✓	-
Marsh Inundation Index (MII)	-	✓	-	-
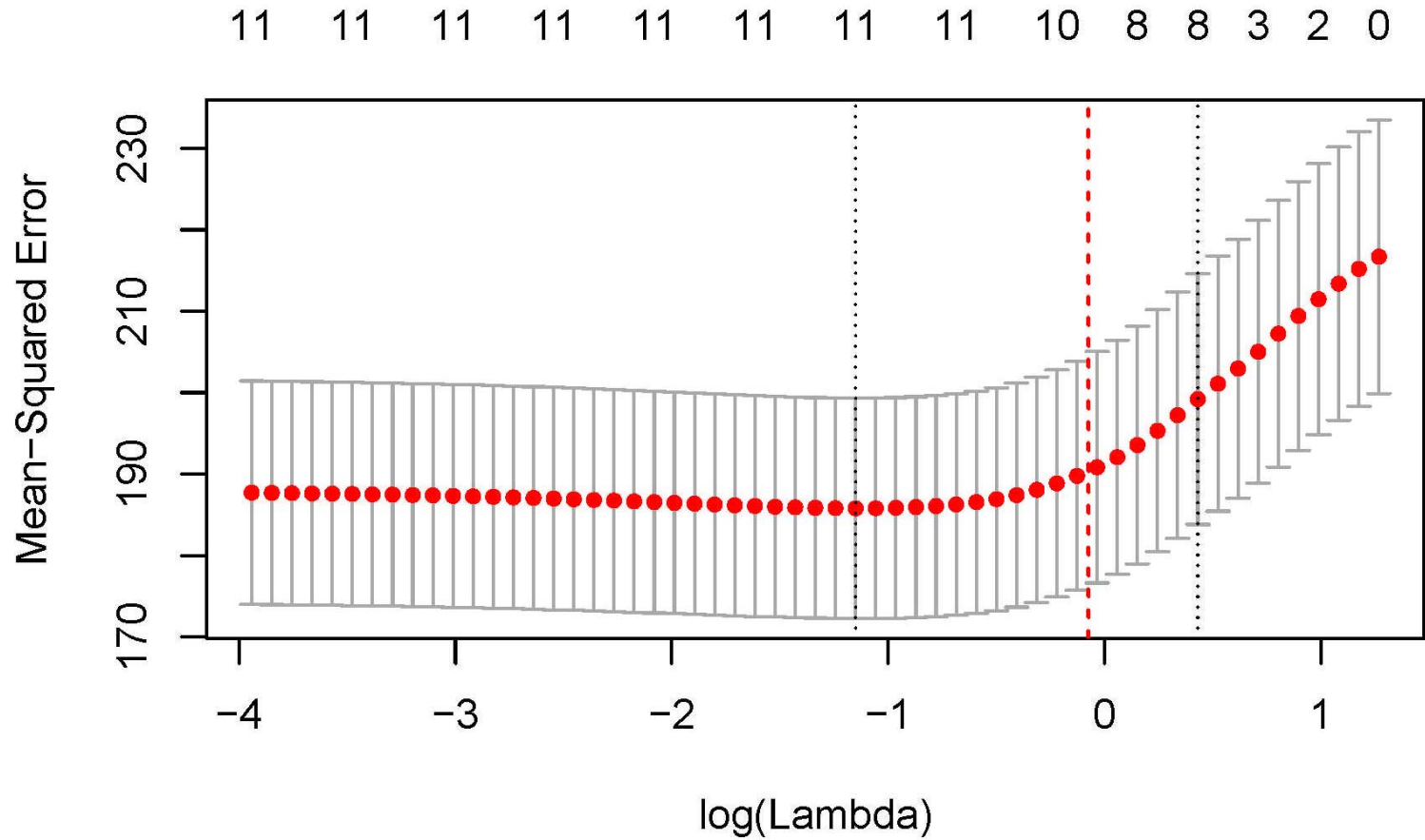
Figure 3.17:   Lambda selection based on the MSE calculated for the entire dataset using a general linear model with Lasso regularization and 10-fold cross validation. The x axis for each graph is the log of lambda, the y axis is the mean square error, and the top x axis shows the number of parameters associated with each lambda selected value. Error bars are ±1SE, dashed gray lines are minimum and +1SE of the minimum lambda selection. The dashed red vertical line is the +0.5SE lambda selection.
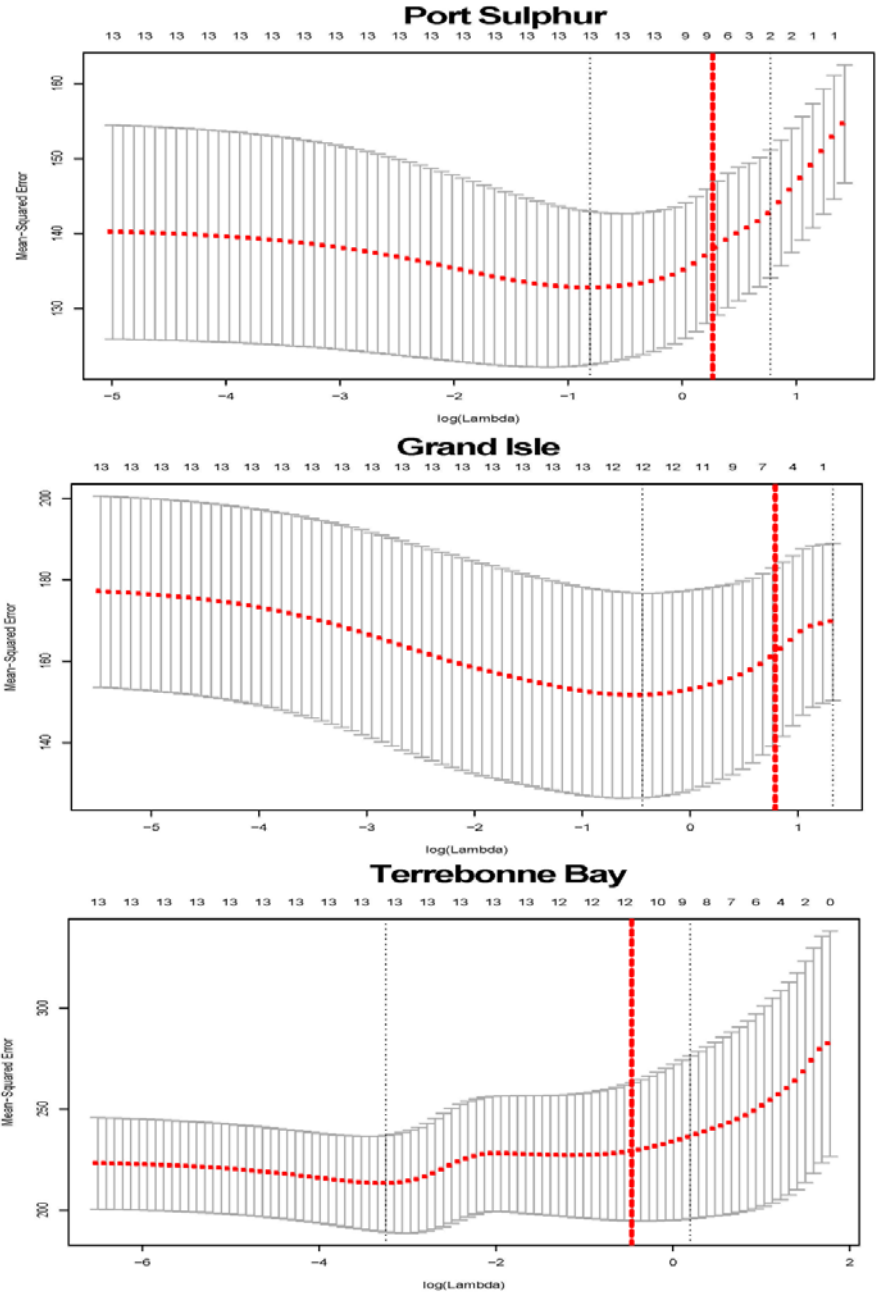
Figure 3.18: Lambda selection based on the MSE calculated for each region using a general linear model with Lasso regularization and 5-fold cross validation. The x axis for each graph is the log of lambda, the y axis is the mean square error, and the top x axis shows the number of parameters associated with each lambda selected value. Error bars are ±1SE, dashed gray lines are minimum and +1SE of the minimum lambda selection. The dashed red vertical line is the +0.5SE lambda selection.

The model results indicated that the MII value did not have predictive power in explaining the bacterial composition at Grand Isle or Terrebonne Bay, but was predictive at Port Sulphur (Table 3.4). The parameters of vegetation coverage, edge water pH, LMW *n*-alkanes, and water height over the marsh also all had predictive power in the model. CPI was the only parameter not predictive at Port Sulphur and not influential at Terrebonne Bay. At Grand Isle, the MII value and CRMS-recorded salinity were not influential, yet all other parameters were. Terrebonne Bay had the least number of parameters that had predictive power in explaining the bacterial communities, yet the model explained the most deviance out of all that were run.

Of these results, salinity was evaluated as being correlated with changes in bacterial community compositions (Jackson and Vallaire, 2009). Salinity data collected on site (i.e., not CRMS-collected) were compared to calculated Chao1 α-diversity index values. Minimal changes in bacterial diversity at Port Sulphur and Grand Isle were noted, but a positive increase in diversity with salinity was observed for Terrebonne Bay samples (Figure 3.19).

Flooding Controls on Bacterial Community Diversity

The MII values were used in multivariate analysis to determine the effect of flooding and inundation on the soil bacterial communities. Unlike PCA that is unconstrained, CCA used transformed environmental data to text for potential relationships between the bacterial communities constrained by specific environmental parameters. Many parameters could be evaluated, and flooding history based on MII values was selected for this thesis. Statistical significance of $\alpha = 0.05$ was assessed for the constraining variables and overall model using an ANOVA-like permutation test with 999 permutations (Table A.2) (Oksanen et al., 2007).
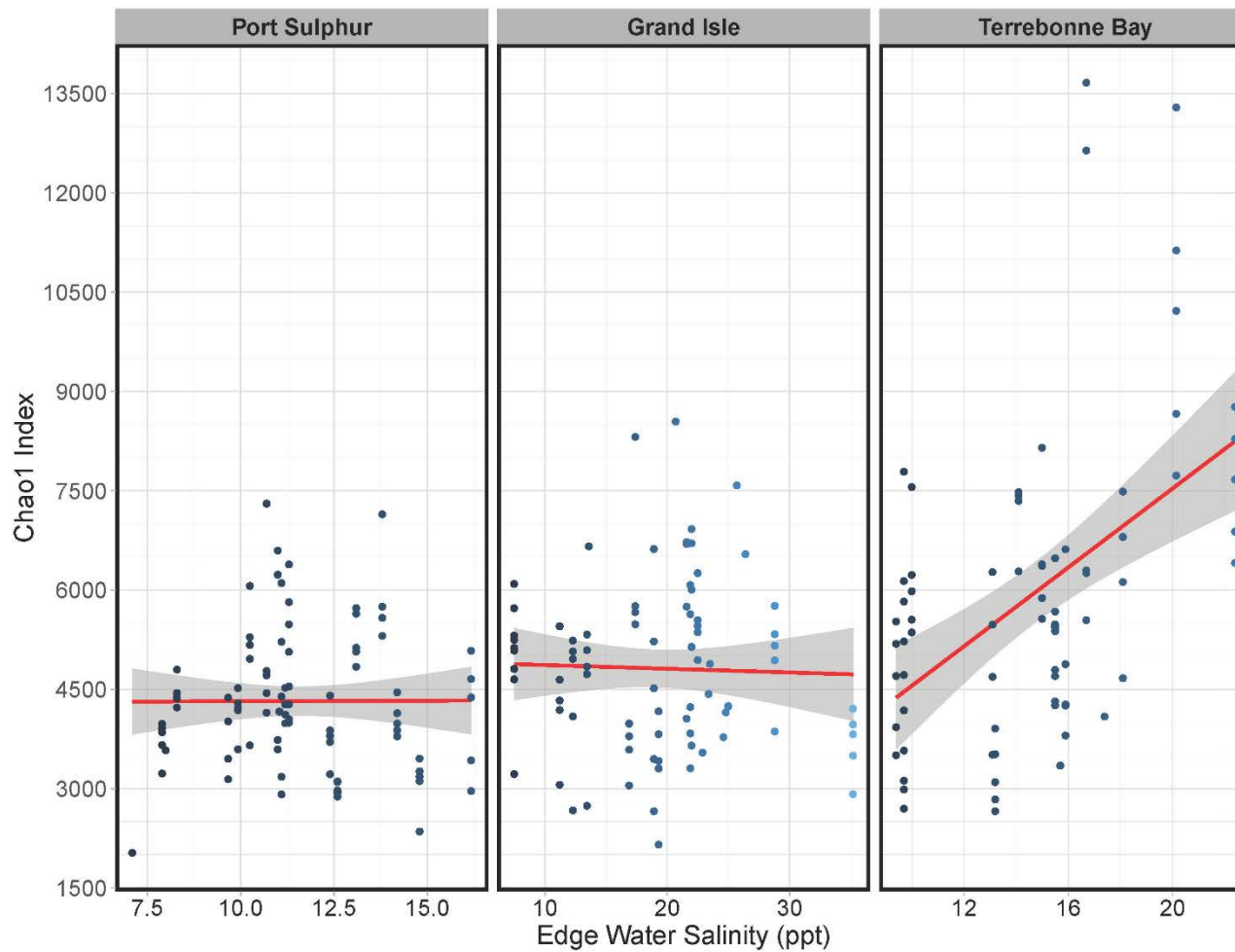
Figure 3.19: Chao1 species richness values versus edge water salinity from all samples compared by region. The diversity was calculated from 95% similarity threshold OTU analysis of each sample. Terrebonne Bay was the only significant ($R^2 = 0.22$, P-value <0.001) linear correlation between Chao1 diversity and salinity, all other regions were not significant.

Five different CCA models were completed: 1) all samples constrained by MII and region (Figure 3.20); 2) only samples with MII 0 or 3 constrained by MII (Figure 3.21); 3) Port Sulphur communities constrained by MII and sample depth (Figure 3.22); 3) Grand Isle communities constrained by MII and sample depth (Figure 3.23); and 5) Terrebonne Bay communities constrained by MII and depth (Figure 3.24). In all CCAs analyzed, the MII value was significant (P-value <0.05) for the Port Sulphur region, but not in the other two regions (P-value = 0.08) (Table A.3), as also indicated by Lasso parameter selection results.

The CCA of all samples (n = 245) used MII values and regional information as the constraining variables, and the overall model was significant (P-value = 0.001), as was MII value (P-value = 0.009) and regional classification (P-value = 0.001) (Table A.3). However, the constrained axes (CCA1 to CCA3) explained 9% of the total variation in bacterial composition at the class level (Table A.2). The first axis explained 5.1% of the variance, both the MII and regional differences were explained with the environmental loadings. The variation in CCA1 was predominantly due to the scores of GIF9, Candidate Division OP9, Dehalococcoidetes, and Fusobacteria (Table A.4). The second axis (CCA2) explained 2.9% of the variation and separated the regions of Port Sulphur and Grand Isle. The largest scores of CCA2 were for Candidate Division OP11, Fusobacteria, OPB35, and Cyanobacteria Subsection II.

The second CCA model was created using only the samples that were categorized as either MII 0 or 3, the largest MII value in the sampling set during sampling, and using the MII value as the only constraining variable (Figure 3.20). The plot was completed using a total of 53 samples from Terrebonne Bay and Port Sulphur.
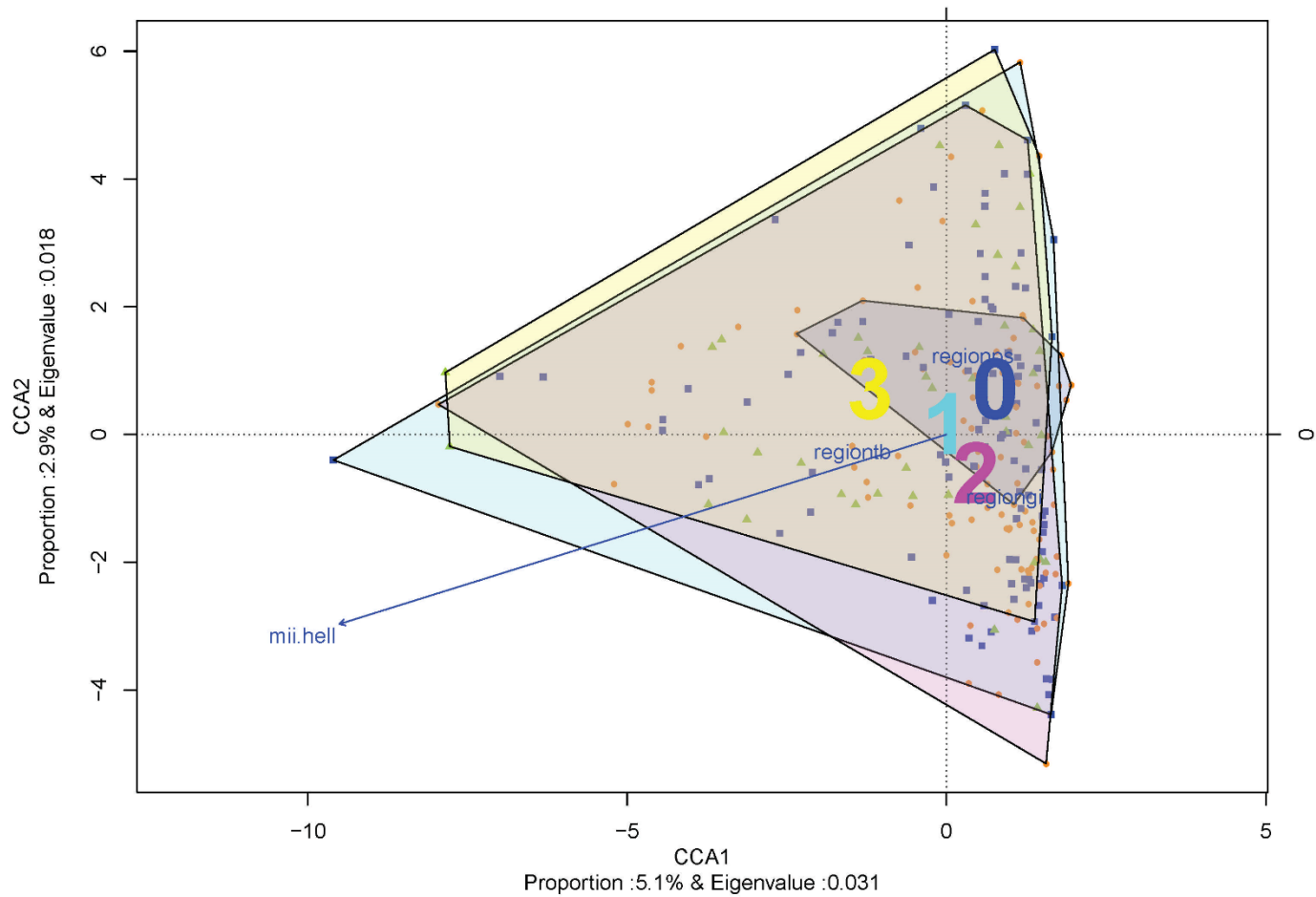
Figure 3.20: CCA of all samples with the MII value and region as constraining variables, grouped by MII value. The relative proportion of each axis variance and Eigenvalue are listed along the axis. Each ordinal hull is colored and labeled by MII value, with the sample also labeled by color.
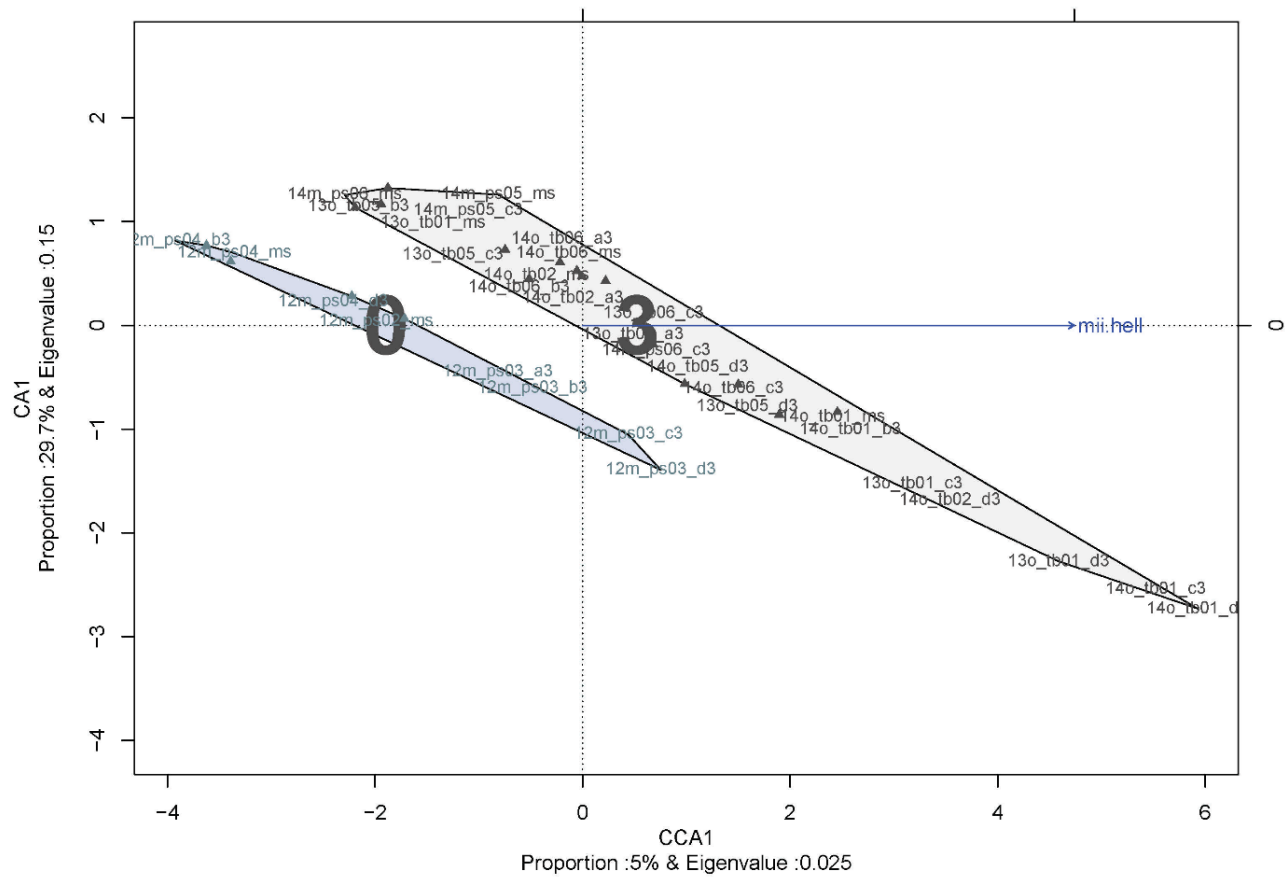
Figure 3.21: Ordination of the CCA with only samples of MII 0 and 3 with MII value as the constraining variable and samples grouped by MII value. Each grouping and samples within each grouping are color coordinated with the MII value displayed. The variance of each axis is displayed, the only constrained axis is CCA1. The secondary axis on the top of the graph denotes the strength of the constraining variable vector (MII) from 0 at the axis intercept to 1 at the first tick.
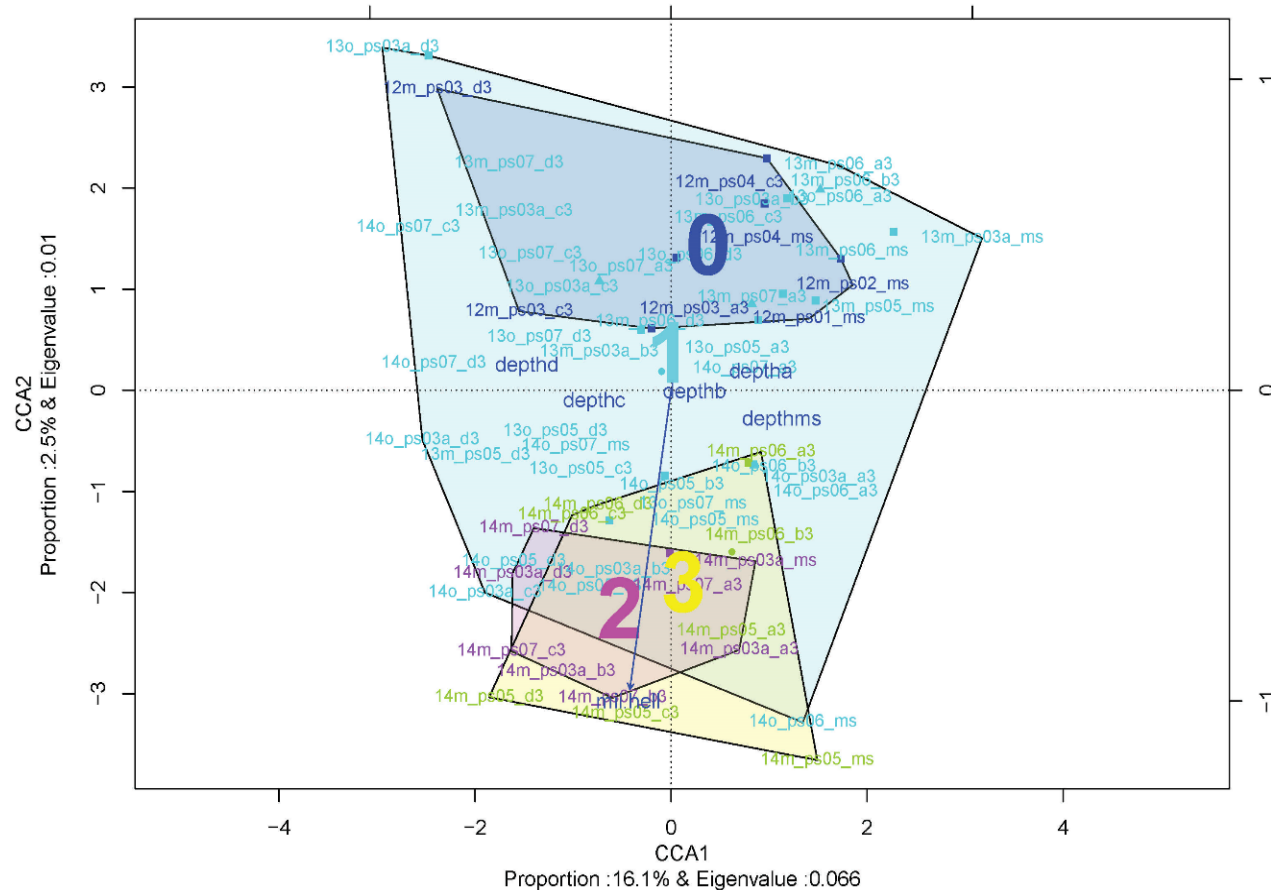
Figure 3.22: Ordination of the CCA with only samples from Port Sulphur with MII value and depth as the constraining variables, grouped by MII value. Each grouping and samples within each grouping are color coordinated with the MII value displayed. The variance of each axis is displayed. The secondary axis on the top and right of the graph show the strength of the constraining variable vector (MII) from zero to 1, with the scaled centroids of depth also plotted.

Figure 3.23: Ordination of the CCA with only samples from Grand Isle and with MII value and depth as the constraining variables, grouped by MII value. Each grouping and samples within each grouping are color coordinated with the MII value displayed. The variance of each axis is displayed. The secondary axis on the top and right of the graph show the strength of the constraining variable vector (MII) from zero to 1, with the scaled centroids of depth also plotted.

Figure 3.24: Ordination of the CCA with only samples from Terrebonne Bay, with MII value and depth as the constraining variables, grouped by MII value. Each grouping and samples within each grouping are color coordinated with the MII value displayed. The variance of each axis is displayed. The secondary axis on the top and right of the graph show the strength of the constraining variable vector (MII) from zero to 1, with the scaled centroids of depth also plotted.

MII 0 conditions were only met during May 2012 in Port Sulphur, but the MII 3 conditions were met by samples in both Terrebonne Bay and Port Sulphur. The MII value (P-value = 0.017) and overall model (P-value = 0.01) were both significant (Table A.3). The single constrained axis (CCA1) explained 5% of the bacterial variation, due to the scores of Candidate Division OP11, SAR202, SO85, Dehalococcoidetes, and uncultured Cyanobacteria (Table A.4). The second axis was unconstrained (CA1), and explained 35% of the variation unexplained by the MII due to scores for GIF9, unclassified TA06, Candidate Division OP9, and uncultured Cyanobacteria.

The sampling depth was used as the other environmental constraining variable for each regional CCA and grouped by the MII value classification. For Port Sulphiur, a CCA model was run with 88 samples using the Hellinger-transformed MII values and depth data as constraining variables. There were 22 MS samples and 18 core depths (A-D) with only one sample missing (Table 2.1). The constraining variables explained 20.6% of the variance in the bacterial communities. The cumulative proportion of the first two axes (Table A.2) explained 18.7% of the variance. CCA 1 explained 16.1% of the variance due to the scores of Dehalococcoidetes, Epsilonproteobacteria, Candidate Division OP9, and Cyanobacteria Subsection 1. CCA2 explained 2.5% of the variance due to the scores of KD4-96, Cyanobacteria Subsections IV and III, and Candidate Divisions OP11 and OP10. The vector of MII value was associated with CCA2, and the sampling depths were associated with CCA1. For Grand Isle, there were 22 MS samples and 15 core samples from all depths (Table 2.1). Constraining variables in the Grand Isle CCA explained 22.2% of the total variation, with CCA1 explaining 17.8% of the variation and CCA2 explaining 2.5% (Table A.2), predominately due to Dehalococcoidetes, CD-TG-1 Lineage IV, unclassified WCHB1-60, vadin BA26, and, in the positive direction, Cyanobacteria

Subsection I. Along CCA2, the bacterial classes that explained variation included Fusobacteria, vadinHA49, Dehalococoidetes, and Cyanobacteria Subsection II, which were closely associated with the MII vector. For the Terrebonne Bay CCA, there were samples (n = 75) collected during MII values 1 through 3 (Figure 3.23), which comprised 15 samples per depth. Depth was significant in explaining community variance (P-value = 0.001), but MII values were not (P-value = 0.08) (Table A.3). The overall CCA model was significant (P-value = 0.001) and all constraining variables explained 17.7% of the variance. CCA1 explained 13.6% of the variance and changes in depth, influenced by RF3, Lineage I Endomicrobia, Epsilonproteobacteria, Dehalococcoidetes, and vadinBA26 (Figure A.6). CCA2 explained 2.2% of the variance and was associated with the MII vector, and was explained by SAR202, Epsilonproteobacteria, Spartobacteria, and WD272.

CHAPTER FOUR - DISCUSSION

Microbial communities in coastal salt marshes are responsible for important biogeochemical processes, including organic matter decomposition, nitrogen fixation, sulfate reduction, and methanogenesis. A better understanding of the processes that govern salt marsh microbial ecosystems has been needed because many of the earlier studies, particularly focused in the marshes in southern Louisiana, have been done at broad, ecosystem-scales (Kirby and Gosselink, 1976; Gosselink and Pendleton, 1984; Sasser, 1994; Visser et al., 1998). At the microbial scale, the taxonomic diversity and inferred ecological function of bacterial communities can indicate overall marsh system health (Blum et al., 2004; Bowen et al., 2009; Jackson and Vallaire, 2009; Beazley et al., 2012; Bowen et al., 2012; Mahmoudi et al., 2013; Graves et al., 2016), particularly in light of the impacts of natural and anthropogenic stressors to these systems (Rabalais et al., 2002; Mendelssohn et al., 2012; Zou et al., 2015). Yet, few studies have identified the diversity, taxonomic representation, and community structure of bacterial communities from Louisiana marshes, or characterized how diversity changes are affected by environmental conditions. Therefore, the goals of this thesis were to use 16S rRNA gene sequences to uncover bacterial diversity in salt marsh soils and to determine which environmental parameters, including water inundation frequency and depth, vegetation, and salinity, contributed to the most variance in the taxonomic diversity of marsh soil microbiomes through time. The analyses required a multidisciplinary, data-driven approach to determine what environmental measurements would be useful in predicting bacterial community changes, especially changes in marsh elevation over time and the impact of marsh flooding.

Similarity of Marsh Soil Microbiomes

According to the α-diversity indices, the soil samples had high bacterial diversity, but there was no distinct core microbiome where OTUs with >1% relative abundances were shared across all samples. There were, however, many shared bacterial communities at much lower relative abundances, which may indicate similar taxonomic and functional patterns among the few shared communities with depth at each region (Schimel and Schaeffer, 2015). Moreover, the high diversity translated to there being >80% of the taxonomic representation that was shared at the phylum level, even if there were not shared OTUs, despite geographic separation and seasonal differences.

The Proteobacteria was the most abundant taxonomic group retrieved from all the soil samples, and Proteobacteria were also associated with the majority of shared OTUs. In general, Proteobacteria have been identified previously as the most abundant phylum in the soil samples, and the different proteobacterial communities, along with Bacteroidetes and Actinobacteria, have been associated with the decomposition of plant organic matter, specifically lignocellulose (Buchan et al., 2003) or even oil-related compounds, as was identified after the Deepwater Horizon oil spill (Beazley et al., 2012). The relative abundances of proteobacterial communities, specifically at the class level, from the oil spill research were similar to the relative abundances for the various proteobacterial groups retrieved from this study (Atlas and Hazen, 2011; Beazley et al., 2012; Sims et al., 2013; King et al., 2015)

The greatest differences in bacterial community compositions were between the uppermost soil samples and the deepest sampled depths. Samples at each depth were equally dissimilar to changes temporally or spatially, and were attributed to the same dissimilar

communities. The deposition of organic matter from winter wind-driven flooding or vegetation die-off after the growing season similarly affects upper cores through sampling, and geochemical changes with depth appear to be independent. As accretion rates vary through time, marshes are periodically more or less flooded at each region, yet the underlying processes are consistently changing and affecting the same communities at the surface and at depth similarly According to the literature, the upper few millimeters of marsh soil have negligible dissolved oxygen concentrations due to rapid deposition and decomposition of organic matter by microorganisms (Kirby and Gosselink, 1976; White et al., 1978). It is likely that the shift from oxygen-enriched surface soil to oxygen-depleted soil at depth accounts for the community compositional differences identified in this study. Moreover, the controls on oxygen levels in the soils may be linked to the *S. alterniflora* productivity associated with flooding (Teal and Kanwisher, 1966). Future research should include oxygen measurements from the soils to verify the role of oxygen in controlling bacterial diversity with soil depth. Moreover, the effect of organic matter deposition, which affects marsh accretion rates, should be evaluated against the bacterial community compositions. Rapid rates of marsh accretion that keep up or exceed current rates of sea-level rise should influence the bacterial community diversity and biogeochemical processes.

Influential Environmental Parameters

The changes in microbial community taxonomic representation at the phylum and class levels, while small (<30%), were evaluated against a range of environmental controls. Lasso regularization was used to identify environmental parameters that could predict differences and changes in bacterial community compositions. Terrebonne Bay had fewer predictive parameters compared to the other regions, indicating that controls on bacterial diversity at Terrebonne Bay

were dissimilar to Port Sulphur and Grand Isle communities. Among the parameters, conditions related to vegetation and salinity were the most important in predicting marsh bacterial community changes at all regions.

At least one vegetation-related parameter, such as canopy height, vegetation cover, or species, was useful to explain changes in bacterial diversity at all regions, and all of the vegetation-related parameters were useful in the overall model. Plant communities are known to have distinct rhizosphere microbial communities (Berg and Smalla, 2009) that affect above- and below-ground biomass. Variable density and plant height in each region were influential to explain bacterial diversity, and these parameters have been found by other studies (Blum, 1993; Rooney-Varga et al., 1997; Rietl et al., 2016).

Shared OTUs in deeper soil samples at Port Sulphur were associated with moderate salinity values, which was not comparable to other regions. The salinity measurements at Port Sulphur decreased with periods of flooding, yet this did not influence Chao1 diversity calculations. The only significant change in diversity and salinity occurred at Terrebonne Bay, where higher salinity values correlated to greater taxonomic diversity. There was also a positive relationship between salinity and water height over the marsh for Terrebonne Bay samples.

Salinity typically has a strong effect on bacterial diversity (Weston et al., 2006; Edmonds et al., 2009; Jackson and Vallaire, 2009; Ikenaga et al., 2010; Morrissey et al., 2014); however, few studies have focused on the effects of how decreases in salinity, or freshening of the water, within a region impacts bacterial diversity (Hart et al., 1991; Chambers et al., 2013; Marks et al., 2016). Lower salinity with increased water depth for the Port Sulphur marshes could be

explained by increased freshwater diversions in the region, as well as changes in marsh accretion rates that no longer keep up with sea-level rise.

Lastly, the percentage of low chain *n*-alkanes was predictive at all regions. The selection of short- versus long-chain species was dependent on the VIF, yet the CPI could be used to infer if longer chain *n*-alkanes are predictive, as well. Of all samples, and especially at Grand Isle, both CPI and LMW *n*-alkanes were useful in modeling bacterial community changes. The variation in *n*-alkane chain length and total *n*-alkane concentrations at both Port Sulphur and Terrebonne Bay may be a result of the distance to open ocean, and other marsh processes and conditions that will require further research to elucidate.

Flooding History Controls on Bacterial Communities

Low lying marshes are flooded almost daily, so the duration of flooding likely does not explain changes in microbial communities adapted to those environments. Within all regions, water height over the marsh was predictive, but the MII values were not. When constrained, in all models the MII values identified trends in classes of Cyanobacteria and Chloroflexi. These two phyla are very diverse, and many cyanobacteria are capable of photosynthesis and nitrogen fixation (Church et al., 2005). The predictive power of MII values was only useful for the Port Sulphur communities, which was the region closest to the Mississippi River. In Port Sulphur, the river diversions are caused salinity reduction, and the relative marsh elevations are the highest compared to the other two regions. Port Sulphur marshes had the lowest rate of elevation increase and could be negatively impacted by sea-level rise and flooding more than at the other two regions. The Terrebonne Bay marshes were almost always inundated, and so the MII values and salinity measured in this region were unable to predict changes in the bacterial communities.

Conclusions

Bacterial communities from marsh soils in southern Louisiana share up to 80% of their taxonomic communities in common at the phylum level, despite different sampling depths, regional differences, and seasonal variability. Although inundation duration did not explain changes in the bacterial community compositions over time, the depth of water that had flooded the marshes did predict community changes, as well as salinity, plant biomass, n-alkane chain length measured from the soils. In the future, remediation efforts done to restore coastal salt marshes, and monitoring programs, should include accurate measurements of water flooding depth and salinity when understanding how soil bacterial communities are structured and function ecologically.

REFERENCES

Aeckersberg, F., Rainey, F.A., and Widdel, F., 1998, Growth, natural relationships, cellular fatty acids and metabolic adaptation of sulfate-reducing bacteria that utilize long-chain alkanes under anoxic conditions: Archives of Microbiology, v. 170, p. 361–369, doi: 10.1007/s002030050654.

Amaral-Zettler, L.A., Rocca, J.D., LaMontagne, M.G., Dennett, M.R., and Gast, R.J., 2008, Changes in microbial community structure in the wake of Hurricanes Katrina and Rita: Environmental science & technology, v. 42, p. 9072–9078, http://www.ncbi.nlm.nih.gov/pmc/articles/PMC2668980/.

Angermeyer, A., Crosby, S.C., and Huber, J.A., 2016, Decoupled distance-decay patterns between dsrA and 16S rRNA genes among salt marsh sulfate-reducing bacteria: Environmental Microbiology, v. 18, p. 75–86, doi: 10.1111/1462-2920.12821.

Atlas, R.M., and Hazen, T.C., 2011, Oil biodegradation and bioremediation: a tale of the two worst spills in US history: Environmental science & technology, v. 45, p. 6709–6715.

Beazley, M.J., Martinez, R.J., Rajan, S., Powell, J., Piceno, Y.M., Tom, L.M., Andersen, G.L., Hazen, T.C., van Nostrand, J.D., Zhou, J., Mortazavi, B., and Sobecky, P.A., 2012, Microbial community analysis of a coastal salt marsh affected by the Deepwater Horizon oil spill: PLoS ONE, v. 7, doi: 10.1371/journal.pone.0041305.

Benner, R., Maccubbin, A.E., and Hodson, R.E., 1984, Anaerobic biodegradation of the lignin and polysaccharide components of lignocellulose and synthetic lignin by sediment microflora: Applied and Environmental Microbiology, v. 47, p. 998–1004.

Benner, R., Moran, M.A., and Hodson, R.E., 1986, Biogeochemical cycling of lignocellulosic carbon in marine and freshwater ecosystems: Relative contributions of procaryotes and eucaryotes.: Limnology and Oceanography, v. 31, p. 89–100.

Berg, G., and Smalla, K., 2009, Plant species and soil type cooperatively shape the structure and function of microbial communities in the rhizosphere: FEMS Microbiology Ecology, v. 68, p. 1–13.

Blum, L.K., 1993, *Spartina alterniflora* root dynamics in a Virginia marsh: Marine Ecology Progress Series, v. 102, p. 697178.

Blum, L.K., Roberts, M.S., Garland, J.L., and Mills, A.L., 2004, Distribution of microbial communities associated with the dominant high marsh plants and sediments of the United States East Coast: Microbial Ecology, v. 48, p. 375–388, doi: 10.1007/s00248-003-1051-6.

Boesch, D.F., Josselyn, M.N., Mehta, A.J., Morris, J.T., Nuttle, W.K., Simenstad, C.A., and Swift, D.J.P., 1994, Scientific assessment of coastal wetland loss, restoration and management in Louisiana: Journal of Coastal Research, p. 1–103.

Boustany, R.G., 2010, Estimating the benefits of freshwater introduction into coastal wetland ecosystems in Louisiana: Nutrient and sediment analyses: Ecological Restoration, v. 28, p. 160–174.

Bowen, J.L., Byrnes, J.E.K., Weisman, D., and Colaneri, C., 2013, Functional gene pyrosequencing and network analysis: An approach to examine the response of denitrifying

bacteria to increased nitrogen supply in salt marsh sediments: Frontiers in Microbiology, v. 4, p. 1–12, doi: 10.3389/fmicb.2013.00342.

Bowen, J.L., Crump, B.C., Deegan, L. a, and Hobbie, J.E., 2009, Salt marsh sediment bacteria: their distribution and response to external nutrient inputs.: The ISME journal, v. 3, p. 924–934, doi: 10.1038/ismej.2009.44.

Bowen, J.L., Morrison, H.G., Hobbie, J.E., and Sogin, M.L., 2012, Salt marsh sediment diversity: a test of the variability of the rare biosphere among environmental replicates: The ISME Journal, v. 6, p. 2014–2023, doi: 10.1038/ismej.2012.47.

Bowen, J.L., Ward, B.B., Morrison, H.G., Hobbie, J.E., Valiela, I., Deegan, L.A., and Sogin, M.L., 2011, Microbial community composition in sediments resists perturbation by nutrient enrichment: The ISME journal, v. 5, p. 1540–1548.

Buchan, A., Newell, S.Y., Butler, M., Biers, E.J., Hollibaugh, J.T., and Moran, M.A., 2003, Dynamics of Bacterial and Fungal Communities on Decaying Salt Marsh Grass: Applied and Environmental Microbiology, v. 69, p. 6676–6687, doi: 10.1128/AEM.69.11.6676-6687.2003.

Campbell, B.J., and Kirchman, D.L., 2012, Bacterial diversity, community structure and potential growth rates along an estuarine salinity gradient: ISME Journal, v. 7, p. 210–220, doi: 10.1038/ismej.2012.93.

Center for Operational Oceanographic Products and Services, 2015, Mean Sea Level Trend 1947-2015 at station 8761724 Grand Isle, Louisiana (NOAA, Ed.):, http://tidesandcurrents.noaa.gov/sltrends/sltrends_station.shtml?stnid=8761724.

Cerco, C.F., and Cole, T., 1993, Three dimensional eutrophication model of the Chesapeake Bay: Journal of Environmental Engineering, v. 119, p. 1006–1025, doi: 10.1061/(ASCE)0733-9372(1993)119:6(1006).

Chambers, L., Osborne, T., and Reddy, K., 2013, Effect of salinity-altering pulsing events on soil organic carbon loss along an intertidal wetland gradient: a laboratory experiment: Biogeochemistry, v. 115, p. 363–383, doi: 10.1007/s10533-013-9841-5.

Chmura, G.L., Anisfeld, S.C., Cahoon, D.R., and Lynch, J.C., 2003, Global carbon sequestration in tidal, saline wetland soils: Global Biogeochemical Cycles, v. 17, p. 12, doi: 1111 10.1029/2002gb001917.

Church, M.J., Jenkins, B.D., Karl, D.M., and Zehr, J.P., 2005, Vertical distributions of nitrogen-fixing phylotypes at Stn ALOHA in the oligotrophic North Pacific Ocean: Aquatic Microbial Ecology, v. 38, p. 3–14, doi: 10.3354/ame038003.

Clarke, K.R., 1993, Non-parametric multivariate analyses of changes in community structure: Australian Journal of Ecology, v. 18, p. 117–143.

CO-OPS, and NOAA, 2016, NOAA Water Level (Tidal) Data of 205 Stations for the Coastal United States and Other Non-U.S. Sites:, http://www.tidesandcurrents.noaa.gov/nwlon.html.

Colwell, R.K., 2006, EstimateS.: Robert K. Colwell.

Couvillion, B.R., Barras, J.A., Steyer, G.D., Sleavin, W., Fischer, M., Beck, H., Trahan, N.,

Griffin, B., and Heckman, D., 2011, Land Area Change in Coastal Louisiana from 1932 to 2010 (U S Department of the Interior, Ed.): U.S. Geological Survey Scientific Investigations Map 3164, p. 12, doi: 1411331338.

Couvillion, B.R., Steyer, G.D., Wang, H., Beck, H.J., and Rybczyk, J.M., 2013, Forecasting the Effects of Coastal Protection and Restoration Projects on Wetland Morphology in Coastal Louisiana under Multiple Environmental Uncertainty Scenarios: Journal of Coastal Research, p. 29–50, doi: http://dx.doi.org/10.2112/SI_67_3.

CPRA, 2017a, Coastwide Reference Monitoring System-Wetlands Monitoring Data: Coastal Information Management System (CIMS) Database, http://cims.coastal.louisiana.gov (accessed January 2017).

CPRA, 2017b, Louisiana's Comprehensive Master Plan for a Sustainable Coast:, http://coastal.la.gov/2017-coastal-master-plan/.

Craney, T.A., and Surles, J.G., 2002, Model-dependent variance inflation factor cutoff values: Quality Engineering, v. 14, p. 391–403.

Cronk, J.K., and Fennessy, M.S., 2016, Wetland plants: biology and ecology: CRC press, 210 p.

CWPPRA Task Force, 2015, The 2012 evaluation report to the US congress on the effectiveness of coastal wetlands planning, protection and restoration act projects.:

DeLaune, R.D., and Pezeshki, S.R., 1994, The Influence of subsidence and saltwater intrusion on coastal marsh stability: Louisiana Gulf Coast, U.S.A.: Journal of Coastal Research, p. 77–89, http://www.jstor.org/stable/25735591.

DiMarco, S.F., and Reid, R.O., 1998, Characterization of the principal tidal current constituents on the Texas-Louisiana shelf: Journal of Geophysical Research: Oceans, v. 103, p. 3093–3109.

Dini-Andreote, F., de Cassia Pereira e Silva, M., Triado-Margarit, X., Casamayor, E.O., van Elsas, J.D., and Salles, J.F., 2014, Dynamics of bacterial community succession in a salt marsh chronosequence: evidences for temporal niche partitioning: ISME J, v. 8, p. 1989–2001, http://dx.doi.org/10.1038/ismej.2014.54.

Dowd, S.E., Callaway, T.R., Wolcott, R.D., Sun, Y., McKeehan, T., Hagevoort, R.G., and Edrington, T.S., 2008, Evaluation of the bacterial diversity in the feces of cattle using 16S rDNA bacterial tag-encoded FLX amplicon pyrosequencing (bTEFAP): BMC microbiology, v. 8, p. 125.

Edgar, R.C., Haas, B.J., Clemente, J.C., Quince, C., and Knight, R., 2011, UCHIME improves sensitivity and speed of chimera detection: Bioinformatics, v. 27, p. 2194–2200.

Edmonds, J.W., Weston, N.B., Joye, S.B., Mou, X., and Moran, M.A., 2009, Microbial community response to seawater amendment in low-salinity tidal sediments: Microbial Ecology, v. 58, p. 558–568, doi: 10.1007/s00248-009-9556-2.

Falkowski, P.G., Barber, R.T., and Smetacek, V., 1998, Biogeochemical controls and feedbacks on ocean primary production: Science, v. 281, p. 200–206.

Folse, T.M., West, J.L., Hymel, M.K., Troutman, J.P., Sharp, A., Weifenbach, D., Mcginnis, T.,

and Rodrigue, L.B., 2014, A Standard Operating Procedures Manual for the Coast-Wide Reference Monitoring System- Wetlands: Methods for Site Establishment, Data Collection, and Quality Assurance/Quality Control: Louisiana Coastal Protection and Restoration Authority, v. Methods, p. 228.

Friedman, J., Hastie, T., and Tibshirani, R., 2009, glmnet: Lasso and elastic-net regularized generalized linear models: R package version, v. 1.

Gebrehiwet, T., Koretsky, C.M., and Krishnamurthy, R. V, 2008, Influence of Spartina and Juncus on saltmarsh sediments. III. Organic geochemistry: Chemical Geology, v. 255, p. 114–119.

Glick, P., Clough, J., Polaczyk, A., Couvillion, B., and Nunley, B., 2013, Potential effects of sea-level rise on coastal wetlands in southeastern Louisiana: Journal of Coastal Research, p. 211–233, doi: 10.2112/SI63-0017.1.

Good, I.J., 1953, The population frequencies of spiecies and the estimation of population parameters: Biometrika, v. 40, p. 237–264, doi: 10.1093/biomet/40.3-4.237.

Gosselink, J., and Pendleton, E.C., 1984, The ecology of delta marshes of coastal Louisiana: a community profile: DTIC Document.

Graham, M.H., 2003, Confronting Multicollinearity in Ecological: Ecology, v. 84, p. 2809–2815.

Graves, C.J., Makrides, E.J., Schmidt, V.T., Giblin, A.E., Cardon, Z.G., and Rand, D.M., 2016, Functional responses of salt marsh microbial communities to long-term nutrient enrichment: Applied and Environmental Microbiology, v. 82, p. 2862–2871, doi: 10.1128/AEM.03990-15.

Guerry, P., LeBlanc, D.J., and Falkow, S., 1973, General method for the isolation of plasmid deoxyribonucleic acid: Journal of Bacteriology, v. 116, p. 1064–1066.

Hart, B.T., Bailey, P., Edwards, R., Hortle, K., James, K., McMahon, A., Meredith, C., and Swadling, K., 1991, A review of the salt sensitivity of the Australian freshwater biota: Hydrobiologia, v. 210, p. 105–144, doi: 10.1007/BF00014327.

Hartman, W.H., Richardson, C.J., Vilgalys, R., and Bruland, G.L., 2008, Environmental and anthropogenic controls over bacterial communities in wetland soils: Proceedings of the National Academy of Sciences, v. 105, p. 17842–17847.

Hooper-Bui, L.M., Rabalais, N.N., Engel, A.S., Turner, R.E., McClenachan, G., Roberts, B., Overton, E.B., Justic, D., Strudivant, K., and Brown, K., 2014, Overview of Research into the Coastal Effects of the Macondo Blowout from the Coastal Waters Consortium: A GoMRI Consortium, *in* International Oil Spill Conference Proceedings, American Petroleum Institute, v. 2014, p. 604–617.

Iavorivska, L., Boyer, E.W., and Dewalle, D.R., 2016, Atmospheric deposition of organic carbon via precipitation: Atmospheric Environment, v. 146, p. 153–163, doi: 10.1016/j.atmosenv.2016.06.006.

Ikenaga, M., Guevara, R., Dean, A.L., Pisani, C., and Boyer, J.N., 2010, Changes in community structure of sediment bacteria along the Florida coastal everglades marsh–mangrove–

seagrass salinity gradient: Microbial ecology, v. 59, p. 284–295.

Jackson, C.R., and Vallaire, S.C., 2009, Effects of salinity and nutrients on microbial assemblages in Louisiana wetland sediments: Wetlands, v. 29, p. 277–287.

Joye, S.B., Teske, A.P., and Kostka, J.E., 2014, Microbial dynamics following the Macondo oil well blowout across Gulf of Mexico environments: BioScience, v. 64, p. 766–777, doi: 10.1093/biosci/biu121.

Kaswadji, R.F., Gosselink, J.G., and Turner, R.E., 1990, Estimation of primary production using five different methods in a Spartina alterniflora salt marsh: Wetlands Ecology and Management, v. 1, p. 57–64, doi: 10.1007/BF00177280.

King, G.M., 1988, Patterns of sulfate reduction and the sulfur cycle in a South Carolina salt marsh: Limnology and Oceanography, v. 33, p. 376–390, doi: 10.4319/lo.1988.33.3.0376.

King, G.M., Kostka, J.E., Hazen, T.C., and Sobecky, P.A., 2015, Microbial responses to the Deepwater Horizon oil spill: from coastal wetlands to the deep sea: Annual review of marine science, v. 7, p. 377–401.

Kirby, C.J., and Gosselink, J.G., 1976, Primary production in a Louisiana Gulf Coast Spartina alterniflora marsh: Ecology, v. 57, p. 1052–1059, http://www.jstor.org/stable/1941070.

Kolb, C.R., and Van Lopik, J.R., 1958, Geology of the Mississippi River deltaic plain, southeastern Louisiana: Technical Report, v. I, p. 1–138.

Koretsky, C.M., Van Cappellen, P., DiChristina, T.J., Kostka, J.E., Lowe, K.L., Moore, C.M., Roychoudhury, A.N., and Viollier, E., 2005, Salt marsh pore water geochemistry does not correlate with microbial community structure: Estuarine, Coastal and Shelf Science, v. 62, p. 233–251.

Koretsky, C.M., Haveman, M., Cuellar, A., Beuving, L., Shattuck, T., and Wagner, M., 2008, Influence of Spartina and Juncus on saltmarsh sediments. I. Pore water geochemistry: Chemical Geology, v. 255, p. 87–99.

Koster, D., and Suarcz, J., 1995, Relative contributions of land and ocean processes to precipitation variability: v. 100.

Kostka, J.E., Roychoudhury, A., Cappellen, P. Van, Kostka, J.E., and Roychoudhury, A., 2008, Rates and controls of anaerobic microbial respiration across spatial and temporal gradients in saltmarsh sediments: Biogeochemistry, v. 60, p. 49–76.

Lamers, L.P.M., van Diggelen, J.M.H., Op den Camp, H.J.M., Visser, E.J.W., Lucassen, E.C.H.E.T., Vile, M.A., Jetten, M.S.M., Smolders, A.J.P., and Roelofs, J.G.M., 2012, Microbial Transformations of Nitrogen, Sulfur, and Iron Dictate Vegetation Composition in Wetlands: A Review: Frontiers in Microbiology, v. 3, p. 156, doi: 10.3389/fmicb.2012.00156.

Larsen, L.G., Serena Moseman, Alyson Santoro, Kristine Hopfensperger, and Amy Burgin, 2010, A complex-systems approach to predicting effects of sea level rise and nitrogen loading on nitrogen cycling in coastal wetland ecosystems, *in* Eco-DAS VIII Symposium Proceedings, The American Society of Limnology and Oceanography, Inc., p. 67–92,

http://pubs.er.usgs.gov/publication/70146200.

Legendre, P., and Gallagher, E.D., 2001, Ecologically meaningful transformations for ordination of species data: Oecologia, v. 129, p. 271–280, doi: 10.1007/s004420100716.

Liu, C., 2011, Geomicrobiology of Louisiana coastal marshes before and after the Deepwater Horizon oil spill:

Louisiana Department of Natural Resources, 2011, Louisiana Coastal Facts:, http://www.ocpr.louisiana.gov/coastalfacts.asp.

Lyman, J., and Fleming, R.H., 1940, Composition of sea water: Journal of Marine Reserach, v. 3, p. 134–146.

Mac, M.J., Opler, P.A., Puckett-Haeckler, C.E., and Doran, P.D., 1998, Status and trends of the nation's biological resources: Coastal Louisiana (US Department of the Interior, Ed.): v. 2, p. 385–436.

Magurran, A.E., 2013, Measuring biological diversity: John Wiley & Sons.

Mahmoudi, N., Porter, T.M., Zimmerman, A.R., Fulthorpe, R.R., Kasozi, G.N., Silliman, B.R., and Slater, G.F., 2013, Rapid degradation of Deepwater Horizon spilled oil by indigenous microbial communities in Louisiana salt marsh sediments: Environmental science & technology, v. 47, p. 13303–13312.

Marks, B.M., Chambers, L., and White, J.R., 2016, Effect of fluctuating salinity on potential denitrification in coastal wetland soil and sediments: Soil Science Society of America Journal, v. 80, p. 516–526.

Mason, O.U., Canter, E.J., Gillies, L.E., Paisie, T.K., and Roberts, B.J., 2016, Mississippi River Plume Enriches Microbial Diversity in the Northern Gulf of Mexico: Frontiers in microbiology, v. 7.

Mendelssohn, I.A., Andersen, G.L., Baltz, D.M., Caffey, R.H., Carman, K.R., Fleeger, J.W., Joye, S.B., Lin, Q., Maltby, E., Overton, E.B., and Rozas, L.P., 2012, Oil impacts on coastal wetlands: Implications for the Mississippi River delta ecosystem after the Deepwater Horizon oil spill: BioScience, v. 62, p. 562–574, doi: 10.1525/bio.2012.62.6.7.

Mitchell, K.R., and Takacs-Vesbach, C.D., 2008, A comparison of methods for total community DNA preservation and extraction from various thermal environments: Journal of industrial microbiology & biotechnology, v. 35, p. 1139–1147.

Morales, S.E., Cosart, T.F., Johnson, J. V, and Holben, W.E., 2009, Extensive phylogenetic analysis of a soil bacterial community illustrates extreme taxon evenness and the effects of amplicon length, degree of coverage, and DNA fractionation on classification and ecological parameters: Applied and Environmental Microbiology, v. 75, p. 668–675.

Morris, J.T., 2000, Effects of sea level anomalies on estuarine processes, *in* Estuarine Science: A synthetic approach to Research and Practice, Island Press, p. 107–127.

Morrissey, E.M., Gillespie, J.L., Morina, J.C., and Franklin, R.B., 2014, Salinity affects microbial activity and soil organic matter content in tidal wetlands: Global Change Biology, v. 20, p. 1351–1362.

National Atmospheric Deposition Program, 2015, NTN Precipitation-weighted mean concentrations:

National Oceanic and Atmospheric Association, 2013, NOAA's State of the Coast: Communities: The U.S. Population Living at the Coast, http://stateofthecoast.noaa.gov/population/welcome.html.

Oksanen, J., Kindt, R., Legendre, P., O'Hara, B., Stevens, M.H.H., Oksanen, M.J., and Suggests, M., 2007, The vegan package: Community ecology package, v. 10.

Paliy, O., and Shankar, V., 2016, Application of multivariate statistical techniques in microbial ecology: Molecular Ecology, v. 25, p. 1032–1057, doi: 10.1111/mec.13536.

Penfound, W.T., and Hathaway, E.S., 1938, Plant communities in the marshlands of southeastern Louisiana: Ecological Monographs, v. 8, p. 1–56.

Pennings, S.C., Grant, M.B., and Bertness, M.D., 2005, Plant zonation in low-latitude salt marshes: Disentangling the roles of flooding, salinity and competition: Journal of Ecology, v. 93, p. 159–167, doi: 10.1111/j.1365-2745.2004.00959.x.

Pethick, J.S., 1981, Long-term Accretion Rates on Tidal Salt Marshes: J Sediment Res, v. Vol. 51, p. 571–577, doi: 10.1306/212F7CDE-2B24-11D7-8648000102C1865D.

Pruesse, E., Quast, C., Knittel, K., Fuchs, B.M., Ludwig, W., Peplies, J., and Glöckner, F.O., 2007, SILVA: a comprehensive online resource for quality checked and aligned ribosomal RNA sequence data compatible with ARB: Nucleic acids research, v. 35, p. 7188–7196.

Rabalais, N.N., Turner, E.R., Dortch, Q., Justic, D., Bierman, V.J., and Wiseman, W.J., 2002, Nutrient-enhanced productivity in the northern Gulf of Mexico: past, present and future.: Hydrobiologia, v. 475–476, p. 39–63, doi: doi:10.1023/A:1020388503274.

R Core Team, 2015, R: A Language and Environment for Statistical Computing:, https://www.r-project.org/.

Rao, C.R., 1995, A review of canonical coordinates and an alternative to correspondence analysis using Hellinger distance: Questiio, v. 19, p. 23–63.

Redfield, A.C., 1942, The processes determining the concentration of oxygen, phosphate and other organic derivatives within the depths of the Atlantic Ocean: Papers In Physical Oceanogrphy and Meterology, v. XI.

Rietl, A.J., Overlander, M.E., Nyman, A.J., and Jackson, C.R., 2016, Microbial community composition and extracellular enzyme activities associated with *Juncus roemerianus* and *Spartina alterniflora* vegetated sediments in Louisiana saltmarshes: Microbial Ecology, v. 71, p. 290–303, doi: 10.1007/s00248-015-0651-2.

Roblin, R., 2008, Water quality modeling of freshwater diversions in the Barataria Basin: University of New Orleans Thesis Dissertation, 1-220 p.

Rodriguez-R., L.M., Overholt, W.A., Hagan, C., Huettel, M., Kostka, J.E., Konstantinidis, K.T., Rodriguez-R, L.M., Overholt, W.A., Hagan, C., Huettel, M., Kostka, J.E., and Konstantinidis, K.T., 2015, Microbial community successional patterns in beach sands impacted by the Deepwater Horizon oil spill: Annual Review of Marine Science: ISME

Journal, v. 9, p. 1928–1940, doi: 10.1038/ismej.2015.5.

Rooney-Varga, J.N., Devereux, R., Evans, R.S., and Hines, M.E., 1997, Seasonal changes in the relative abundance of uncultivated sulfate-reducing bacteria in a salt marsh sediment and in the rhizosphere of Spartina alterniflora: Applied and Environmental Microbiology, v. 63, p. 3895–3901.

Rosenberg, E., 2013, The prokaryotes: Alphaproteobacteria and Betaproteobacteria: 1-1012 p., doi: 10.1007/978-3-642-30197-1.

Rueter, P., Rabus, R., Wilkest, H., Aeckersberg, F., Rainey, F.A., Jannasch, H.W., and Widdel, F., 1994, Anaerobic oxidation of hydrocarbons in crude oil by new types of sulphate-reducing bacteria: Nature, v. 372, p. 455–458, doi: 10.1038/372455a0.

Sasser, C.E., 1994, Vegetation dynamics in relation to nutrients in floating marshes in Louisiana, USA: PhD Dissertation, 193 p.

Schimel, J.P., and Schaeffer, S.M., 2015, Microbial control over carbon cycling in soil: The causes and consequences of microbial community structure, p. 155.

Schloss, P.D., Gevers, D., and Westcott, S.L., 2011, Reducing the effects of PCR amplification and sequencing artifacts on 16S rRNA-based studies: PLoS One, v. 6, p. e27310.

Schloss, P.D., and Westcott, S.L., 2011, Assessing and improving methods used in operational taxonomic unit-based approaches for 16S rRNA gene sequence analysis: Applied and Environmental Microbiology, v. 77, p. 3219–3226.

Schloss, P.D., Westcott, S.L., Ryabin, T., Hall, J.R., Hartmann, M., Hollister, E.B., Lesniewski, R.A., Oakley, B.B., Parks, D.H., Robinson, C.J., Sahl, J.W., Stres, B., Thallinger, G.G., Van Horn, D.J., et al., 2009, Introducing mothur: Open-source, platform-independent, community-supported software for describing and comparing microbial communities: Applied and Environmental Microbiology, v. 75, p. 7537–7541, doi: 10.1128/AEM.01541-09.

Schubauer, J.P., and Hopkinson, C.S., 1984, Above- and belowground emergent macrophyte production and turnover in a coastal marsh ecosystem, Georgia: Limnology and Oceanography, v. 29, p. 1052–1065, doi: 10.4319/lo.1984.29.5.1052.

Schulte, E.E., and Hopkins, B.G., 1996, Estimation of soil organic matter by weight loss-on-ignition, *in* Soil Organic Matter: Analysis and Interpretation, Madison, WI, Soil Science Society of America, SSSA Special Publication SV, p. 21–31, doi: 10.2136/sssaspecpub46.c3.

Shade, A., and Handelsman, J., 2012, Beyond the Venn diagram: The hunt for a core microbiome: Environmental Microbiology, v. 14, p. 4–12, doi: 10.1111/j.1462-2920.2011.02585.x.

Shinkle, K.D., and Dokka, R.K., 2004, Rates of vertical displacement at benchmarks in the lower Mississippi Valley and the northern Gulf Coast. NOAA Technical Report NOS/NGS 50 (U S Department of Commerce and Education, Ed.): , p. 135.

Simon, M.R., 2013, East Coast Salt Marsh Response To Sea Level Rise: Microbial Community

Function And Structure:

Sims, A., Zhang, Y., Gajaraj, S., Brown, P.B., and Hu, Z., 2013, Toward the development of microbial indicators for wetland assessment: Water Research, v. 47, p. 1711–1725.

Smith, E.P., and van Belle, G., 1984, Nonparametric estimation of species richness: Biometrics, p. 119–129.

Somerville, C.C., Knight, I.T., Straube, W.L., and Colwell, R.R., 1989, Simple, rapid method for direct isolation of nucleic acids from aquatic environments: Applied and environmental microbiology, v. 55, p. 548–554.

Teal, J.M., and Kanwisher, J.W., 1966, Gas transport in the marsh grass, Spartina alterniflora: Journal of Experimental Botany, v. 17, p. 355–361.

Thomas, G.W., 1996, Soil pH and soil acidity: Methods of soil analysis. Part 3 - chemical methods., p. 475–490, doi: 10.1007/978-94-6091-478-2_16.

Tibshirani, R., 1996, Regression shrinkage and selection via the lasso: Journal of the Royal Statistical Society. Series B (Methodological), p. 267–288.

Tornqvist, T.E., Kidder, T.R., Autin, W.J., and van der Borg, K., 1996, A revised chronology for Mississippi River subdeltas: Science, v. 273, p. 1693.

Turner, R.E., McClenachan, G., and Tweel, A.W., 2016, Islands in the oil: Quantifying salt marsh shoreline erosion after the Deepwater Horizon oiling: Marine Pollution Bulletin, v. 110, p. 316–323, doi: 10.1016/j.marpolbul.2016.06.046.

Turner, R.E., Overton, E.B., Meyer, B.M., Miles, M.S., McClenachan, G., Hooper-Bui, L., Engel, A.S., Swenson, E.M., Lee, J.M., Milan, C.S., and Gao, H., 2014, Distribution and recovery trajectory of Macondo (Mississippi Canyon 252) oil in Louisiana coastal wetlands: Marine Pollution Bulletin, v. 87, p. 57–67, doi: 10.1016/j.marpolbul.2014.08.011.

Turner, R.E., and Rabalais, N.N., 1991, Changes in Mississippi River water quality this century implications for coastal food webs: BioScience, v. 41, p. 140–147.

Turner, R.E., and Swenson, E., 2016, Marsh health and process data collected in the Louisiana Coastal Plain Marshes, 2011-2013: GRIIDC, doi: 10.7266/N72N5065.

Tweel, A.W., and Turner, R.E., 2012, Watershed land use and river engineering drive wetland formation and loss in the Mississippi River birdfoot delta: Limnology and Oceanography, v. 57, p. 18–28.

U.S. Geological Survey, 2016, USGS Surface-Water Monthly Statistics for the Nation USGS 07374525 Mississippi River at Belle Chasse:, https://waterdata.usgs.gov/nwis/inventory?agency_code=USGS&site_no=07374525.

Valiela, I., Cole, M.L., Mcclelland, J., Hauxwell, J., Cebrian, J., and Joye, S.B., 2002, Role of salt marshes as part of coastal landscapes, in Concepts and Controversies in Tidal Marsh Ecology, Springer, p. 23–36.

Valiela, I., and Teal, J.M., 1979, The nitrogen budget of a salt marsh ecosystem: Nature, v. 280, p. 652–656, doi: 10.1038/280652a0.

Valiela, I., Teal, J.M., Volkmann, S., Shafer, D., and Carpenter, E.J., 1978, Nutrient and

particulate fluxes in a salt marsh ecosystem: tidal exchanges and inputs by precipitation and groundwater: Limnology and Oceanography, v. 23, p. 798–812.

Veres, D. ̄, 2002, A comparative study between loss on ignition and total carbon analysis on minerogenic sediments: Geologia, v. 47, p. 171–182.

Visser, J.M., Duke-Sylvester, S.M., Carter, J., and Broussard, W.P.I., 2013, A computer model to forecast wetland vegetation changes resulting from restoration and protection in coastal Louisiana: Journal of Coastal Research, v. 67, p. 51–59, doi: 10.2112/SI.

Visser, J.M., Sasser, C.E., Chabreck, R.H., and Linscombe, R.G., 1998, Marsh vegetation types of the Mississippi River deltaic plain: Estuaries, v. 21, p. 818–828.

Weston, N.B., Dixon, R.E., and Joye, S.B., 2006, Ramifications of increased salinity in tidal freshwater sediments: Geochemistry and microbial pathways of organic matter mineralization: Journal of Geophysical Research: Biogeosciences, v. 111, p. 1–14, doi: 10.1029/2005JG000071.

White, D.A., Weiss, T.E., Trapani, J.M., and Thien, L.B., 1978, Productivity and decomposition of the dominant salt marsh plants in Louisiana: Ecology, p. 751–759.

Wickham, H., 2012, reshape2: Flexibly reshape data: a reboot of the reshape package: R package version, v. 1.

Wickham, H., and Francois, R., 2015, dplyr: A grammar of data manipulation: R package version 0.4, v. 1, p. 20.

Yang, T., Nigro, L.M., Gutierrez, T., D′Ambrosio, L., Joye, S.B., Highsmith, R., and Teske, A., 2014, Pulsed blooms and persistent oil-degrading bacterial populations in the water column during and after the Deepwater Horizon blowout: Deep Sea Research Part II: Topical Studies in Oceanography, doi: http://dx.doi.org/10.1016/j.dsr2.2014.01.014.

Zhou, J., Bruns, M.A., and Tiedje, J.M., 1996, DNA recovery from soils of diverse composition: Applied and environmental microbiology, v. 62, p. 316–322.

Zou, L., Kent, J., Lam, N.S.-N., Cai, H., Qiang, Y., and Li, K., 2015, Evaluating Land Subsidence Rates and Their Implications for Land Loss in the Lower Mississippi River Basin: Water, v. 8, p. 10.

APPENDICES
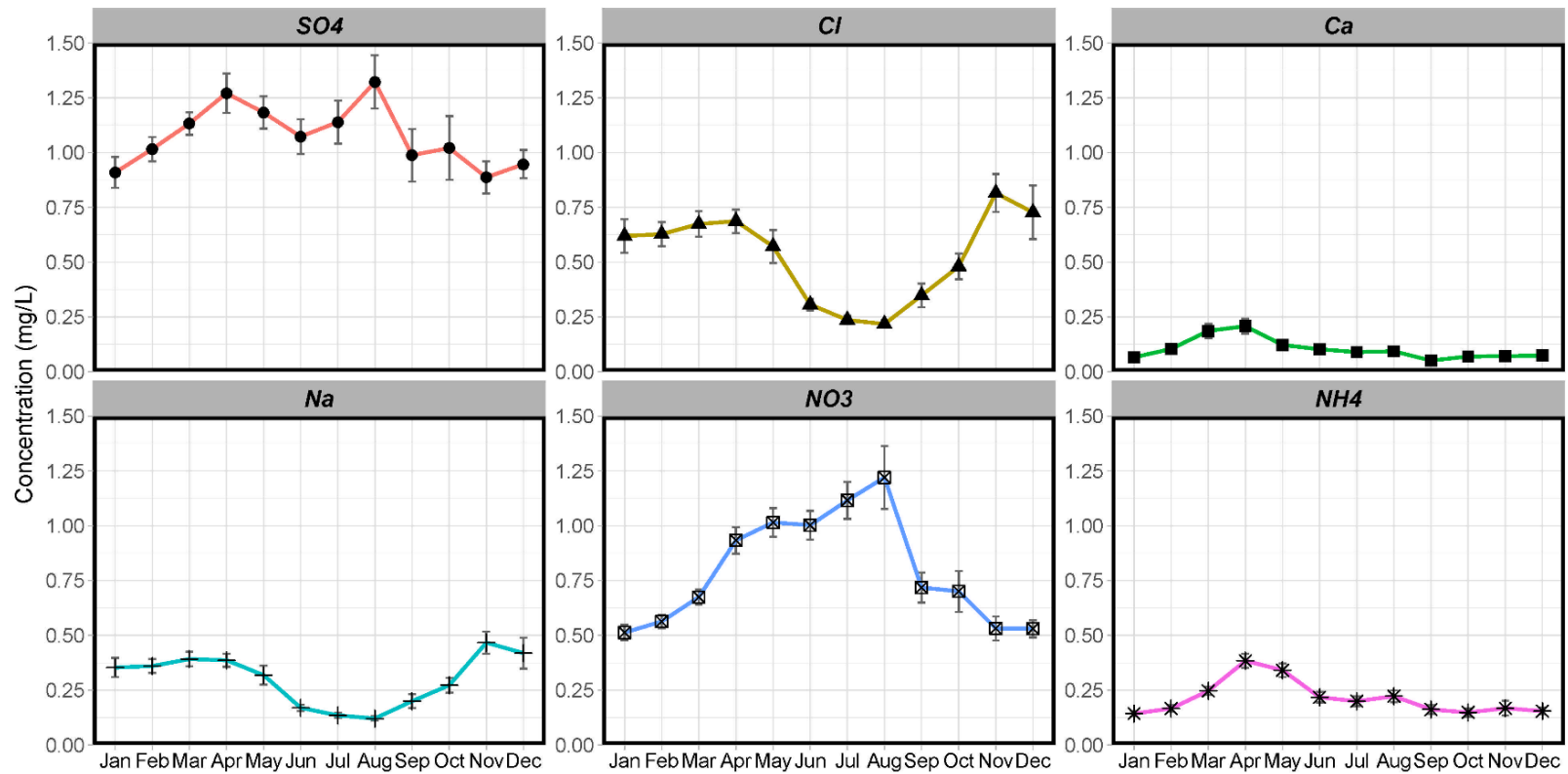
Figure A.1: Monthly mean concentrations of selected ions from precipitation in southern Louisiana 1983 to 2015 from NADP site LA30.

Table A.1: PCA Loadings of the 5 most explanatory phylum level loadings in the positive and negative direction. The eigenvalue and variance as a percentage, are displayed in the upper portion. In the lower portion, the individual class level bacterial are listed with their loadings for the first 3 principal component axes, only 1 and 2 were plotted.

PC 1		PC 2		PC 3	
Eigenvalue	96.89	40.22		22.92	
% variance	45.60	18.93		10.79	
Bacterial Class Loadings					
Deltaproteobacteria	0.4743	Alphaproteobacteria	0.2938	Betaproteobacteria	0.4488
Anaerolineae	0.1480	Epsilonproteobacteria	0.1487	Chlorobia	0.4049
Chlorobia	0.1155	Chlorobia	0.1474	Deltaproteobacteria	0.3793
Epsilonproteobacteria	0.0991	Anaerolineae	0.1432	Alphaproteobacteria	0.2470
vadinBA26	0.0938	vadinBA26	0.1137	Acidobacteria	0.1932
Sphingobacteria	-0.0978	Planctomycetacia	-0.0653	Sphingobacteria	-0.1502
Gammaproteobacteria	-0.0979	Chloroplast	-0.0718	vadinBA26	-0.1815
Planctomycetacia	-0.1494	Flavobacteria	-0.1888	Flavobacteria	-0.2016
Flavobacteria	-0.1497	Sphingobacteria	-0.1895	GIF9	-0.2651
Alphaproteobacteria	-0.7956	Gammaproteobacteria	-0.8434	Epsilonproteobacteria	-0.3317

Figure A.2: PCA of phylum level bacterial relative abundance with the vectors indicating the loadings of specific phyla. The ordinal hulls are grouping bacteria by sampling year.
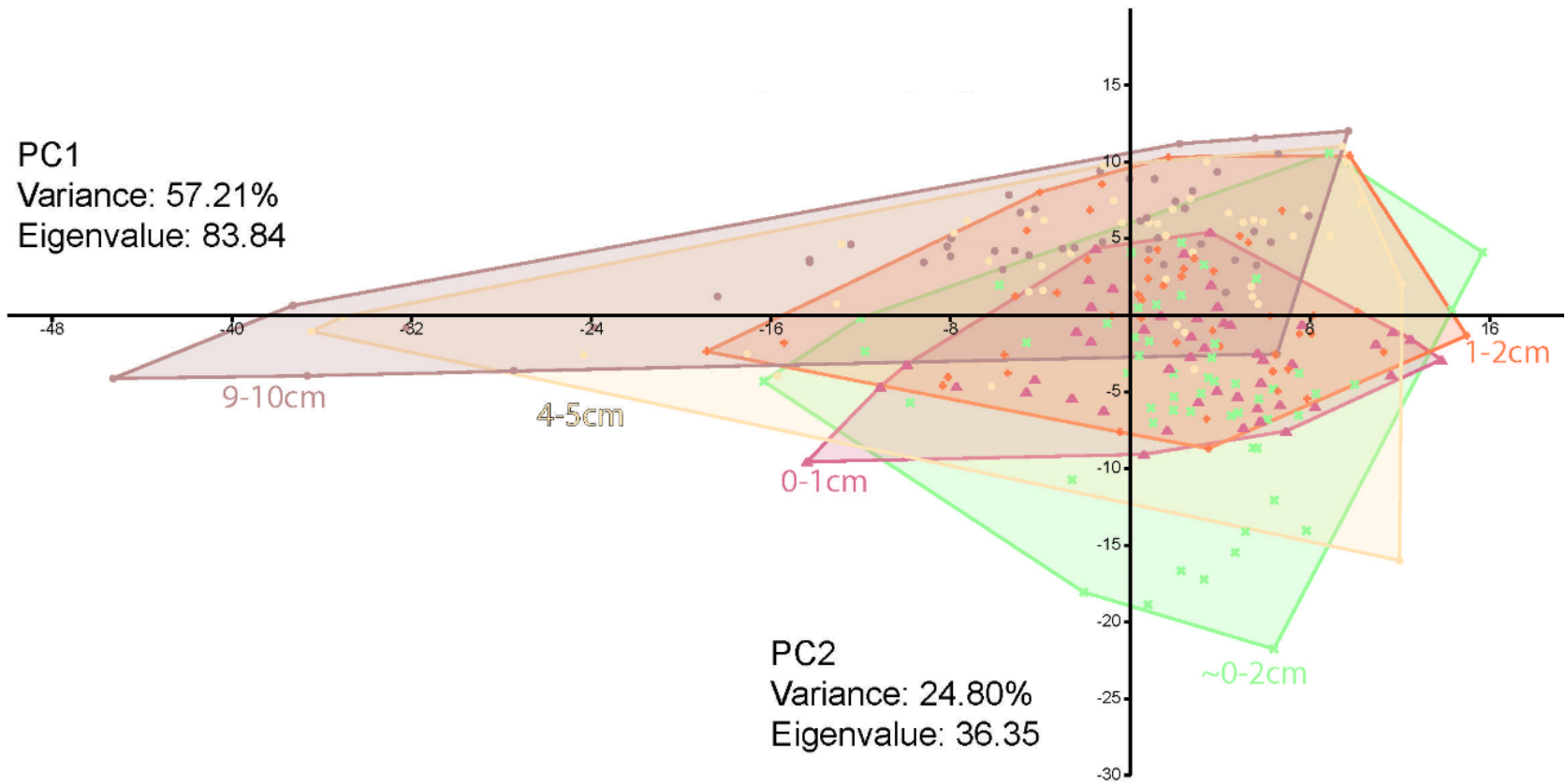
Figure A.3: PCA of phylum level bacterial relative abundance with the vectors indicating the loadings of specific phyla. The ordinal hulls are grouping bacteria by sampling depth.
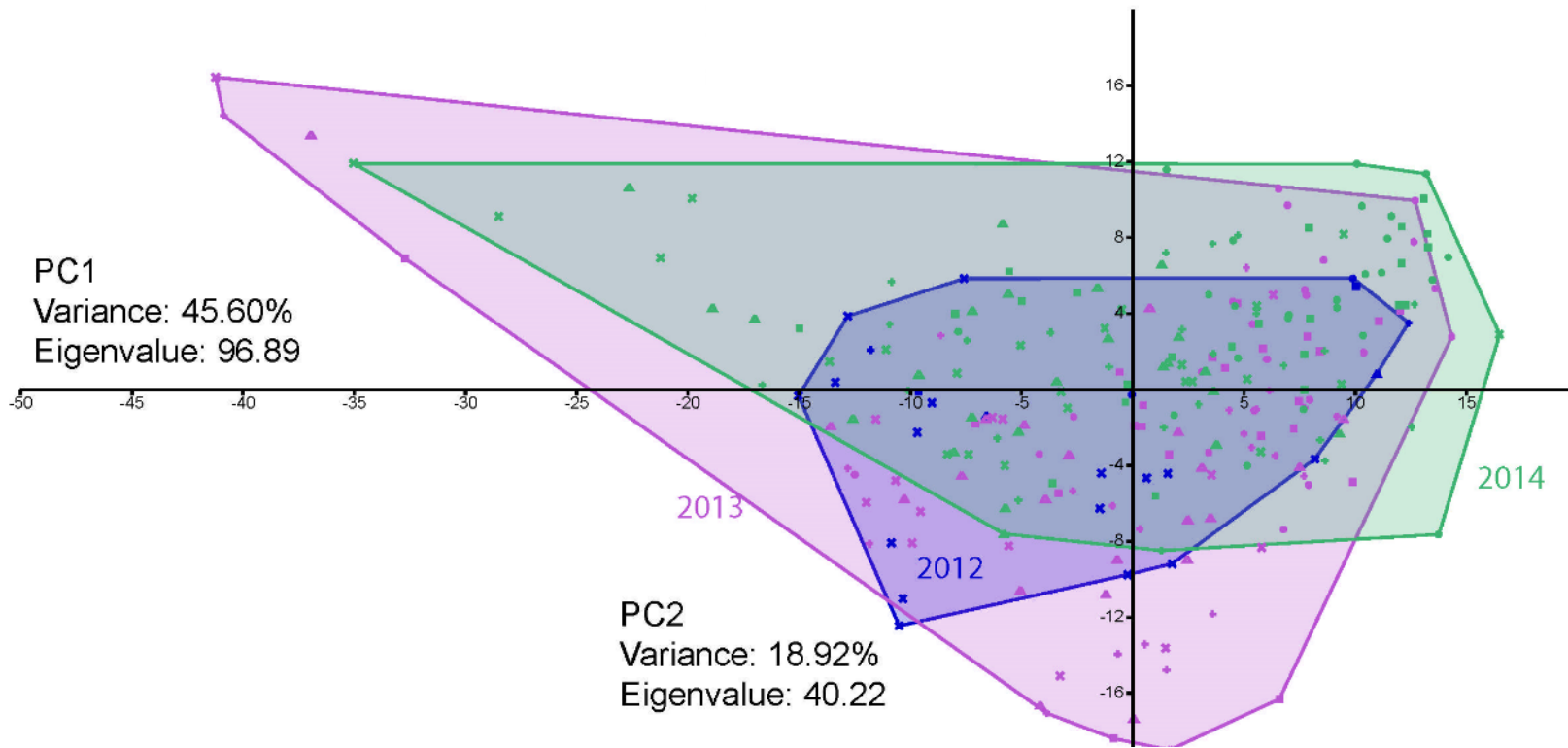
Figure A.4: PCA of Class level bacterial relative abundance with the vectors indicating the loadings of specific phyla. The ordinal hulls are grouping bacteria by sampling year.

Table A.2: CCA overall proportion of the constrained axes from the second hypothesis. Each eigenvalue and proportion are from the constrained axes, with the cumulative proportion is calculated as a percentage of the total variance represented by the CCA model. The Axis for the MII samples labeled CA1 is the proportion of the model which is unconstrained, in which only MII is used as an environmental variable. Beyond the cumulative proportion of variance explained by the models, the remaining variance is unexplained by the supplied variables. For all models, MII was the first constraining variable. For all samples Region was the input, and for all regional models Depth was the constraining variables

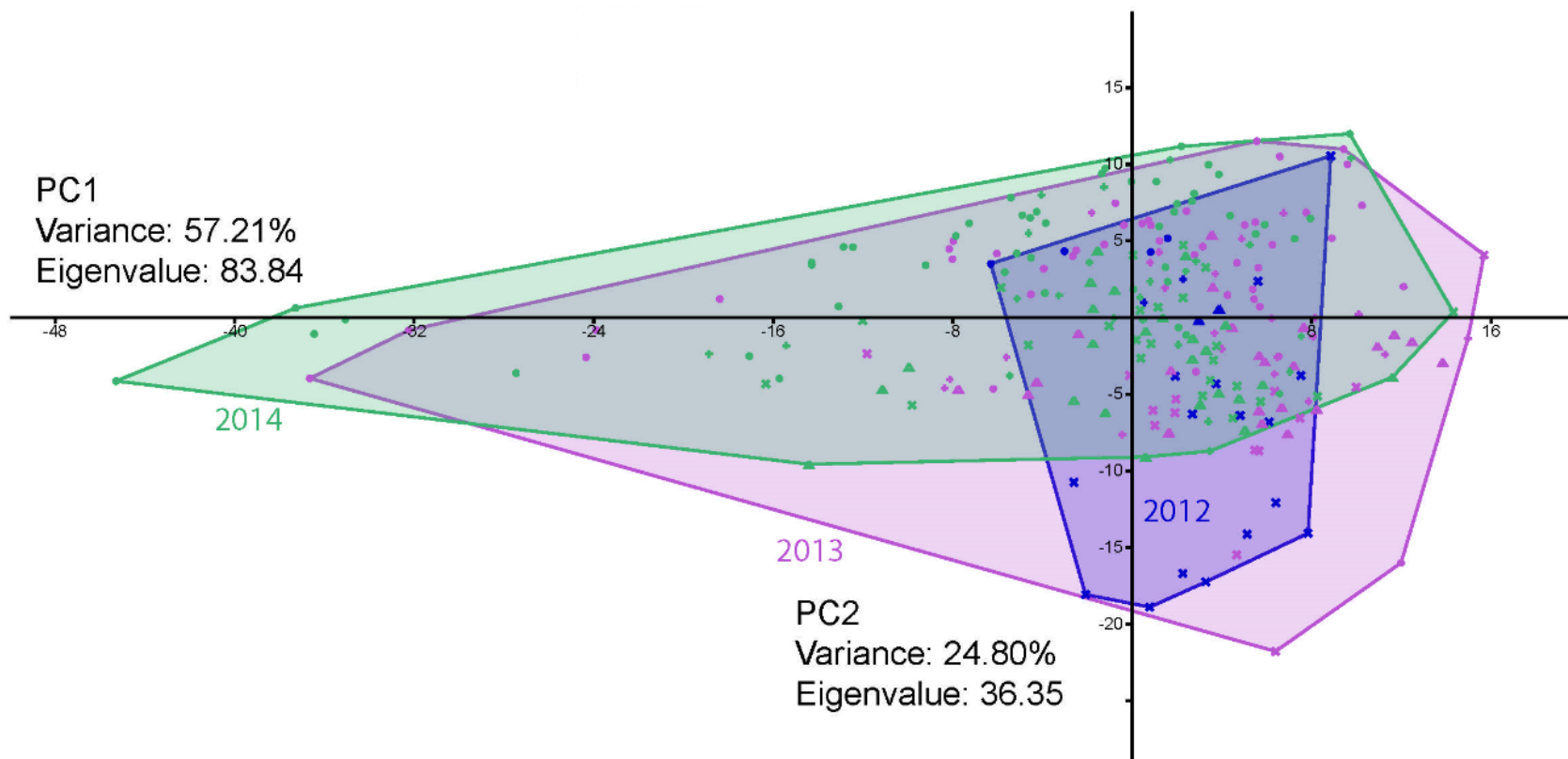| CCA - All			
Variable	**CCA1**	**CCA2**	**CCA3**
Eigenvalue	0.031	0.018	0.003
Proportion Explained	0.051	0.029	0.006
Cumulative Proportion (%)	5.00	8.00	9.00

CCA - MII-0 and MII-3 Samples		
Variable	**CCA1**	**CA1**
Eigenvalue	0.025	0.150
Proportion Explained	0.050	0.297
Cumulative Proportion (%)	0.05	0.35

CCA - Port Sulphur					
Variable	**CCA1**	**CCA2**	**CCA3**	**CCA4**	**CCA5**
Eigenvalue	0.066	0.010	0.006	0.001	0.001
Proportion Explained	0.161	0.025	0.014	0.003	0.003
Cumulative Proportion (%)	16.1	18.7	20.1	20.4	20.6

CCA - Grand Isle					
Variable	**CCA1**	**CCA2**	**CCA3**	**CCA4**	**CCA5**
Eigenvalue	0.081	0.011	0.006	0.002	0.001
Proportion Explained	0.178	0.025	0.012	0.005	0.001
Cumulative Proportion (%)	17.8	20.3	21.5	22.1	22.2

CCA - Terrebonne Bay					
Variable	**CCA1**	**CCA2**	**CCA3**	**CCA4**	**CCA5**
Eigenvalue	0.091	0.015	0.008	0.004	0.002
Proportion Explained	0.136	0.022	0.011	0.005	0.003
Cumulative Proportion (%)	13.6	15.8	16.9	17.5	17.7

Table A.3: Results of Anova-like permutation tests run for each CCA. The results for the whole CCA model as a sum of constraint eigenvalues is shaded blue, and the permutation test for each constraining variable in the model for each CCA is unshaded. The type of transformation is listed at the end of the name of each variable, ".hell" is a Hellinger transformation performed on all values of the dataset for that measurement. Categorical variables in the model were not transformed and were used in the model as binary values to explain the data, thus there are differing degrees of freedom within the model based on the number of individual categorical values. Each categorical value is displayed in the plots without a vector to identify their centroid and loading of the model.

CCA-All Samples				
Variable	**Df**	**ChiSquare**	**F**	**Pr(>F)**
Model	3	0.053	7.600	0.001
Residual-Model	241	0.555		
mii.hell	1	0.006	2.689	0.009
region	2	0.046	10.055	0.001
Residual-Env. Variables	241	0.555		

CCA - MII-0 and MII-3 Samples				
Variable	**Df**	**ChiSquare**	**F**	**Pr(>F)**
Model	1	0.025	2.783	0.01
Residual-Model	53	0.481		
mii.hell	1	0.025	2.783	0.017
Residual	53	0.481		

CCA - Port Sulphur				
Variable	**Df**	**ChiSquare**	**F**	**Pr(>F)**
Model	5	0.085	4.265	0.001
Residual-Model	82	0.326		
mii.hell	1	0.011	2.749	0.011
depth	4	0.074	4.643	0.001
Residual-Env. Variables	82	0.326		

CCA - Grand Isle				
Variable	**Df**	**ChiSquare**	**F**	**Pr(>F)**
Model	5	0.101	4.339	0.001
Residual-Model	76	0.354		
mii.hell	1	0.008	1.737	0.08
depth	4	0.093	4.990	0.001
Residual-Env. Variables	76	0.354		

CCA - Terrebonne Bay				
Variable	**Df**	**ChiSquare**	**F**	**Pr(>F)**
Model	5	0.118	2.972	0.001
Residual-Model	69	0.550		
mii.hell	1	0.014	1.757	0.08
depth	4	0.104	3.275	0.001
Residual-Env. Variables	69	0.550		

Table A.4: Scores of individual CCA models with up to two variables, MII and region or nothing. The MII 0 and 4 CCA has no second constraining variable, and thus the CA1 is the first unconstrained axis. Each chart shows the first two constrained axes and the scores of each bacterial class.

All Samples			
CCA1		**CCA2**	
Fusobacteria	0.418	CD_OP11-unclassified	0.770
Cyanobacteria-uncultured	0.316	OPB35	0.556
JTB23	0.268	Acidimethylosilex	0.445
Opitutae	0.252	KD4-96	0.440
CD_TM7-unclassified	0.248	Lineage_IV	0.411
Hyd24-12-unclassified	-0.693	Acaryochloris	-0.239
TA06-unclassified	-0.717	VC2.1	-0.304
Dehalococcoidetes	-0.754	Deinococcales	-0.442
CD_OP9-unclassified	-0.840	SubsectionII	-0.555
GIF9	-0.843	Fusobacteria	-0.641

MII 0 & 3			
CCA1		**CA1**	
CD_OP11-unclassified	0.528	Cyanobacteria-uncultu	0.655
Dehalococcoidetes	0.455	CD_TM7-unclassified	0.577
KD3-62	0.452	KD4-96	0.562
GIF9	0.427	S085	0.551
Caldilineae	0.408	SAR202	0.542
SubsectionIV	-0.400	Lineage_I_Endomicrob	-1.009
Acidimethylosilex	-0.430	OPS8-unclassified	-1.060
Cyanobacteria-uncultured	-0.455	CD_OP9-unclassified	-1.072
S085	-0.457	TA06-unclassified	-1.192
SAR202	-0.516	GIF9	-1.273

Table A.5:   Scores from regional CCA models. Each chart shows the first two constrained axes and the scores of each bacterial class.

Port Sulphur			
CCA1		CCA2	
SubsectionI	0.712	SubsectionIV	0.459
Flavobacteria	0.643	SubsectionIII	0.378
SubsectionIII	0.538	Candidatus_Kuenenia	0.375
SubsectionII	0.529	Cyanobacteria-uncultured	0.353
Acaryochloris	0.471	Thermodesulfobacteria	0.336
GIF9	-0.640	OPB35	-0.252
vadinBA26	-0.686	Chrysiogenetes	-0.266
CD_OP9-unclassified	-0.746	CD_OP10-unclassified	-0.304
Epsilonproteobacteria	-0.895	CD_OP11-unclassified	-0.415
Dehalococcoidetes	-0.938	KD4-96	-0.466

Grand Isle			
CCA1		CCA2	
SubsectionI	0.544	Fusobacteria	0.981
Flavobacteria	0.509	Dehalococcoidetes	0.530
SM1A07	0.436	SubsectionII	0.479
TA18	0.385	Deinococcales	0.468
Acidimethylosilex	0.343	Hyd24-12-unclassified	0.449
vadinBA26	-0.838	TK10	-0.279
CD_OP11-unclassified	-0.890	Cyanobacteria-uncultured	-0.318
WCHB1-60-unclassified	-0.900	Lineage_I_Endomicrobia	-0.356
Lineage_IV	-0.985	WD272	-0.441
Dehalococcoidetes	-1.193	vadinHA49	-0.556

| Terrebonne Bay			
CCA1		CCA2	
RF3	0.867	SAR202	0.602
SubsectionIII	0.691	Epsilonproteobacteria	0.432
SubsectionII	0.655	RF3	0.293
SubsectionI	0.617	Fusobacteria	0.283
Spartobacteria	0.468	OPS8-unclassified	0.281
GIF9	-0.662	CD_OP11-unclassified	-0.293
vadinBA26	-0.710	Lineage_I_Endomicrobia	-0.298
Dehalococcoidetes	-0.827	SubsectionIII	-0.300
Epsilonproteobacteria	-0.846	WD272	-0.313
Lineage_I_Endomicrobia	-0.861	Spartobacteria	-0.323
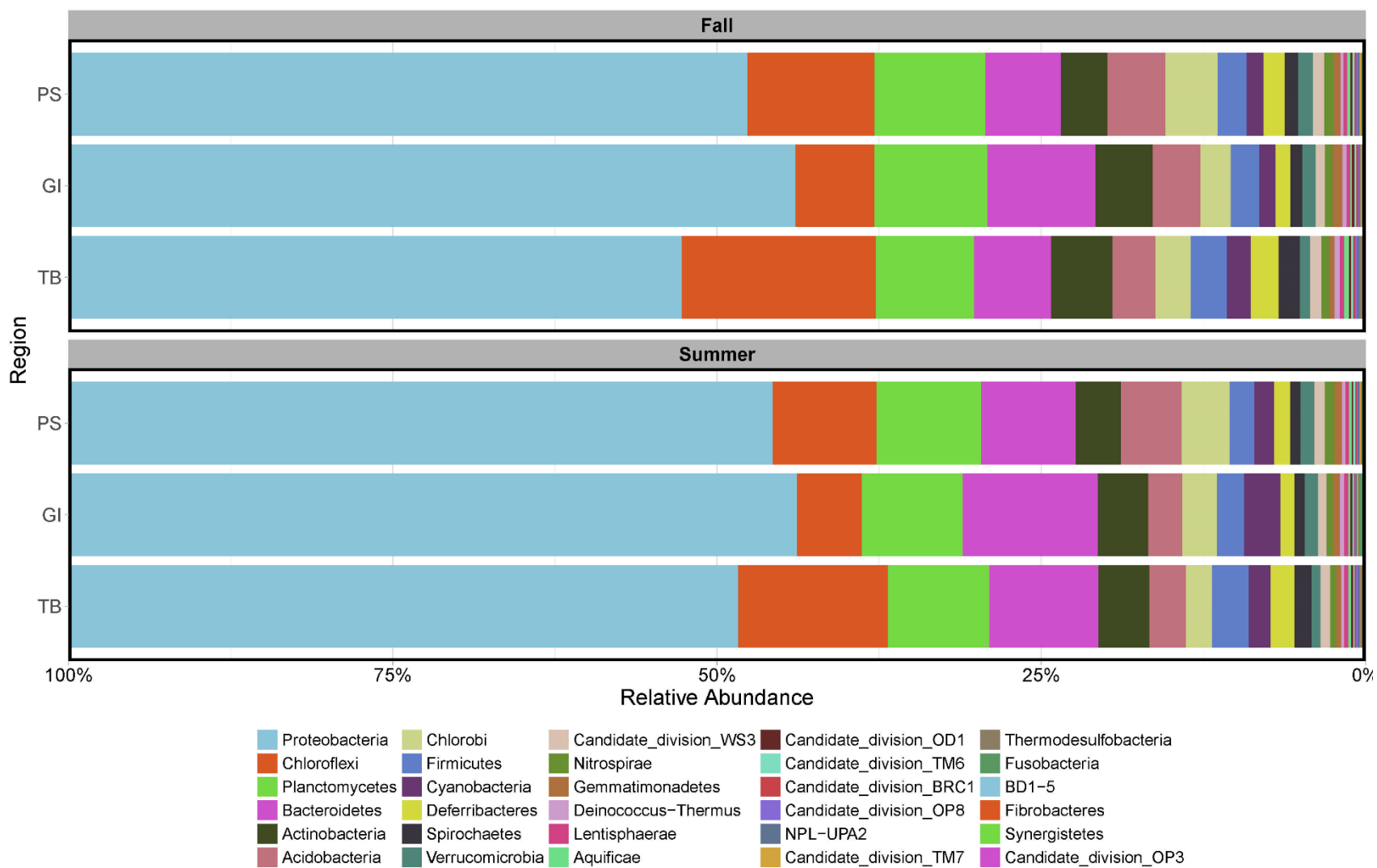
Figure A.5: Average bacterial relative abundance of the top 99% of bacterial phyla by region and season.

Figure A.6: CCA of all samples showing the species scores with the MII and region as constraining variables. The relative proportion of each axis variance and eigenvalue are listed along the axis. Each ordinal hull is colored and labeled by MII value with the sample point is also labeled with the corresponding color. The secondary axis on the top and right of the graph show the strength of the constraining variable vector, of MII and regional centroids.
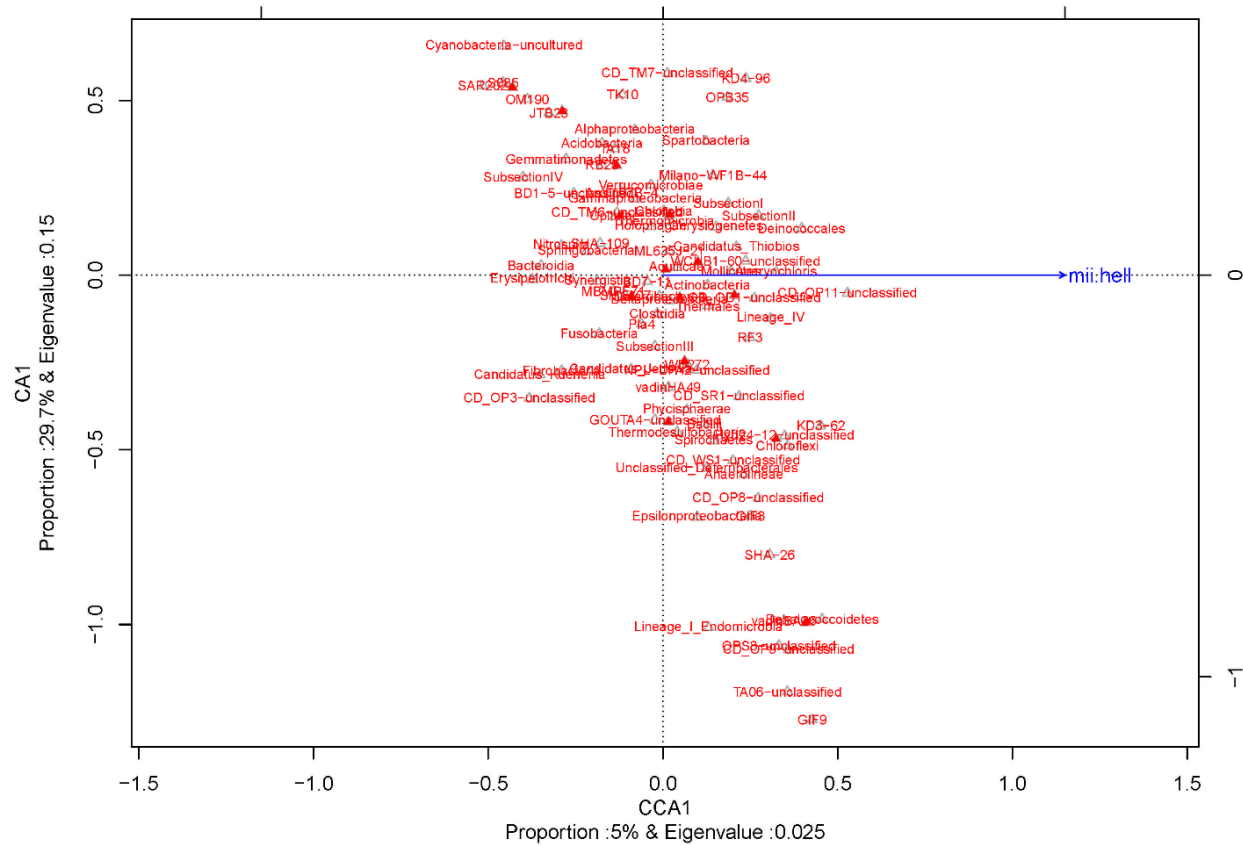
111

Figure A.7: Ordination of the CCA with only bacterial communities of MII 0 and 4 with MII as the constraining variable. The proportion of the variance of each axis is displayed, the only constrained axis is CCA1. The secondary axis on the top and right of the graph show the strength of the constraining variable vector (MII) from zero to 1.
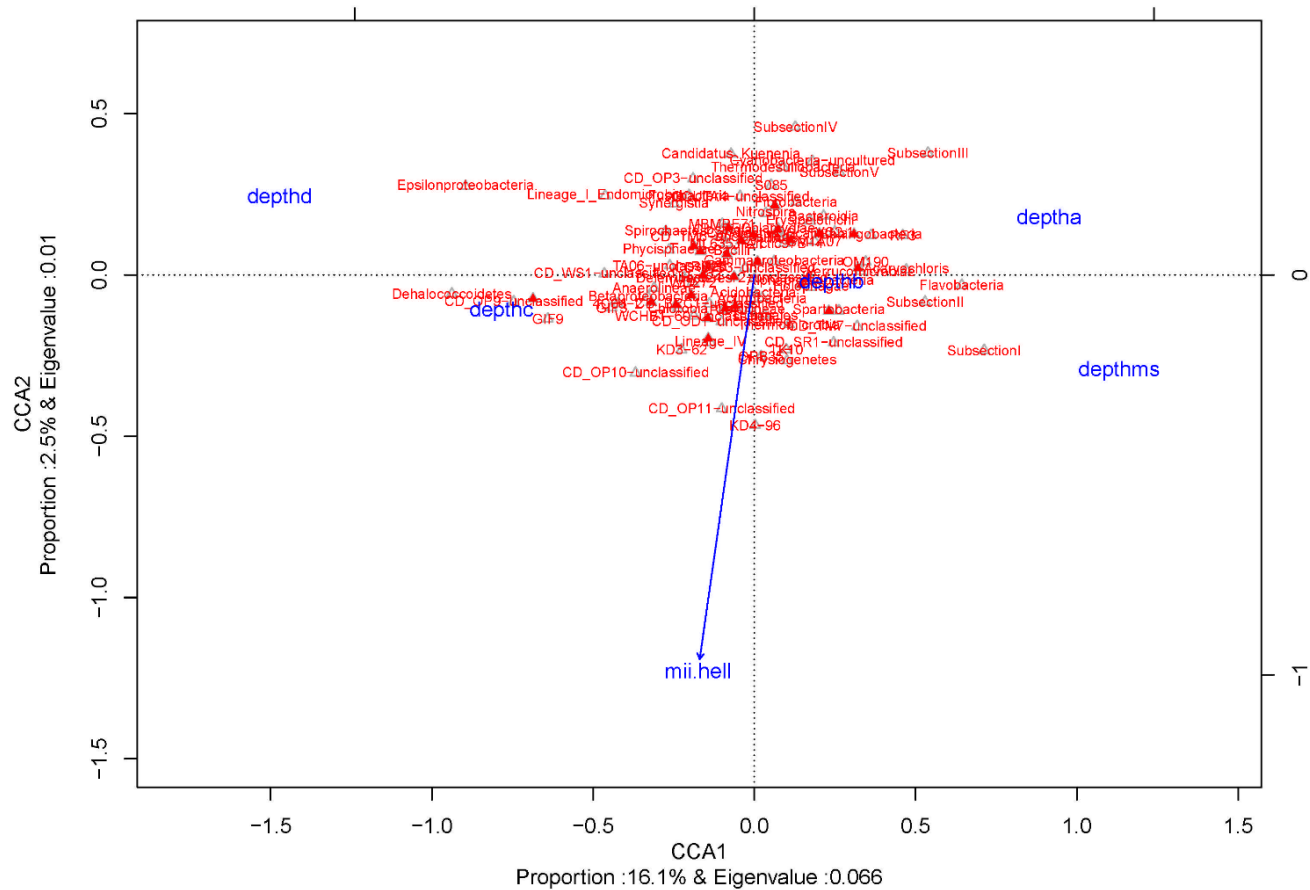
Figure A.8: Ordination of the CCA with only bacterial communities from Port Sulphur with MII and depth as the constraining variables. The proportion of the variance of each axis is displayed. The secondary axis on the top and right of the graph show the strength of the constraining variable vector (MII) from zero to 1, and the centroid of each depth category on the same scale.

Figure A.9: Ordination plot of the CCA with only bacterial communities from Grand Isle with MII and depth as the constraining variables. The proportion of the variance of each axis is displayed. The secondary axis on the top and right of the graph show the strength of the constraining variable vector (MII) from zero to 1, and the centroid of each depth category on the same scale.
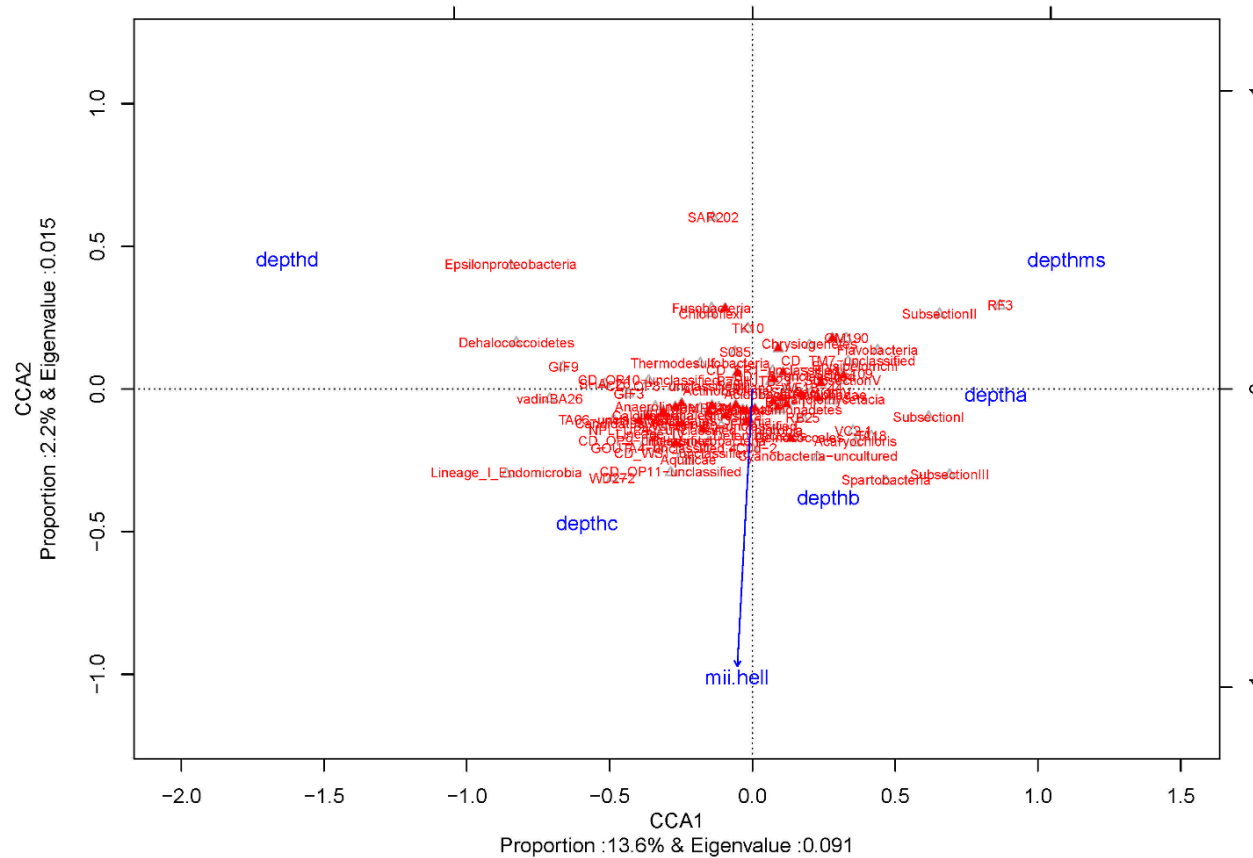
Figure A.10: Ordination plot of the CCA with only bacterial communities from Terrebonne Bay with MII and depth as the constraining variables. The proportion of the variance of each axis is displayed. The secondary axis on the top and right of the graph show the strength of the constraining variable vector (MII) from zero to 1, and the centroid of each depth category on the same scale.

VITA

Brandon Bagley was born in Portland, Maine, on May 30, 1984. After elementary school, Brandon and his family moved to North Carolina where he graduated high school and obtained a Bachelor's of Art, with a concentration in Photography, and a Bachelor's of Science in Earth Science at the University of North Carolina at Charlotte. After graduation in 2011 he entered the workforce in environmental consulting in Cincinnati, Ohio, before obtaining a Master's in Geology at the University of Tennessee, Knoxville.